Simulating dynamics of two electron spins in a SI-based double quantum dot

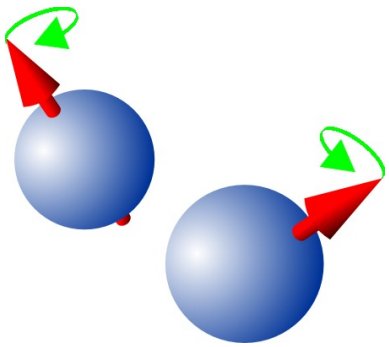

THESIS

submitted in partial fulfillment of the
requirements for the degree of

MASTER OF SCIENCE
in
PHYSICS

Author :	Ahmad Jamalzada
Student ID :	s1145657
Supervisor :	Dr. Wolfgang Löffler
2nd corrector :	Dr. Thorsten Last

Leiden, The Netherlands, July 24, 2019

Simulating dynamics of two electron spins in a SI-based double quantum dot

Ahmad Jamalzada

Huygens-Kamerlingh Onnes Laboratory, Leiden University
P.O. Box 9500, 2300 RA Leiden, The Netherlands

July 24, 2019

Abstract

This thesis is concerned with the design of numerical methods for solving the Schrödinger equation for a system of two-electrons in a double quantum dot. Theoretical background is presented for the physics of a two-electron quantum dot. Implementation of the double dot system is via the QuTiP library is discussed and a numerical approach for the treatment of the system using the density matrix formalism is presented

Contents

Chapter 1

Introduction

The size of the fundamental building block of the digital computers, the transistor is quickly approaching its limit, and with that limit the computational power of the transistor based computer will also reach its limit. Today we are approaching the point where computer chips are so small, that the quantum mechanical effects are becoming apparant. The quantum computer was proposed to harness the quantum phenomona for computational calculations. In 1985 the concept of a Universal Quantum Computer, which is the quantum analog of the Universal Turing Machine was developed by David Deutsch. He provided a physical model for quantum computation, and also provided one of the first examples of a problem that a quantum computer is able to solve exponentially faster than any algorithm on a classical computer.[1] The quantum mechanical analog of a bit, which can take the value of 0 and 1, is called a quantum bit (qubit) and it is basically a quantum mechanical two level system that can take the value 0 and 1 but also a superposition of these values. There are many different methods for implementing qubits, one of the most promising one is to encode qubits in electron spins trapped in a semi-conductor quantum dot. The spins in the quantum dots can then be controlled through conventional Nuclear Magnetic Resonance techniques (NMR) and electrical pulsing to acquire one and two-qubit operations. This thesis will discuss the simulation of a two-electron quantum dot system and implementation of the two qubit system to perform simple gate operations. The thesis is meant as a summary or guide for people who have interest in quantum dot based spin systems. All of the code is written with Python, so that it can be easily followed and edited. The thesis is organized as follows. Chapter 2 provides an overview to the realization of semi-conductor quantum dots and the physicsal description of the spin model. In Chapter 3, basic theory of NMR is discussed and how it can be used for quantum computation. Finally in Chapter 4, the computational methods used are reviewed.

Chapter 2

Spins in quantum dots

2.1 Quantum Dots

A quantum dot is the most extreme example of an artificially structured, low-dimensional semicondcutor. These structures bind a small number of electrons to a region within the semiconductor that is of the order of the Broglie wavelength of the electrons $\lambda = h/2m_e^\star E$ where E is the kinetic energy of the electrons which causes discrete energy levels to form. A general understanding of low-dimensional semiconductors comes from treating the semiconductor as a three-dimensional box that confines the conduction electrons. These electrons behave approximately like free particles, with an effective mass, trapped in a box. By solving the Schrödinger equation, we can find the number of allowed electron states per volume at a given energy or the density of states. In 3D given a box with size L, the normalized wavefunction solution is:

$$\psi(x,y,z) = \sqrt{\frac{8}{L^3}} \sin(k_x x) \sin(k_y y) \sin(k_z z) \tag{2.1}$$

where k_x, k_y and k_z are the wavevectors for an electron in the x, y, and z directions. The allowed wavevectors satifsy:

$$k_{x,y,z} = \frac{n_{x,y,z}\pi}{L}, n_{x,y,z} = 1, 2, 3 \ldots \tag{2.2}$$

and the allowed energies are

$$E_{n_x n_y n_z} = \frac{\hbar^2}{2m}\left(\frac{n_x^2}{L} + \frac{n_y^2}{L} + \frac{n_z^2}{L}\right) = \frac{\hbar^2 k^2}{2m_e^*} \tag{2.3}$$

This enforces that the wavefunction will be zero at the boundaries of the box.

To find the number of states we can imagine a three-dimensional space, with axes k_x, k_y, k_z (k-space) where each state occupies a volume of π^3/L^3. The electrons will then

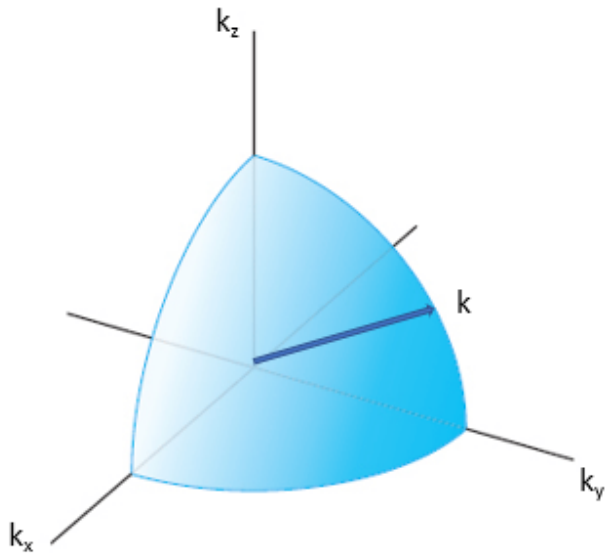

Figure 2.1: *One octant of a sphere in k-space*

fill up one octant of a sphere of radius k in k-space. The number of states within this sphere is given by the following:

$$\frac{1}{8}\left(\frac{4}{3}\pi k^3\right) = \frac{N}{2}\left(\frac{\pi^3}{L^3}\right) \tag{2.4}$$

Where the factor of $1/2$ is required because two electrons can occupy the same state due to spin degeneracy. The density of states can be calculated by the following:

$$g(E) = \frac{dN}{dk} = \frac{dN}{dk}\frac{dk}{dE} = \frac{1}{2\pi^2}\left(\frac{2m^*}{\hbar^2}\right)^{3/2}\sqrt{E} \tag{2.5}$$

By decreasing the dimensions of the box in one direction, we can treat the semiconductor effectively as a two-dimensional material. The electrons in the 2D case can only be excited along two motional degree of freedoms. It is possible to decrease the size of the box along a second dimension. This results in a structure known as a quantum wire which only allows electrons to be excited along one motional degree of freedom. Fig 2.2 shows a simple outline of how quantum wells and wires might be fabricated. 2D materials can be created by interfacing two dissimilar semiconductors resulting in a 2 dimensional electron gas (2DEG), which is a thin layer of highly mobile electrons that are free to move within a plane. Further etching of the material will leave a free standing strip of a quantum well material, where the electrons are confined along x-and z-axis (a quantum wire).

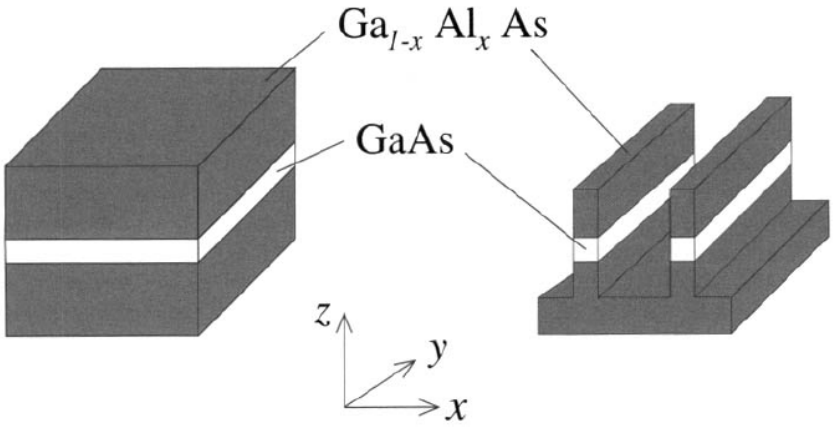

Figure 2.2: *Fabrication of quantum wires.[2]*

The resulting density of states for 2D and 1D are given by the following:

$$g_{2D}(E) = \frac{m^*}{\pi\hbar^2} \tag{2.6}$$

$$g_{1D}(E) = \frac{1}{\pi\hbar}\sqrt{\frac{m^*}{2E}} \tag{2.7}$$

If all dimensions of the box are decreased sufficiently in size, the electrons will lose their motional degree of freedoms in every direction and are not able to move like free particles. Beause there is no k-space to be filled with electrons and all available states exist only at discrete energies, the density of states for 0D is given by delta functions:

$$g_{0D}(E) = 2\sum_i \delta(E - E_i) \tag{2.8}$$

As previously mentioned, the size of the order of confinement is given by the de Broglie wavelength of the electrons $\lambda = h/2m^*E$. At these length scales quantum dots can be considered as artificial atoms, where the discrete energy levels are similar to the orbitals in a free atom. It turns out that an electron confined in a very small box of $L = 20$nm, has a ground state energy of only 1 meV, which is negligible at room temperature($\approx$ 23 meV). [3] To observe the quantum effects of quantum dots, temperature needs to be reduced and also the size of the structures need to be very small to increase the energy of the states $E \sim \frac{1}{L^2}$.

2.2 Lateral gate-defined semiconductor quantum dots

In this thesis we will be discussing quantum dots based on lateral semiconductor physics. In these devices electrons are trapped within a 2 dimensional plane and form a 2 dimensional electron gas (2DEG). Further confinement is achieved electrostatically by using gate

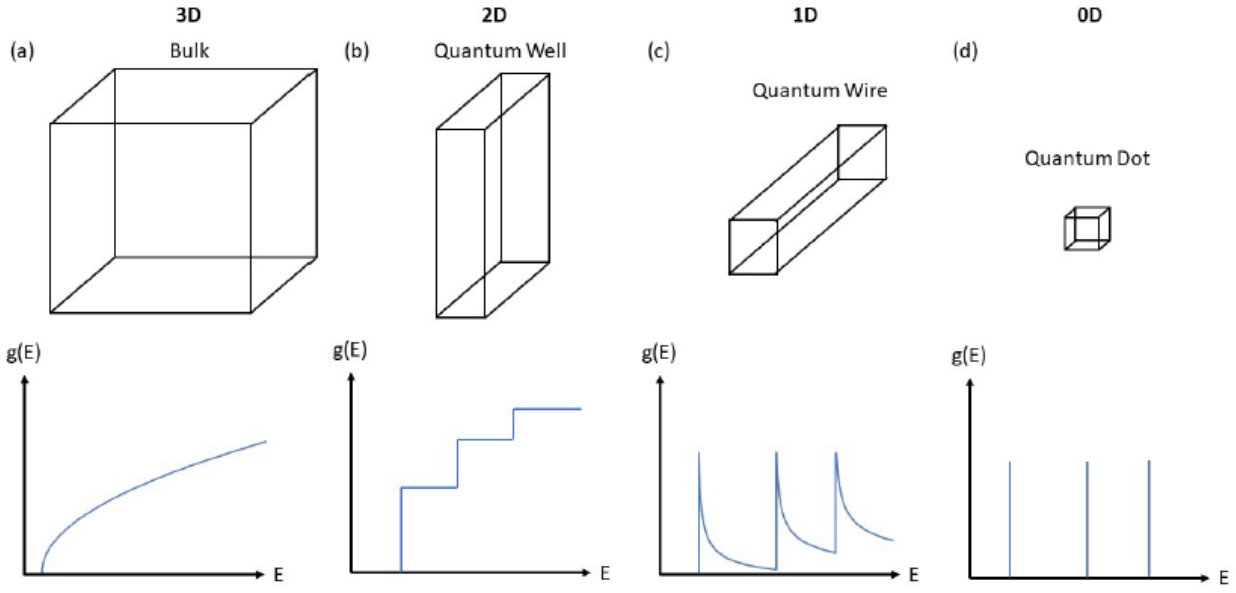

Figure 2.3: *Electron density of states $g(E)$ for different dimensions.*

voltages that induce electric fields which confine the movement of the electrons within the plane to a very small region, resulting in a quantum dot. A typical architecture of materials is the heterostructure of GaAs and AlGaAs which is grown using Molecular Beam Epitaxy, see fig. 2.4. The 2DEG is achieved by doping the AlGaAs layer with Si, which provide the free electrons. The conduction band can of the materials can be seen on the right. At the interface between the AlGaAs and GaAs layers, the dopants of AlGaAs are ransferred to GaAs and the Fermi-levels of the materials are matched which results in a sharp bending of their energy bands. The electrons are strongly confined in this electrical potential minimum along the z-direction (growth direction) in such a way that their movement in that direction can be neglected and thus a 2DEG is formed. The gate electrodes are then used to create a potential landscape which further confines the electrons in a small island within the 2DEG, called quantum dot. An example can be seen in figure 2.5 The quantum dots are connected to electron reservois via ohmic contacts (low-resistance leads). The electron ransport through the dots can be measured as a current which characterizes the electrical properties of the quantum dot. An addition of quantum point contacts (QPC) nearby the quantum dots can be used to measure the charge inside the quantum dot. This allows a non-distubing probing of the properties of the quantum dot.[5] It is also possible to farbricate coupled quantum dots, the first demonstration of a lateral double quantum dot (DQD) system was achieved by Ezlerman et al. (see fig. 2.5c) [6].

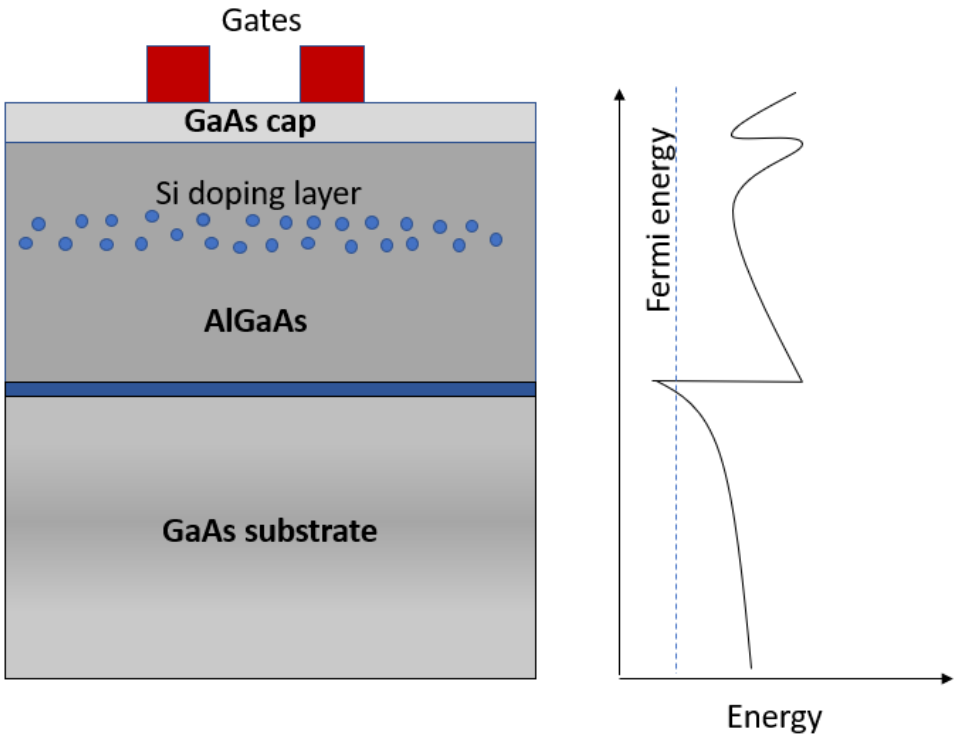

Figure 2.4: *Electron density of states $g(E)$ for different dimensions.*

2.3 Transport through Quantum Dots

2.3.1 Single Quantum Dot

It is useful to understand the framework that describes the classical view of electron transport in quantum dots. We will discuss the Constant Interaction (CI) model. In this model the quantum dot is considered as a metallic island with a self-capacitance C_{Dot} that is weakly coupled to a source and drain via tunnel barriers. This self-capicitance is given by the sum of the capcitances between the dot and the source, drain and gate: $C_{dot} = C_S + C_D + C_G$. We assume that the single-particle energy levels ψ_i (due to space confinement) are unaffected by the Coulomb interactions.

The charge induced on the quantum dot Q_{dot} by the electrostatic potentials V_i on the source and drain contacts and the gate is given by:

$$\begin{aligned} Q_{Dot} &= \sum C_i V_i \\ &= (V_{Dot} - V_S)C_S + (V_{Dot} - V_D)C_D + (V_{Dot} - V_G)C_G \end{aligned} \tag{2.9}$$

(2.10)

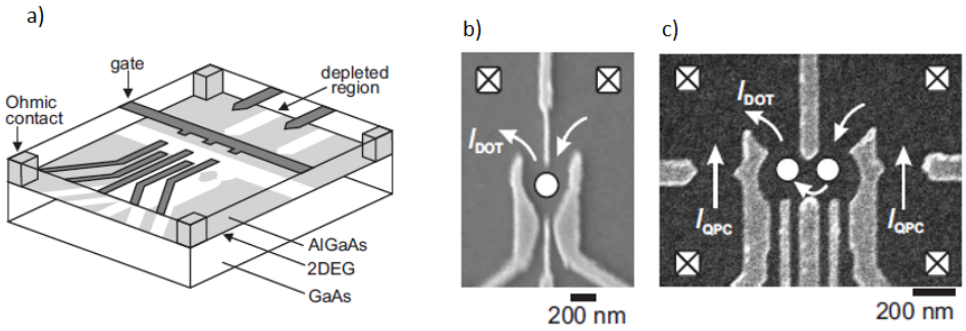

Figure 2.5: *a) Schematic view of a lateral gate defined quantum dot.[4] The 2DEG is formed between the AlGaAs an GaAs layers. Metal gates are used to control the potential of the dot and the number of electrons in it. b)-c) A scanning tunneling micrograph of a single quantum dot and a double quantum dot. The gate electrodes are light gray and the two white circles represent the locations of the dots. The electron occupancy can be measured with QPCs.*

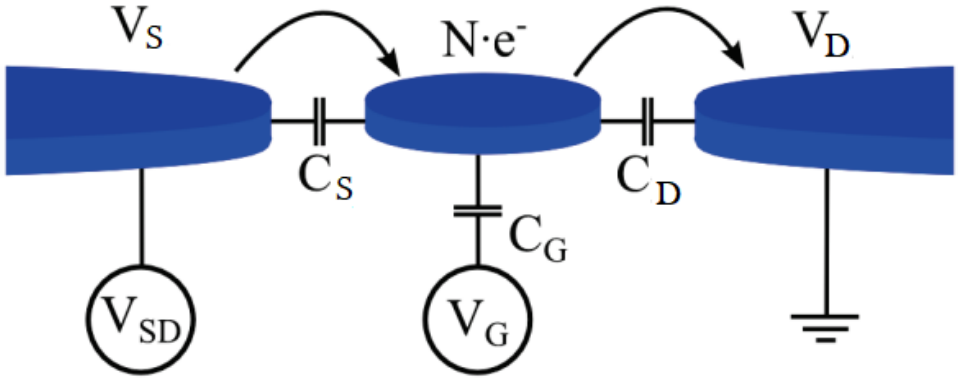

Figure 2.6: *Schematic drawing of the capacitance model of a quantum dot.[3]*

With a bit of rewriting:

$$Q_{Dot} + C_S V_S + C_D V_D + C_G V_G = C_{Dot} V_{Dot} \tag{2.11}$$

Due to charge quantization of electrons we can write the total charge as an integer number time the charge quantum $Q_{dot} = e^- N$. The energy of the dot is then given by (following ref [7]):

$$U(N) = \frac{(e^- N + C_S V_S + C_D V_D + C_G V_G)^2}{2C_{Dot}} + \sum_{i=1}^{N} \epsilon_i \tag{2.12}$$

where the last term is a sum over the occupied single-particle energy levels ϵ_i. Eq. 2.12 has a quadratic dependency on the voltages and occupation numbers. If we plot the energy

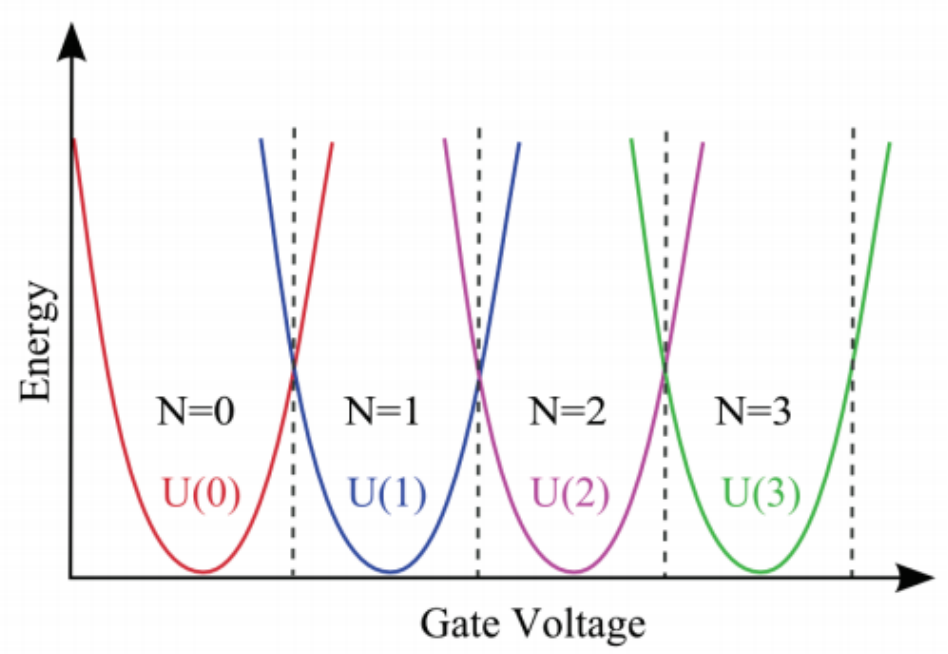

Figure 2.7: *Energy of the quantum dot for different values of electron occupation N[3]*

of the dot for multiple fixed electron numbers while varying one of the gate voltages, we obtain Fig. 2.7

On the lower end of the gate voltage value, the branch with zero electrons has minimal energy, thus the quantum dot is unoccupied. When the gate voltage is increased, a new branch will obtain the minimum energy and so it will be energetically favourable for an electron to occupy the dot. This way it is possible to sequentially fill the quantum dot with electrons. Since the dot is coupled to a reservoir (source and drain), it can always relax to the ground state by exchanging an electron with the reservoir, therefore it will always go to the branch with minimal energy. In this case it is useful to define a electrochemical potential $\mu(N)$ for the dot:

$$\begin{aligned}\mu(N) &\equiv U(N) - U(N-1) \\ &= \left(N - \frac{1}{2}\right) E_C + \frac{E_C}{e^-}\left(C_S V_S + C_D V_D + C_G V_G\right) + \epsilon_N \end{aligned} \tag{2.13}$$

where $E_C = e^2/C_{dot}$ is the charging energy. This equation can be interepreted as the amount of energy required to transition between the N-electron ground state and the $(N-1)$-electron ground state. The energy required to add an electron to the dot is given by the *addition energy*:

$$E_{add}(N) = \mu(N+1) - \mu(N) = E_C + \epsilon_{N+1} - \epsilon_N = E_C + \Delta E \tag{2.14}$$

The 2DEG is an electron reservoir with a chemical potential equal to its Fermi energy $\mu_S = \mu_D = \varepsilon_F$. The reservoir will therefore fill up the quantum dot with electrons until $\mu_{Dot}(N+1) > \epsilon_F$, this can be seen in Fig. 2.8a. The electron number is fixed at N.

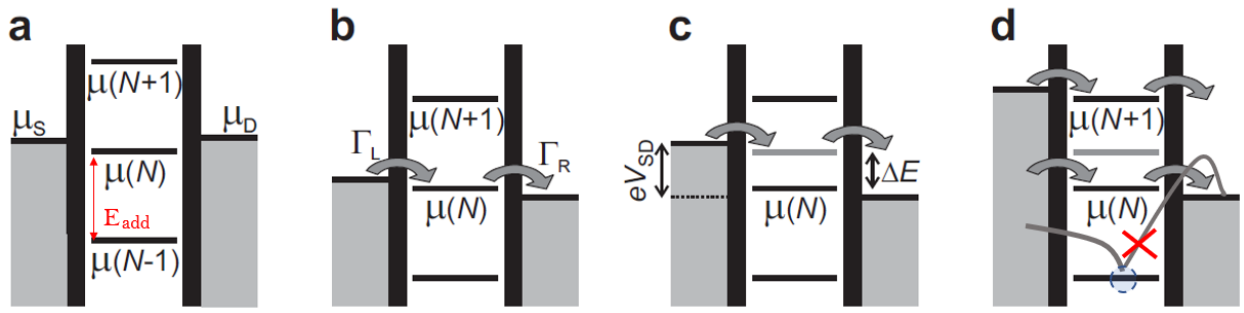

Figure 2.8: *[8]*

If the chemical potentials of the left and right reservoirs are not equal, then the quantum dot will mediate tunneling of an electron from the source to the drain. However this is only possible if the chemical potential of the dot is between the chemical potentials of the source and drain $\mu_S > \mu_{Dot}(N) > \mu_D$ as depicted in Fig. 2.8b, here the chemical potential of the dot has been changed with respect to the source/drain by chaging the gate voltage. An electron tunnels from the left reservoir into the quantum dot filling up the $\mu(N)$ state. Since the state in the source will be filled up again rapidly, this process is not reversible. The Fermi energy of the right reservoir is lower than the chemical potential of the quantum dot , so the electron can tunnel to an unoccupied state in the right reservoir, resulting in a transport of a single electron through the dot. The electron number will alternate between $N-1$ and N. The energy difference between the Fermi energies of the two reservoirs are called the bias windows $e^{-}V_{SD} = \mu_S - \mu_D$. As long as the chemical potential of the dot falls within this windows, electron transport is possible. It's also possible to increase the range of the bias windows, as depicted in Fig. 2.8c, here an electron is able to tunnel via the ground state but also an excited state. Fig. 2.8d shows an even bigger bias window, here the number of electrons alternate between $N-1$, N and $N+1$. Note that in all cases it is transport from the $N-1$ state to the right reservoir is blocked because the chemical potential of the dot is higher than the chemical potential of the right reservoir, this is also called the Coulomb blockade. In measurements one usually fixes V_{SD} and changes V_G. This way it is possible to control the number of electrons confined in a dot, by tuning V_G.

2.3.2 Double Quantum Dot

A double quantum dot can be understood similarly to the single quantum dot via the CI model.

The dots are modeled as a network of tunnel resistors and capacitors Fig. 2.9, where each dot is coupled by a capacitance to a gate voltage V_{gi}, $i = 1, 2$ and to the source and drain contct via a tunnel barrier represented by a tunnel resistor $R_{L(R)}$ and a capacitor $C_{(L(R)}$. The dots are also coupled to each other via a tunnel barrier represented by a tunnel resistor R_m and a capacito C_m. In this system one can define the electrochemical potentials $\mu_1(N1, N2)$ and $\mu_2(N1, N2)$, where N_1 and N_2 are the electron occupation numbers of dot

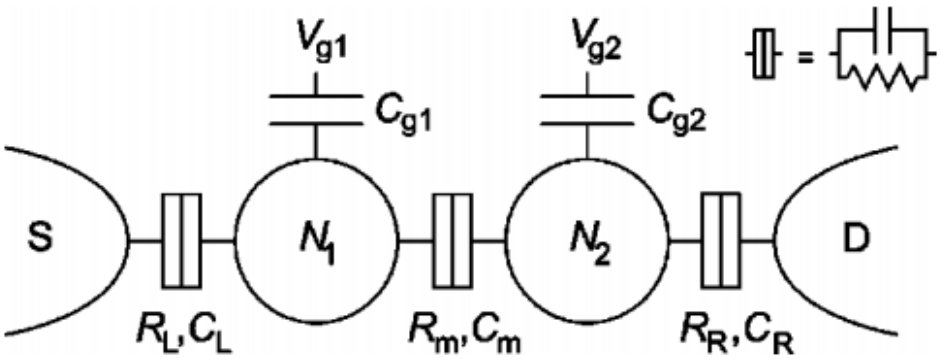

Figure 2.9: *Charge stability diagram as a function of gate voltages. Coupling the quantum dots through via a capacitance will skew the charge configuration lines[7]*

1 and 2 respectively as the following:

$$\mu_1(N_1,N_2) = U(N_1,N_2) - U(N_1-1,N_2) = \tag{2.15}$$
$$= (N_1 - 1/2)\,E_{C1} + N_2 E_{Cm} - (1/|e|)\,(C_{g1}V_{g1}E_{C1} + C_{g2}V_{g2}E_{Cm})$$
$$\mu_2(N_1,N_2) = U(N_1,N_2) - U(N_1,N_2-1) = \tag{2.16}$$
$$= (N_2 - 1/2)\,E_{C2} + N_1 E_{Cm} - (1/|e|)\,(C_{g1}V_{g1}E_{Cm} + C_{g2}V_{g2}E_{C2})$$

where E_{Ci} are the addition energies of the dots. E_{CM} is the change in energy generated on one dot when an extra electron is added or removed from the other one. The capacitive coupling between the dots results in a change of the electrostatic energy of one dot due to the addition of an electron to the other dot. From the chemical potentials in Eqs. 2.15 and 2.16 one can construct a charge stability diagram Fig. 2.10. Similarly to a single dot, by varying the gate voltages of the dots it is possible to control the electron occupations of the dots. The diagram is constructed by denoting the electron combination numbers (N_1, N_2) in the phase space of the gate voltages (V_{g1}, V_{g2}). This diagram gives the equilibrium electron occupation numbers N_1 and N_2 as a function of the gate voltages V_{g1} and V_{g2}.

One can define the electrochemical potentials of the left and right reservoirs to be zero if no bias voltage is applied $\mu_L = \mu_R = 0$. If the chemical potentials $\mu_1(N_1, N_2)$ and $\mu_2(N_1, N_2)$ are less than zero but $\mu_1(N_1 + 1, N_2)$ and $\mu(N_1, N_2 + 1)$ are larger than zero, then the charge configuration (N_1, N_2) is the equilibrium situation. Otherwise electrons are able to escape to the reservoirs. This contraint, and the fact that N_1 an N_2 are integers, results into the hexagonal domains in the charge stability diagram. Fig. 2.10a shows the diagram if the dots are not coupled ($C_M = 0$). In this case the change of the gate voltage $V_{g1(2)}$ changes the charge on one dot but does not affect the charge on the other dot. If there is a finite coupling, ($C_M \neq 0$), then the domains become hexagonal (Fig.2.10b). This diagram can be used to identify the double quantum dot charge configuration and shows us how to move between different charge configurations.[9]

The regime of the charge stability diagram we will be discussing is the two-electron regime, where the occupancy of the double dot can be (0,2), (1,1), or (2,0).

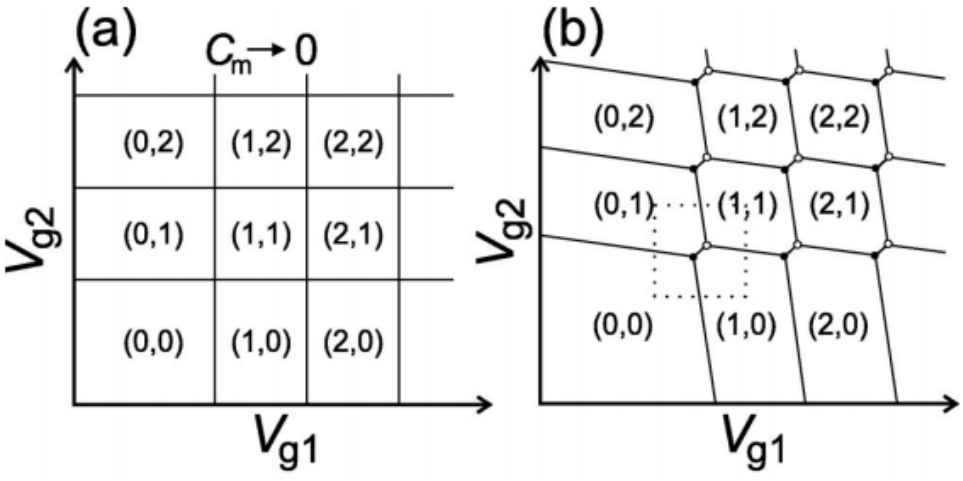

Figure 2.10: *Capacitance model of the coupled quantum dots [7]*

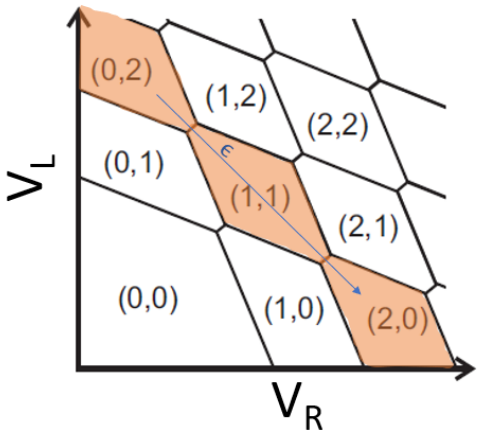

Figure 2.11: *Charge stability diagram of a double quantum dot as a function of the gate voltages. The detuning ϵ is defined as the axis along the (0,2), (1,1) and (2,0) regime of the diagram.[4]*

The levels of the two dots are controlled by the gate voltages V_L and V_R. The *detuning* $\epsilon = |e|(V_L - V_R)$ denotes how the levels in the two dots are detuned with respect to eachother and determines the charge state along the two-electron regimes.

The electrons can be separated by changing the potential energy of the two dots, while making exchange between the dots possible via a tunnel barrier. As the detuning changes, the energy levels of the two dots with respect to each other shifts and changes the ground-state of the configuration. Tunneling between the dots will result in change of configuration from two electrons in one dot to one electron in each dot (Fig. 2.12).

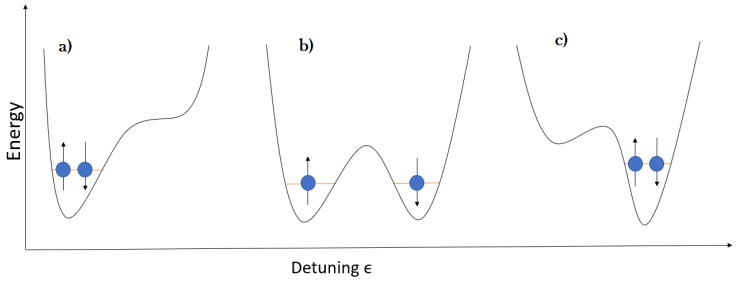

Figure 2.12: *Schematic of the double dot potential along the detuning axis. (a), (b) and (c) show the elctrostatic potential along the x-axis for decreasing ϵ from the left to the right.*

2.4 Spin states in quantum dots

One of the early experimental evidence for the existence of electron spin came from the Stern-Gerlach experiment, performed in 1922. They found that an electron passing through a magnetic field will be deflected in one of two possible directions. (Historically they observed that silver atoms had two possible discrete angular momenta despite having no orbital angular momentum). This could be explained by an intrinsic magnetic moment being carried by the electron. A simple physical interpretation of this was suggested in 1925 by George Uhlenbeck and Samuel Goudsmit at Leiden University: a particle spinning around its own axis, hence this intrinsic magnetic moment is coined "spin". The interaction of a particle carrying a magnetic moment, $\boldsymbol{\mu}$ with a magnetic field $\mathbf{B}$ is described by the hamiltonian

$$H = -\boldsymbol{\mu} \cdot \mathbf{B} \tag{2.17}$$

where the minus indicates that it is energetically favorable for a magnetic dipole to be aligned along the direction of the magnetic field. The magnetic moment of a electron due to its spin is given by:

$$\boldsymbol{\mu}_e = g_e \frac{\mu_B}{\hbar} \mathbf{S} = g_e \frac{e}{2m_e} \mathbf{S} \tag{2.18}$$

where $\mathbf{S}$ is the spin quantum number, m_e and e respectively the mass and charge of the electron, μ_B is the bohr magneton and g_e is the *g-factor* which arises due to relativistic effects and relates the observed magnetic moment of the electron to its spin quantum number. The value g_e is approximately equal to 2 and is in excellent agreement with experiments. [10]

The spin $\mathbf{S}$ of an electron is a quantum mechanical observable similar to the quantum mechanical angular momentum $\mathbf{L}$ and thus it follows the same rules. It is represented by the operators $\hat{S}^2 = \hat{S}_x^2 + \hat{S}_y^2 + \hat{S}_z^2$. Where $\hat{S}_i$ are the projections of the spin onto the Cartesian axes. Analogous to the quantum number l, we can introduce a spin quantum number s, thus the multiplicity of the spin component in a given direction is $(2s + 1)$. For fermions, e.g. electrons, the spin value is $s = 1/2$ which means that the multiplicity of the spin operators are 2. When referring to the spin state of an electron, what is usually meant

is the eigenstates of the $\hat{S}_z$ operator, corresponding to its two eigenvalues $\hbar/2$ and $-\hbar/2$ ($m\hbar$ with $m = -s, -s+1 \ldots, s = -1/2, 1/2$). These eigenstates are called the spin down and spin up states and are also represented by $|\downarrow\rangle$ and $|\uparrow\rangle$.

In the most simple case, a quantum dot containing just a single electron being subject to a static external magnetic field B, the spin results into splitting of the orbitals into Zeeman doublets [6] (more detailed analysis is given in section ...). Where the ground state is given by the by state of the electron spin pointing up $|\uparrow\rangle$ and the excited state is given by the electron spin pointing down $|\downarrow\rangle$. The difference in energy between the two states $E_\uparrow$ and $E_\downarrow$ is given by the Zeeman energy: $\Delta E = E_\downarrow - E_\uparrow = g\mu_B B$. Loss et al. proposed in 1998 [11] to use the spin property of electrons as the qubit states $|0\rangle \equiv |\uparrow\rangle$ and $|1\rangle \equiv |\downarrow\rangle$. Oscillating magnetic fields can be used that couples to the magnetic momentum of the electron which can alter the spin state. This mechanism can be used to create one-qubit gates required for universality.

2.4.1 Two-electron spin states

The two-electron spin operator is simply the sum of the operators of each spin $\mathbf{S} = \mathbf{S}_1 + \mathbf{S}_2$ and $\hat{S}^2 = \hat{S}_1^2 + \hat{S}_2^2$. Each electron can have spin up or spin down, so there are four possible spin configurations $\uparrow\uparrow$, $\uparrow\downarrow$, $\downarrow\uparrow$, $\downarrow\downarrow$. Since electrons are fermions, the complete two-electron state $\Psi = \chi(s_1, s_2)\psi(\mathbf{r_1}, \mathbf{r_2})$ (consisting of spin $\chi(s_1, s_2)$ and the spatial part (orbitals) $\psi(\mathbf{r_1}, \mathbf{r_2})$) has to be anti-symmetric under exchange of the particle variables. This means in the case that the spatial part is anti-symmetric, the spin state must be symmetric and if the spatial is symmetric, the spin part must be anti-symmetric. The eigenstates of the two-electron spin operators are given by the anti-symmetric so-called singlet state that has total spin $s = 0$ and $m = 0$,

$$\chi(s_1, s_2) = |S\rangle = \frac{1}{\sqrt{2}}(|\uparrow\rangle_1 \otimes |\downarrow\rangle_2 - |\downarrow\rangle_1 \otimes |\uparrow\rangle_2) = \frac{1}{\sqrt{2}}(|\uparrow\downarrow\rangle - |\downarrow\uparrow\rangle) \tag{2.19}$$

and the three symmetric triplet states,

$$\begin{aligned} |T_-\rangle &= |\downarrow\downarrow\rangle \\ |T_0\rangle &= \frac{1}{\sqrt{2}}(|\uparrow\downarrow\rangle + |\downarrow\uparrow\rangle) \\ |T_+\rangle &= |\uparrow\uparrow\rangle \end{aligned} \tag{2.20}$$

that have total spin $s = 1$. The states $|T_\pm\rangle$ have the quantum number $m = \pm 1$ (corresponding to the z component of the spin) and the state $|T_0\rangle$ has $m = 0$. The complete

wavefunctions are given by:

$$\begin{aligned}\Psi_S =& \frac{|\uparrow\downarrow\rangle - |\downarrow\uparrow\rangle}{\sqrt{2}} \otimes \psi_{\mathrm{S}}(\mathbf{r}_1, \mathbf{r}_2) \\ \Psi_{T_0} =& \frac{|\uparrow\downarrow\rangle + |\downarrow\uparrow\rangle}{\sqrt{2}} \otimes \psi_{\mathrm{AS}}(\mathbf{r}_1, \mathbf{r}_2) \\ \Psi_{T_+} =& |\uparrow\uparrow\rangle \otimes \psi_{\mathrm{AS}}(\mathbf{r}_1, \mathbf{r}_2) \\ \Psi_{T_-} =& |\downarrow\downarrow\rangle \otimes \psi_{\mathrm{AS}}(\mathbf{r}_1, \mathbf{r}_2)\end{aligned} \tag{2.21}$$

Where $\psi_{(A)S}(\mathbf{r}_1, \mathbf{r}_2)$ stands for the (anti-)symmetric combination of the right and left orbital envelopes $\Psi_R(\mathbf{r})$ and $\Psi_L(\mathbf{r})$.[12]

$$\begin{aligned}\psi_{\mathrm{S}}(\mathbf{r}_1, \mathbf{r}_2) &= \frac{\lambda_S}{\sqrt{2}} \left(\Psi_L(\mathbf{r}_1)\Psi_R(\mathbf{r}_2) + \Psi_R(\mathbf{r}_1)\Psi_L(\mathbf{r}_2)\right) \\ \psi_{\mathrm{AS}}(\mathbf{r}_1, \mathbf{r}_2) &= \frac{\lambda_{AS}}{\sqrt{2}} \left(\Psi_L(\mathbf{r}_1)\Psi_R(\mathbf{r}_2) - \Psi_R(\mathbf{r}_1)\Psi_L(\mathbf{r}_2)\right)\end{aligned} \tag{2.22}$$

where $\lambda_{(A)S}$ are normalization factors. The symmetrization requirement of the wave function results in the so-called exchange force, which is not a real force, but rather a purely geometrical consequence of the symmetrization requirement.[13] This exchange interaction results in an effective attractive force between bosons and an effective repulsive force between fermions. When the electrons are in the singlet state, having a symmetrical spatial wave function, they effectively behave as bosons and the exchange interaction causes an attraction between the electrons. In the triplet state, having an anti-symmetrical spatial wave function, the exchange interaction results in an effective repulsive force between the electrons. The difference in the energy of the triplet $|T_0\rangle$ and singlet $|S\rangle$ is called the exchange energy J.[14]

2.4.2 Hamiltonian model

The Hamiltonian of the double quantum dots is described by the Hubbard model. This model was introduced as a simple approximation of interacting particles in a lattice with only two terms in the Hamiltonian, the on-site interaction (Coulomb interaction) energy U and a tunneling term t. Other effects such as the Zeeman-splitting and quantum effects can be readily accomodated in the generalized Hubbard model, making it a suitable model for the spin physics in quantum dots.[15] We will consider only the low energy states in the (1,1) charge regime $|\uparrow,\uparrow\rangle$, $|\downarrow,\uparrow\rangle$, $|\uparrow,\downarrow\rangle$, $|\uparrow,\uparrow\rangle$, and the states in the singlet states in the (2,0) and (0,2) charge regime $|S(2,0)\rangle = |S,0\rangle$, $|S(0,2)\rangle = |0,S\rangle$. The triplet states in the (0,2) and (2,0) charge regime are much higher in energy and will be neglected. [4]

The two-electron double dot Hamiltonian is given by the following:

$$\hat{H} = \hat{H}_\epsilon + \hat{H}_t + \hat{H}_U + \hat{H}_Z \tag{2.23}$$

Here $\hat{H}_\epsilon$ is the detuning term, describing the gate-controlled energy shift ϵ of the dots with respect to each other. $\hat{H}_t$ describes the hopping (tunneling) term of the electrons from

one dot to the other. The third term $\hat{H}_U$ accounts for the on-site interaction (Coulomb interaction). The last term $\hat{H}_Z$ describes the Zeeman coupling when external magnetic fields are introduced. The Hamiltonian terms are:

$$\hat{H}_\epsilon = -\epsilon \sum_{i,\sigma} c^\dagger_{i\sigma} c_{i\sigma} \tag{2.24}$$

$$\hat{H}_t = t \sum_{i,j,\sigma} c^\dagger_{i\sigma} c_{j\sigma}, \quad \text{where } i \neq j \tag{2.25}$$

$$\hat{H}_U = \sum_i U_i n_{i\uparrow} n_{i\downarrow} \tag{2.26}$$

$$\hat{H}_Z = \sum_i \frac{E_{zi}}{2} (n_{i\uparrow} - n_{i\downarrow}) \tag{2.27}$$

where $c^\dagger_{i\sigma}$ and $c_{i\sigma}$ are the creation and annihilation operators respectively, where $i = 1, 2$ and $\sigma = \uparrow, \downarrow$ indicate the index of the dot and the spin respectively. The operators obey the canonical fermion commutation rules,

$$c^\dagger_{i\alpha} c_{j\beta} + c_{j\beta} c^\dagger_{i\alpha} = \delta_{i,j}\delta_{\alpha,\beta}, \quad c^\dagger_{i\alpha} c^\dagger_{i\alpha} = 0, \quad c^\dagger_{i\alpha} c^\dagger_{j\beta} = -c^\dagger_{j\beta} c^\dagger_{i\alpha} \tag{2.28}$$

The number operators $n_{i\sigma} \equiv c^\dagger_{i\sigma} c_{i\sigma}$ gives the number of electrons in dot i with spin σ. The term E_{zi} describes the Zeeman energy dot i and is proportional to the magnetic field $E_{zi} = g\mu_B B_i$. This can be different for each dot due to inhomogeneity of the magnetic field. In the basis $\{|\downarrow,\downarrow\rangle, |\downarrow,\uparrow\rangle, |\uparrow,\downarrow\rangle, |\uparrow,\uparrow\rangle, |S,0\rangle, |0,S\rangle\}$ the Hamiltonian reads:

$$\hat{H} = \begin{pmatrix} -\bar{E}_z & 0 & 0 & 0 & 0 & 0 \\ 0 & -\Delta E_z & 0 & 0 & t & t \\ 0 & 0 & \Delta E_z & 0 & -t & -t \\ 0 & 0 & 0 & \bar{E}_z & 0 & 0 \\ 0 & t & -t & 0 & U_1 + \epsilon & 0 \\ 0 & t & -t & 0 & 0 & U_2 - \epsilon \end{pmatrix} \tag{2.29}$$

Where $\bar{E}_z = (E_{z1} + E_{z2})/2$ is the average Zeeman energy of the dots and $\Delta E_z = (E_{z1} - E_{z2})/2$ is the difference in Zeeman energy between the dots. We also define $|S(1,1)\rangle = \frac{1}{\sqrt{2}}(|\uparrow,\downarrow\rangle - |\downarrow,\uparrow\rangle)$ and $|T_0(1,1)\rangle = \frac{1}{\sqrt{2}}(|\uparrow,\downarrow\rangle + |\downarrow,\uparrow\rangle)$ with one electron in each dot. If we consider only the singlet state $|S(2,0)\rangle$ and the singlet state in the (1,1) configurationl $|S(1,1)\rangle$ we obtain after projection:

$$\hat{H}_{singlet} = \begin{pmatrix} 0 & t \\ t & \epsilon \end{pmatrix} \tag{2.30}$$

Here we set the charging energy $U_1 = 0$ and the magnetic field $B_1 = 0$ as these will result in nothing more than a shift in the energies. We see that at $\epsilon = 0$ the singlet states between the (1,1) and (2,0) charge regime are degenerate and the new eigenstates are symmetric

and anti-symmetric superpositions of the two singlet states with a splitting of $2t$. This results in a hybridization of the states and electron exchange is possible. The eigenvalues (energies) of the matrix can be found by diagonalizing the matrix : $E_{\pm} = \frac{\epsilon \pm \sqrt{\epsilon^2 + 4t^2}}{2}$

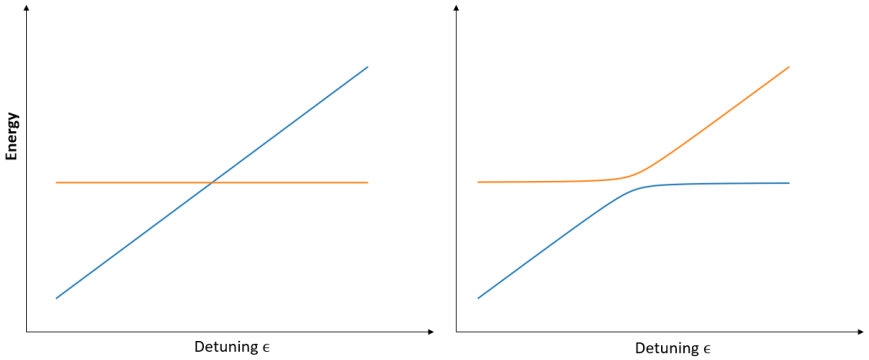

Figure 2.13: *The left plot shows the eigenvalues of the hamiltonian as a function of the detuning for $t = 0$. The right plot shows the eigenvalues for $t = 100$, the states hybridize and exchange is possible*

For a complete understanding of the spin states, the eigenvalues of the full Hamiltonian are plotted against the detuning ϵ to obtain the energy dispersion of the double dot system. in Fig. 2.15. For zero magnetic fields and no tunnel coupling, the states have a linear dispersion relation and the ground state changes from singlet with both electrons in the left dot (2,0) to the configuration (1,1) where the triplet $\uparrow\uparrow$, $\downarrow\downarrow$ and the anti-parallel states are degenerate, to the singlet with the (0,2) configuration. The width of the split region is given by the charging energies U_1 and U_2, in this example both chosen $U_1 = U_2 = 1000$ (Fig. 2.15a). A finite magnetic field introduces the Zeeman energies E_{z1} and E_{z2} and results in a lifting of the degeneracy of the triplet states and the anti-parallel states (Fig. 2.15b). The sign of the Lande factor determines whether the spin up or spin down is lower in energy and shifts the triplet $T_{\_}$ and T_+ states accordingly, in this case T_+ is shifted down while $T_{\_}$ is shifted up the singlet branch. Due to the inhomogeneity of the magnetic field, the degeneracy of the anti-parallel is also lifted. Finally when a tunnel-coupling is introduced as in Fig. 2.15c, we see that the anti-parrallel states are shifted down in energy as ϵ moves away from zero. This can be understood if we write the anti-parallel state as:

$$
\begin{aligned}
|\uparrow,\downarrow\rangle &= \frac{1}{\sqrt{2}}(|S(1,1)\rangle + |T_0(1,1)\rangle) \\
|\downarrow,\uparrow\rangle &= \frac{1}{\sqrt{2}}(|T_0(1,1)\rangle - |S(1,1)\rangle)
\end{aligned}
\tag{2.31}
$$

Because the anti-parallel states have a $|S(1,1)\rangle$ component and as we've seen before the $|S(1,1)\rangle$ state has an avoided crossing with the $|S(2,0)\rangle$ and $|S(0,2)\rangle$ states, there is an anti-crossing between the (1,1) anti-parallel states and the singlets $|S(0,2)\rangle$ and $|S(2,0)\rangle$. The decrease of the energy of the anti-parallel states is denoted by $J(\epsilon)/2$, where $J(\epsilon)$ is

the exchange coupling of the two electron spins (Fig.2.14). This controllable exchange interaction $J(\epsilon)$ will serve as the basis for generating two-qubit gate operations.

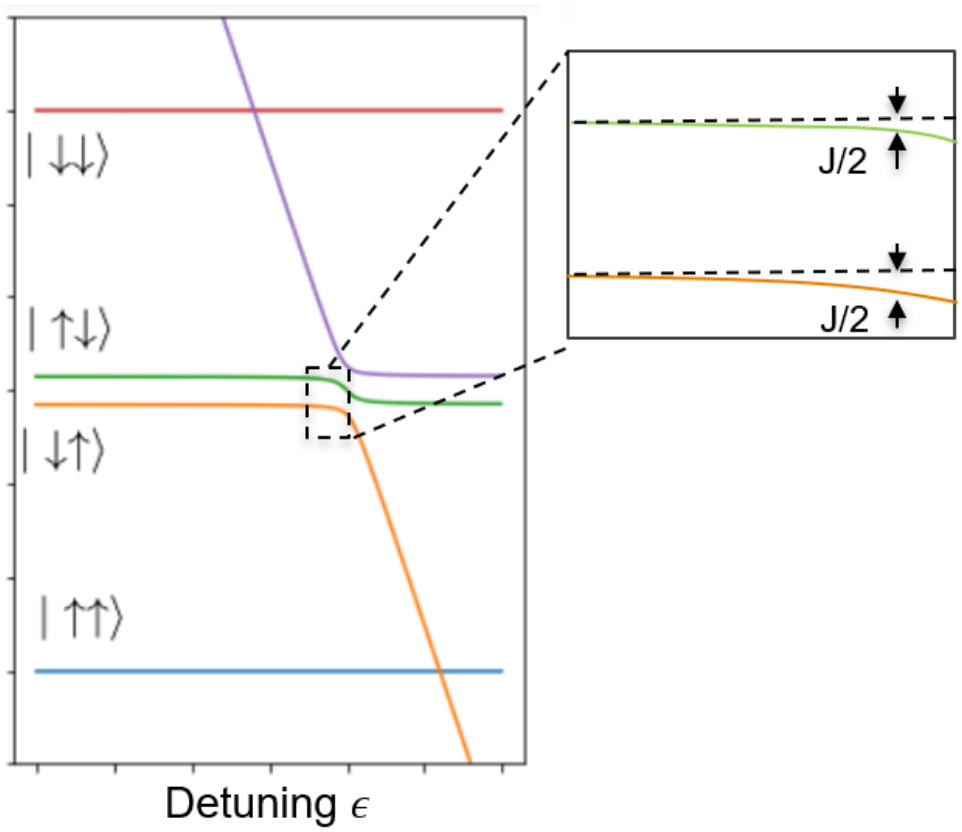

Figure 2.14: *Energy dispersion of the double dot system as a functino of the detuning ϵ. At high detuning the energies of the anti-parallel spin states are dereased by the exchange interaction $J(\epsilon)$.*

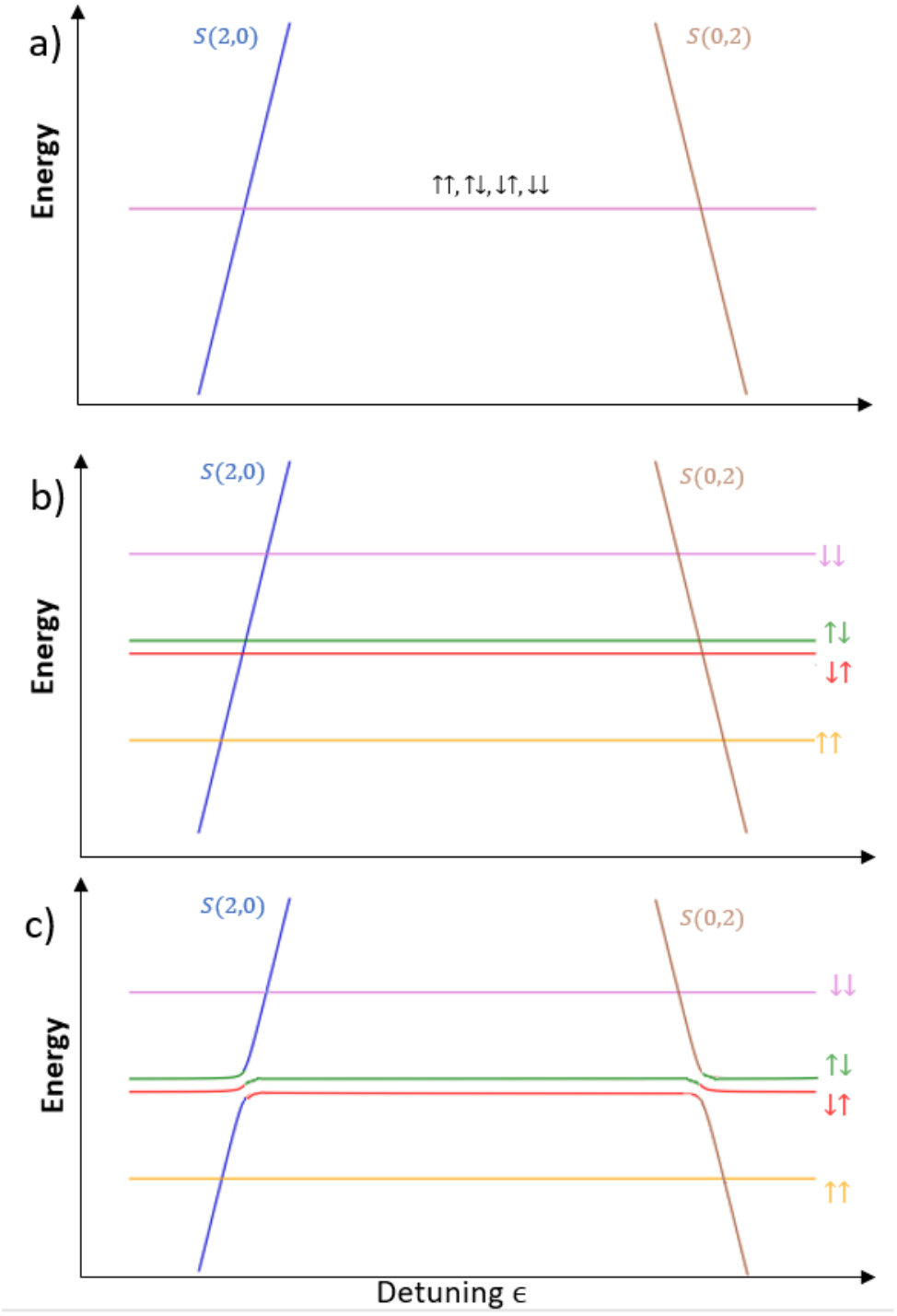

Figure 2.15: *The energy dispersion of the double dot Hamiltonian for different values of magnetic fields and tunnel-coupling.* ***a)*** *Uncoupled Hamiltonian with $B_1 = B_2 = 0$ and $t = 0$.* ***b)*** *Uncoupled Hamiltonian with $B_1 = B_2 \neq 0$ and $t = 0$.* ***c)*** *Coupled Hamiltonian with finite magnetc fields and tunnel-coupling.*

Chapter 3

Spin Qubit Control for Quantum Computation

3.1 Quantum computation

A qubit is a quantum mechanical two-level system spanned by the states $|0\rangle$ and $|1\rangle$. It can be realized either by a true two-level system (like the polarization angles of a photon, or the spin of an electron) or a system in which there are two states (usually the ground state and first excited state) that are seperable in energy from the rest of the eigenstates of the system or in some way decoupled from them. For example consider an electron moving in the potential from the nucleus of an atom. The eigenstates are given by $\Psi_n(x,t) = \Psi_n(x)e^{-iE_nt/\hbar}$ and satisfy the time-independent Schrödinger equation

$$\hat{H}\Psi_n(x) = E_n\Psi_n(x) \tag{3.1}$$

Where the solutions are the different atomic orbitals ($1s, 2p, 3d, \dots$). Another well known system is the quantum harmonic oscillator where the states are related to Hermite polynomials with corresponding energy levels: $E_n = \hbar\omega\Big(n + \frac{1}{2}\Big), n = 0, 1, 2, 3, \dots$

A more simpler model is the one-dimensional particle in a box of size L, where the states are given by:

$$\Psi_n(x) = \sqrt{\frac{2}{L}}\sin\Big(\frac{n\pi x}{L}\Big), \quad E_n = \frac{n^2\hbar^2\pi^2}{2mL^2}, \quad n = 1, 2, 3, \dots \tag{3.2}$$

Then to limit the dynamics of the system to the ground state Ψ_0 and first excited state Ψ_1, so that only transitions between these two states is possible. Besides spin qubits, there are many other realizations for qubits, for example superconducting qubits[16] and atoms and ions[17]. In general the state of a two-level system can be written by a wavefunction:

$$\Psi(x,t) = c_0(t)\Psi_0(x) + c_1(t)\Psi_1(x) \tag{3.3}$$

The dynamics of the system is determined by the time-dependent coefficients $c_0(t)$ and $c_1(t)$ and the probability of finding the particle in a state Ψ_i is simply $P_i(t) = |c_i(t)|^2$. To induce transitions between the two states we need to change the Hamiltonian. We assume that this time-dependent hamiltonian is a transformation that leaves the states in the space spanned by Ψ_0 and Ψ_1 (so it doesn't transition to some other states). Given that the states are orthonormal:

$$\int dx|\Psi_0(x)|^2 = \int dx|\Psi_1(x)|^2 = 1, \quad \int dx\Psi_0^*(x)\Psi_1(x) = 0 \tag{3.4}$$

We can find a general time-dependent hamiltonian $\hat{H}(t)$ that can be written in the form:

$$\begin{aligned}&\hat{H}(t)\Psi(x,t) = \hat{H}(t)\left[c_0(t)\Psi_0(x) + c_1(t)\Psi_1(x)\right] = \\ =&c_0(t)\hat{H}(t)\Psi_0(x) + c_1(t)\hat{H}(t)\Psi_1(x) = \\ &c_0(t)\left[h_{00}(t)\Psi_0(x) + h_{10}(t)\Psi_1(x)\right] + c_1(t)\left[h_{01}(t)\Psi_0(x) + h_{11}(t)\Psi_1(x)\right]\end{aligned}$$

where

$$\begin{aligned}h_{00}(t) &= \int dx\Psi_0^*(x)\hat{H}(t)\Psi_0(x) \\ h_{10}(t) &= \int dx\Psi_1^*(x)\hat{H}(t)\Psi_0(x) \\ h_{11}(t) &= \int dx\Psi_1^*(x)\hat{H}(t)\Psi_1(x) \\ h_{01}(t) &= \int dx\Psi_0^*(x)\hat{H}(t)\Psi_1(x)\end{aligned}$$

3.1.1 Qubit formalism

In general the time-dependent state of a qubit is given by:

$$|\Psi(t)\rangle = c_0(t)|0\rangle + c_1(t)|1\rangle \tag{3.5}$$

where $c_i(t)$ are time-dependent complex functions. This state is normalized so $|c_0(t)|^2 + |c_1(t)|^2 = 1$ and it satisfies the Schrödinger equation

$$i\hbar\frac{\partial}{\partial t}|\Psi(t)\rangle = \hat{H}(t)|\Psi(t)\rangle \tag{3.6}$$

where

$$\hat{H}(t) = h_{00}(t)|0\rangle\langle 0| + h_{01}(t)|0\rangle\langle 1| + h_{10}(t)|1\rangle\langle 0| + h_{11}(t)|1\rangle\langle 1| \tag{3.7}$$

is the time-dependent Hamiltonian operator.

The qubit states obey the following relations:

$$\begin{array}{ll} \langle 0|0\rangle = \langle 1|1\rangle = 1 & \text{normalization} \\ \langle 0|1\rangle = \langle 1|0\rangle = 0 & \text{orthogonality} \\ |0\rangle\langle 0| + |1\rangle\langle 1| = \hat{1} & \text{completeness} \end{array} \tag{3.8}$$

We can label our basis states with vectors in the following way:

$$|0\rangle = \begin{pmatrix} 1 \\ 0 \end{pmatrix} \quad \langle 0| = (10) \tag{3.9}$$

$$|1\rangle = \begin{pmatrix} 0 \\ 1 \end{pmatrix} \quad \langle 1| = (01) \tag{3.10}$$

$$|0\rangle\langle 0| = \begin{pmatrix} 1 & 0 \\ 0 & 0 \end{pmatrix} \quad |0\rangle\langle 1| = \begin{pmatrix} 0 & 1 \\ 0 & 0 \end{pmatrix} \tag{3.11}$$

$$|1\rangle\langle 0| = \begin{pmatrix} 0 & 0 \\ 1 & 0 \end{pmatrix} \quad |1\rangle\langle 1| = \begin{pmatrix} 0 & 0 \\ 0 & 1 \end{pmatrix} \tag{3.12}$$

The Schrödinger equation in this basis is given by:

$$i\hbar \begin{pmatrix} \dot{c}_0(t) \\ \dot{c}_1(t) \end{pmatrix} = \begin{pmatrix} h_{00}(t) & h_{01}(t) \\ h_{10}(t) & h_{11}(t) \end{pmatrix} \begin{pmatrix} c_0(t) \\ c_1(t) \end{pmatrix} \tag{3.13}$$

3.1.2 Bloch sphere

A general qubit state $|\psi\rangle$ can be written as

$$|\psi\rangle = c_0\,|0\rangle + c_1\,|1\rangle \tag{3.14}$$

where c_0 and c_1 are complex values numbers satisfying the normalization condition $|c_o|^2 + |c_1|^2 = 1$. Using Euler's formula we can write the complex numbers in polar form:

$$c_0 = r_0 e^{i\phi_0} \quad \text{and} \quad c_1 = r_1 e^{i\phi_1} \tag{3.15}$$

Multiplying a state with a complex number, does not change the physical state, i.e. $|\psi\rangle \to \lambda\,|\psi\rangle$. Choosing $\lambda = e^{-i\phi_0}$ then our equivalent state is:

$$e^{-i\phi_0}\,|\psi\rangle = e^{-i\phi_0} \cdot \left(r_0 e^{i\phi_0}|0\rangle + r_1 e^{i\phi_1}|1\rangle\right) = r_0\,|0\rangle + r_1 e^{i(\phi_1-\phi_0)}\,|1\rangle \tag{3.16}$$

This means that we are interested in the relative phase $\phi = \phi_1 - \phi_0$ between the two states and not their absolute phases. Using the normalization condition we obtain $r_0^2 + r_1^2 = 1$, this reduces the degree of freedom to 2. Setting $r_0 = \cos\theta$ and $r_1 = \sin\theta$ we obtain an equivalent representation of $|\psi\rangle$

$$|\psi\rangle = \cos\theta\,|0\rangle + e^{i\phi}\sin\theta\,|1\rangle \tag{3.17}$$

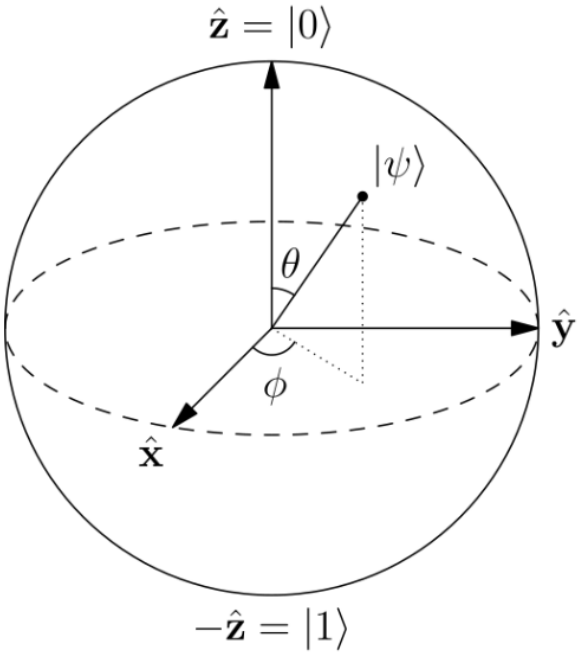

Figure 3.1: *The bloch sphere representation*

This representation can be visualized by the Bloch sphere, which is a unit 2-sphere. Due to the symmetry, any state can be written as:

$$|\psi(\theta,\phi)\rangle = \cos\frac{\theta}{2}|0\rangle + e^{i\phi}\sin\frac{\theta}{2}|1\rangle \tag{3.18}$$

where θ and ϕ are such that they cover the whole sphere without periodicity; $\theta \in [0,\pi)$ and $\phi \in [0,2\pi)$. Rotation of a qubit state around the axes for an angle α are given in terms of the pauli matrices:

$$\sigma_x = \begin{pmatrix} 0 & 1 \\ 1 & 0 \end{pmatrix}, \quad \sigma_y = \begin{pmatrix} 0 & -i \\ i & 0 \end{pmatrix}, \quad ,\sigma_z = \begin{pmatrix} 1 & 0 \\ 0 & -1 \end{pmatrix} \tag{3.19}$$

Rotations of the qubit state around the axes can be performed with the following transformations:

$$R_x(\alpha) = e^{-i\frac{\alpha}{2}\sigma_x} = \cos\frac{\alpha}{2}\mathbb{I} - i\sin\frac{\alpha}{2}\sigma_x = \begin{pmatrix} \cos\frac{\alpha}{2} & -i\sin\frac{\alpha}{2} \\ -i\sin\frac{\alpha}{2} & \cos\frac{\alpha}{2} \end{pmatrix} \tag{3.20}$$

$$R_y(\alpha) = e^{-i\frac{\alpha}{2}\sigma_y} = \cos\frac{\alpha}{2}\mathbb{I} - i\sin\frac{\alpha}{2}\sigma_y = \begin{pmatrix} \cos\frac{\alpha}{2} & -\sin\frac{\alpha}{2} \\ \sin\frac{\alpha}{2} & \cos\frac{\alpha}{2} \end{pmatrix} \tag{3.21}$$

$$R_z(\alpha) = e^{-i\frac{\alpha}{2}\sigma_z} = \cos\frac{\alpha}{2}\mathbb{I} - i\sin\frac{\alpha}{2}\sigma_z = \begin{pmatrix} e^{-i\alpha/2} & 0 \\ 0 & e^{i\alpha/2} \end{pmatrix} \tag{3.22}$$

Using spherical coordinates we can define a unit Bloch vector

$$\mathbf{r} = (\cos\phi\cos\theta, \sin\phi\sin\theta, \cos\theta) \tag{3.23}$$

Now we see that the expectation values of the Pauli matrices $\sigma_{x,y,z}$ have the form of a projection on the respective axes:

$$\langle\psi|\,\sigma_x\,|\psi\rangle = \frac{e^{i\phi}+e^{-i\phi}}{2}2\sin\frac{\theta}{2}\cos\frac{\theta}{2} = \qquad \cos\phi\sin\theta \tag{3.24}$$

$$\langle\psi|\,\sigma_y\,|\psi\rangle = -i\frac{e^{i\phi}-e^{-i\phi}}{2}2\sin\frac{\theta}{2}\cos\frac{\theta}{2} = \qquad \sin\phi\sin\theta \tag{3.25}$$

$$\langle\psi|\,\sigma_y\,|\psi\rangle = \cos^2\frac{\theta}{2}-\sin^2\frac{\theta}{2} = \qquad \cos\theta \tag{3.26}$$

3.2 Two-level system

Most important concepts in quantum computing can be illustrated with nuclear magnetic resonance (NMR). Electron spins trapped in lateral gate defined Quantum Dots were proposed as qubits by Loss et al. in 1998 [11] and the first quantum factoring algorithm was implemented with NMR quantum computing [18]. In this chapter we will discuss electron spin resonance (EPR), which is conceptually analogous to NMR but instead of spins of atomic nuclei, it is electron spins that are excited.

3.2.1 Single spin Hamiltonian

The spin of an electron is 1/2 which makes it a two level system and an excellent candidate for quantum bits. In this section we will discuss the characterstics of a spin 1/2 system. Since all quantum mechanical two - level systems correspond to the spin 1/2 system, the following results are quite general and can be transferred to other two - level systems for realization of quantum bits. The spin up $\uparrow$ and spin down $\downarrow$ states of an electrons can be mapped to the blochsphere $|\uparrow\rangle \equiv |0\rangle$ and $|\downarrow\rangle \equiv |1\rangle$. As we've seen, the expectation value of the pauli matrices provide the projection of the Bloch vector to one of the axes, hence the spin operator can be written in terms of the Pauli matrices:

$$\hat{S}_x = \frac{\hbar}{2}\sigma_x, \quad \hat{S}_y = \frac{\hbar}{2}\sigma_y, \quad \hat{S}_z = \frac{\hbar}{2}\sigma_z \tag{3.27}$$

The magnetic moment $\boldsymbol{\mu}$ of a spin 1/2 particle is given by (in this case the electron):

$$\boldsymbol{\mu} = g\frac{\mu_B}{\hbar}\mathbf{S} \tag{3.28}$$

In a magnetic field $\mathbf{B}_z(t) = B_z(t)\hat{\mathbf{z}}$ along the $\hat{\mathbf{z}}$ axis, the Hamiltonian of the particle is given by:

$$\mathcal{H} = -\boldsymbol{\mu}\cdot\mathbf{B}_z(t) = -g\frac{\mu_B}{\hbar}\mathbf{B}_z(t)\cdot\mathbf{S} = -g\frac{\mu_B}{\hbar}B_z(t)S_z \tag{3.29}$$

$$= -\frac{g}{2}\mu_B B_z(t)\sigma_z \tag{3.30}$$

The Schrödinger equation (eq. 2.13) with this hamiltonian is the following:

$$i\hbar \begin{pmatrix} \dot{c}_0(t) \\ \dot{c}_1(t) \end{pmatrix} = -\frac{g\mu_B}{2} \begin{pmatrix} B_z(t) & 0 \\ 0 & -B_z(t) \end{pmatrix} \begin{pmatrix} c_0(t) \\ c_1(t) \end{pmatrix} \tag{3.31}$$

These are two uncoupled first order linear differential equation and the solution can be easily found through seperation of variables, giving the following:

$$\begin{pmatrix} c_0(t) \\ c_1(t) \end{pmatrix} = \begin{pmatrix} e^{i\Delta/2} & 0 \\ 0 & e^{-i\Delta/2} \end{pmatrix} \begin{pmatrix} c_0(0) \\ c_1(0) \end{pmatrix}, \Delta = \frac{g\mu_B}{\hbar} \int_0^t dt' B_z(t') \tag{3.32}$$

Comparing this to rotation matrices equation(2.22) of a general qubit we see that the unitary operator has the form of a rotation around the z-axis $R_z(-\Delta)$ with an angle $-\Delta$:

$$U = R_z(-\Delta) = \begin{pmatrix} e^{i\Delta/2} & 0 \\ 0 & e^{-i\Delta/2} \end{pmatrix} \tag{3.33}$$

Applying this operator to a general qubit state:

$$R_z(-\Delta) |\psi(\theta, \phi)\rangle = |\psi(\theta, \phi - \Delta)\rangle \tag{3.34}$$

More insight can be gained by using the Bloch sphere equations: if the magnetic field is time independent, $\mathbf{B}_z(t) = \mathbf{B}_0 = B_0\hat{\mathbf{z}}$, the hamiltonian is given in the $|0\rangle$ and $|1\rangle$ basis:

$$\mathcal{H} = -\boldsymbol{\mu} \cdot \mathbf{B}_0 = -\frac{g\mu_B}{2} B_0 \sigma_z = \begin{pmatrix} -\hbar\omega_0/2 & 0 \\ 0 & \hbar\omega_0/2 \end{pmatrix} \tag{3.35}$$

Here $\omega_0/2\pi$ is the Larmor frequency and is defined by $\omega_0 \equiv \frac{g\mu_B}{\hbar} B_0$. We have chosen to place the energy zero half way between our two states, this means that the hamiltonian tells us that the energy of the $|0\rangle$ or $|\uparrow\rangle$ is lower than the $|1\rangle$ or $|\uparrow\rangle$ by $\hbar\omega_0$ (see figure 3.2)

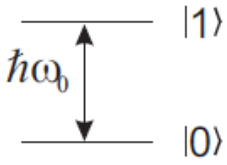

Figure 3.2: *Zeeman splitting of the two spin states by an energy $\hbar\omega_0$[19]*

Now let's consider the time evolution of a state $|\psi(t)\rangle$ with initial condition $|\psi(0)\rangle = \cos\frac{\theta_0}{2}|0\rangle + e^{i\phi_0}\sin\frac{\theta_0}{2}|1\rangle$. Since the hamiltonian is time-independent, the evolution is given by:

$$|\psi(t)\rangle = U(t)|\psi(0)\rangle = e^{-iHt}|\psi(0)\rangle \tag{3.36}$$

Now using the hamiltonian and initial state:

$$\begin{aligned}|\psi(t)\rangle &= e^{-i\frac{\omega_0}{2}t\sigma_z}\left(\cos\frac{\theta_0}{2}|0\rangle + e^{i\phi_0}\sin\frac{\theta_0}{2}|1\rangle\right)\\ &= e^{-i\frac{\omega_0}{2}t}\cos\frac{\theta_0}{2}|0\rangle + e^{i\frac{\omega_0}{2}t}e^{i\phi_0}\sin\frac{\theta_0}{2}|1\rangle\\ &= \cos\frac{\theta_0}{2}|0\rangle + e^{i(\phi_0+\omega_0 t)}\sin\frac{\theta_0}{2}|1\rangle\end{aligned}$$

In the third equality we used the freedom to multiply the state with an arbitrary phase, in this case $e^{i\omega_0/2}$. Comparing this to the general qubit state, the phase ϕ is evolving in time as $\phi(t) = \phi_0 + \omega_0 t$. This means that the Bloch vector is processing around the applied magnetic field with a frequency $\omega_0 = \frac{g\mu_B}{\hbar}B_0$, as mentioned previously, known as the Larmor frequency. (see figure 3.3)

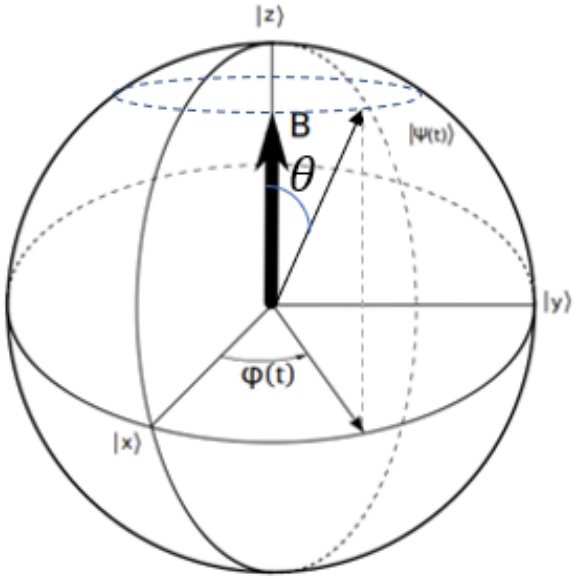

Figure 3.3: *Bloch sphere representation a spin state precessing around a constant magnetic field*

3.2.2 Control Hamiltonian

To control the state of the spin 1/2 particle in a static magnetic field $B_0\hat{\mathbf{z}}$, an oscillating magnetic field $\mathbf{B}_1(t)$ can be applied along the $\hat{\mathbf{x}}$-axis with frequency ω. The Hamiltonian

of this system is given by:

$$H(t) = -\frac{g\mu_B}{2}(B_0\sigma_z + B_1\cos(\omega t+\varphi)\sigma_x) \tag{3.37}$$
$$= \begin{pmatrix} -\frac{\hbar\omega_0}{2} & 0 \\ 0 & \frac{\hbar\omega_0}{2} \end{pmatrix} - \begin{pmatrix} 0 & \frac{\hbar\omega_1}{2}\cos(\omega t+\varphi) \\ \frac{\hbar\omega_1}{2}\cos(\omega t+\varphi) & 0 \end{pmatrix} = H_0 + V(t)$$

where $\omega_0 \equiv \frac{g\mu_B}{\hbar}B_0$ and $\omega_1 \equiv \frac{g\mu_B}{\hbar}B_1$. We set the phase $\varphi = 0$ as it is unimportant for the calculation of the probabilities. Note that $[H(t), H(t')] \neq 0$, thus we are not able to write the time evolution operator in the regular way $U(t) = \exp\left(-i\int_0^t H(t')dt'\right)$. To solve this problem time-dependent perturbation theory can be used with the Dyson series, but this gives us only an approximate solution. Instead it is possible to obtain an exact closed form solution with the *ansatz* that the eigenstates $|\Psi(t)\rangle$ of $H(t)$ can be expanded as a linear combination of the stationary eigenstates of the unperturbed Hamiltonian H_0:

$$|\psi(t)\rangle = c_0(t)e^{-i\omega_0 t/2}|0\rangle + c_1(t)e^{i\omega_0 t/2}|1\rangle \tag{3.38}$$

Inserting this in the Schrödinger equation results in [20]:

$$|c_1|^2 = \frac{\omega_1^2}{(\omega-\omega_0)^2+\omega_1^2}\sin^2\left(\frac{t}{2}\Omega\right) \tag{3.39}$$

This is the Rabi formula, it gives the probability of the spin flipping or transitioning to the $|1\rangle$ state, with $\Omega \equiv \sqrt{(\omega-\omega_0)^2+\omega_1^2}$ the Rabi frequency. For most values of ω, $|c_1|^2 \approx \frac{\omega_1^2}{(\omega-\omega_0)^2+\omega_1^2} \ll 1$ and hence the transition is negligible. However on the resonance frequency $\omega = \omega_0$, the probability is $|c_1|^2 = \sin^2\left(\frac{\omega_1 t}{2}\right)$ which means that is oscillates between 0 and 1 with frequency ω_1 Fig. 3.4.

More insight into this problem can be gained by using the rotating frame transformation and the vector model which we'll discuss next. We will look in the reference frame that is rotating at the Larmor frequency. To transform the Hamiltonian to the rotating frame, we can use the unitary operator $\hat{U} = e^{-i\frac{\omega_{rf}}{2}t\sigma_z}$ where ω_{rf} is the frequency of the rotating frame. The Hamiltonian in the rotating frame is then given by the following transformation:

$$\hat{H}_{rot} = \hat{U}\hat{H}\hat{U}^\dagger + i\hbar\frac{\partial\hat{U}}{\partial t}\hat{U}^\dagger \tag{3.40}$$

First calculating the 2nd term in 3.40:

$$i\hbar\frac{\partial\hat{U}}{\partial t}\hat{U}^\dagger = i\hbar\begin{pmatrix} -i\omega_{rf}/2e^{-i\omega_{rf}t/2} & 0 \\ 0 & i\omega_{rf}/2e^{i\omega_{rf}t/2} \end{pmatrix}\begin{pmatrix} e^{i\omega_{rf}t/2} & 0 \\ 0 & e^{-i\omega_{rf}t/2} \end{pmatrix}$$
$$= \begin{pmatrix} \hbar\omega_{rf}/2 & 0 \\ 0 & -\hbar\omega_{rf}/2 \end{pmatrix} \tag{3.41}$$

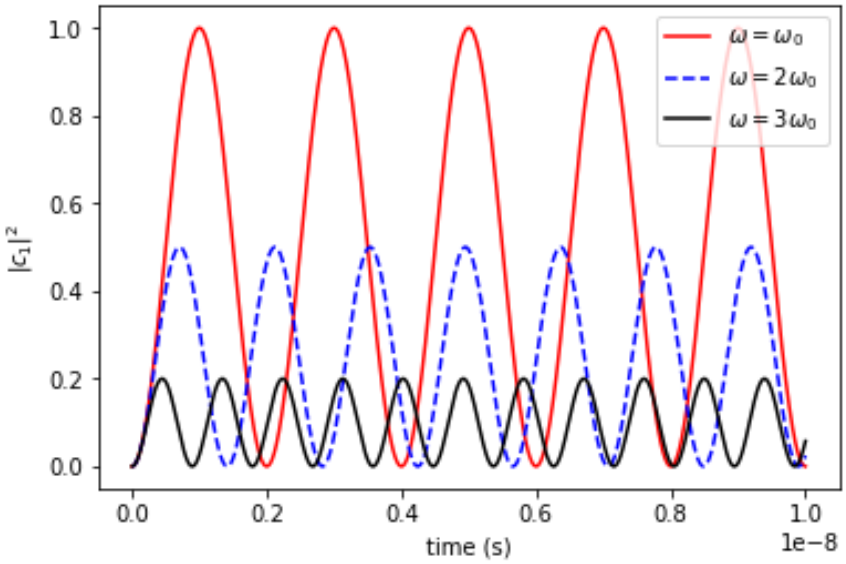

Figure 3.4: *Rabi oscillations of a two-level system. The probability of finding a particle spin state that is subjected to oscillating magnetic fields, in the excited state $|1\rangle$ as a function of time t. Here the zeeman frequency of the two-level system is $\omega_0 = 500$ MHz. The probability has been plotted for three different values of the frequency of the magnetic field, between ω_0 and $3\omega_0$*

The Hamiltonian of the system was given by 3.37:

$$\hat{H} = -\frac{\hbar\omega_0}{2}\sigma_z - \frac{\hbar\omega_1}{2}\cos(\omega t + \varphi)\sigma_x = \hat{H}_0 + \hat{V}(t) \tag{3.42}$$

Since $\hat{H}_0$ and $\hat{U}$ are both given by σ_z, they commute, so

$$\hat{U}\hat{H}_0\hat{U}^\dagger = \hat{U}\hat{U}^\dagger\hat{H}_0 = \hat{H}_0 = \begin{pmatrix} -\hbar\omega_0/2 & 0 \\ 0 & \hbar\omega_0/2 \end{pmatrix} \tag{3.43}$$

Now calculating the time-dependent part in the rotating frame $\hat{U}\hat{V}(t)\hat{U}^\dagger$

$$\begin{aligned}\hat{U}\hat{V}(t)\hat{U}^\dagger &= \begin{pmatrix} e^{-i\omega_{rf}t/2} & 0 \\ 0 & e^{i\omega_{rf}t/2} \end{pmatrix}\begin{pmatrix} 0 & -\frac{\hbar\omega_1}{2}\cos(\omega t+\varphi) \\ -\frac{\hbar\omega_1}{2}\cos(\omega t+\varphi) & 0 \end{pmatrix}\begin{pmatrix} e^{i\omega_{rf}t/2} & 0 \\ 0 & e^{-i\omega_{rf}t/2} \end{pmatrix} \\ &= -\frac{\hbar\omega_1}{2}\begin{pmatrix} 0 & \cos(\omega t+\varphi)e^{-i\omega_{rf}t)} \\ \cos(\omega t+\varphi)e^{i\omega_{rf}t} & 0 \end{pmatrix}\end{aligned} \tag{3.44}$$

Using Euler's formula to decompose the oscillating terms into two counter-rotating terms we obtain:

$$\begin{aligned}\hat{U}\hat{V}(t)\hat{U}^\dagger &= -\frac{\hbar\omega_1}{2}\begin{pmatrix} 0 & \frac{1}{2}(e^{i(\omega t+\varphi)} + e^{-i(\omega t+\varphi)})e^{-i\omega_{rf}t} \\ \frac{1}{2}(e^{i(\omega t+\varphi)} + e^{-i(\omega t+\varphi)})e^{i\omega_{rf}t} & 0 \end{pmatrix} \\ &= -\frac{\hbar\omega_1}{2}\begin{pmatrix} 0 & \frac{1}{2}(e^{i(\omega-\omega_{rf})t+i\varphi} + e^{-i(\omega+\omega_{rf})t-i\varphi}) \\ \frac{1}{2}(e^{i(\omega+\omega_{rf})t+i\varphi} + e^{-i(\omega-\omega_{rf})t-i\varphi}) & 0 \end{pmatrix}\end{aligned} \tag{3.45}$$

Here we have a slowly rotating $\omega - \omega_{rf}$ and a quickly rotating term $\omega + \omega_{rf}$. If the time evolution induced by the applied field is much slower than ω_0, we can neglect the quickly rotating terms. This approximation is called the Rotating Wave Approximation (RWA). By setting $\omega_{rf} = \omega_0$, we set the reference frame to the frame that is rotating with the Larmor frequency. By also setting the frequency of the applied magnetic field to the transition frequency ω_0 we obtain:

$$\hat{U}\hat{V}(t)\hat{U}^{\dagger} = -\frac{\hbar\omega_1}{2}\begin{pmatrix} 0 & \frac{1}{2}(e^{i\varphi} + e^{-i2\omega_0 t - i\varphi}) \\ \frac{1}{2}(e^{i2\omega_0 t + i\varphi} + e^{-i\varphi}) & 0 \end{pmatrix} \tag{3.46}$$

$$\tag{3.47}$$

Applying the RWA results in:

$$\hat{U}\hat{V}(t)\hat{U}^{\dagger} = -\frac{\hbar\omega_1}{4}\begin{pmatrix} 0 & e^{i\varphi} \\ e^{-i\varphi} & 0 \end{pmatrix} = -\frac{\hbar\omega_1}{4}(\cos(\varphi)\sigma_x - \sin(\varphi)\sigma_y) \tag{3.48}$$

The total Hamiltonian is given by adding 3.41, 3.43 and 3.48.

$$\hat{H}_{rot} = -\frac{\hbar}{2}(\omega_0 - \omega_{rf})\sigma_z - \frac{\hbar\omega_1}{4}(\cos(\varphi)\sigma_x - \sin(\varphi)\sigma_y) \tag{3.49}$$

However we set $\omega_{rf} = \omega_0$ so the first term vanishes. The introduction of the phase φ results in a parameter that allows us to generate Hamiltonians proportional to σ_x or σ_y or any angle between them. This allows rotations of the qubit state round any axis in the xy-plane. For example by setting $\phi = 0$ we obtain rotations around the x-axis. In the rotating frame the spin will precess around the x-axis similarly to the precession of the spin around the z-axis when applying a static magnetic field along the z-axis. In the lab frame, there will be a combination of precession around the x- and z-axis.

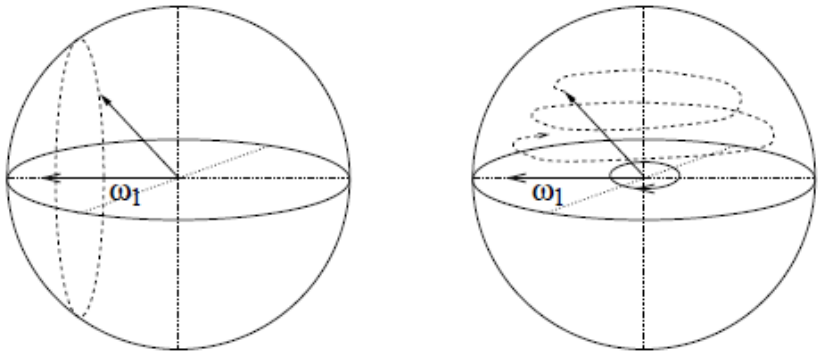

Figure 3.5: *Evolution of a spin in the rotating frame (left) and lab frame (right). [19]*

3.3 Single-qubit gates

Single-spin manipulations provide the basic one-qubit gates needed for universal quantum computation. In general, a one-qubit gate will consist of a sequence of oscilliating magnetic field pulses of different lengths (to control the amount of rotation) and a sequence of phases (to select the rotation axis). For quantum information processing it is necessary for the spin to reach any specified point on the Bloch sphere by a unitary operation U. A rotation around an arbitrary axis $\hat{n}$ can be defined as

$$R_{\hat{n}}(\theta) \equiv \exp\left[-\frac{i\theta\hat{n}\cdot\hat{\sigma}}{2}\right] \tag{3.50}$$

Where $\hat{n}$ is the axis of rotation, θ is the angle of rotation and $\hat{\sigma}$ is a vector of Pauli matrices. Since qubit-unitaries are just 3D rotations with a phase, it is also possible to use Euler's rotation theorem to realize any qubit rotation using a sequence of rotations about just two axes. For any single-qubit rotation $R_{\hat{n}}$, there are real numbers α, β, γ, and δ such that

$$R_{\hat{n}}(\theta) = e^{i\alpha}R_z(\beta)R_y(\gamma)R_z(\delta). \tag{3.51}$$

The Pauli spin matries themselves are also quantum logic gates, for example $\sigma_x = iR_x(\pi)$ which is analogous to the classical NOT gate, which flips the $|\uparrow\rangle$ to $|\downarrow\rangle$. Other useful quantum gates are the Hadamard gate, H and the phase gate Z_ϕ,

$$H = e^{i\frac{\pi}{2}}R_z(\pi)R_y(-\pi/2) = \frac{1}{\sqrt{2}}\begin{pmatrix}1 & 1\\ 1 & -1\end{pmatrix} \tag{3.52}$$

which maps the state $|0\rangle$ to $(|0\rangle + |1\rangle)/\sqrt{2}$ and $|1\rangle$ to $(|0\rangle - |1\rangle)/\sqrt{2}$, which means that the states are in a superposition,

$$Z_\phi = e^{\frac{i\phi}{2}}R_z(\phi) = \begin{pmatrix}1 & 0\\ 0 & e^{i\phi}\end{pmatrix} \tag{3.53}$$

which leaves the basis gate $|0\rangle$ unchanged and maps $|1\rangle$ to $e^{i\phi}|1\rangle$.

3.4 Two-qubit gates

A classical system of two bits is represented by the four states 00, 01, 10, and 11, similarly a two qubit system as four computational basis states denoted by $|00\rangle$, $|01\rangle$, $|10\rangle$, $|11\rangle$. However a quantums state can also exist in a superposition of these four states

$$|\psi\rangle = \alpha_{00}|00\rangle + \alpha_{01}|01\rangle + \alpha_{10}|01\rangle + \alpha_{11}|11\rangle \tag{3.54}$$

so that it occupies a four-dimensional Hilbert space. In general a system of n qubits inhabits an 2^n dimensional Hilbert space. This exponential increase in the size of the Hilbert

space with linear increase in the number of qubits underlies the power of quantum computers. To describe the qubit operators in matrix notation we define the *Kronecker product* $\otimes$ as the following: Given an $m \times n$ matrix A and a $p \times q$ matrix B then $A \otimes B$ is the $mp \times nq$ matrix:

$$A \otimes B = \begin{pmatrix} a_{11}\mathbf{B} & \cdots & a_{1n}\mathbf{B} \\ \vdots & \ddots & \vdots \\ a_{m1}\mathbf{B} & \cdots & a_{mn}\mathbf{B} \end{pmatrix} \tag{3.55}$$

For example the matrix representation of the $|10\rangle$ state is

$$\begin{pmatrix} 0 \\ 1 \end{pmatrix} \otimes \begin{pmatrix} 1 \\ 0 \end{pmatrix} = \begin{pmatrix} 0 \\ 0 \\ 1 \\ 0 \end{pmatrix} \tag{3.56}$$

The kronecker product can also be used to describe operations applied on only one of the qubits. For example, suppose the Hadamard gate is applied to the second qubit of a system in the state $|00\rangle$

$$|00\rangle = |0\rangle \otimes |0\rangle \xrightarrow{\mathrm{H}_2} |0\rangle \otimes (|0\rangle + |1\rangle)/\sqrt{2} = (|00\rangle + |01\rangle)/\sqrt{2} \tag{3.57}$$

Similarly, kronecker products can be used to write down single-qubit operators in a multi-qubit system without the need for explicit labels. For example $\mathrm{H}_2 = \mathbb{I} \otimes \mathrm{H}$. Which means that nothing is done to the first qubit, while a Hadamard gate is applied to the second qubit. Simultaneous single-qubit operations are represented by $H_{1,2} = H_1 \otimes H_2$. Two qubit gates that can be written in terms of kronecker products are a somewhat trivial extension of the corresponding gates in a single qubit system. A more interesting two-qubit gate is the controlled-NOT gate which is equivalent of the classical XOR gate.

$$U_{CNOT} = \begin{pmatrix} 1 & 0 & 0 & 0 \\ 0 & 1 & 0 & 0 \\ 0 & 0 & 0 & 1 \\ 0 & 0 & 1 & 0 \end{pmatrix} \tag{3.58}$$

This gate can not be written as a kronecker product of two single qubit operations. The CNOT gate in combination with the Hadamard gate and the phase gate form a set of *universal* quantum gates necessary for quantum computation, meaning that any desired operation can be build from a sequence of these gates. An important gate is the controlled-Z gate, which performs the transformation

$$|11\rangle \xrightarrow{CZ} -|11\rangle \tag{3.59}$$

while not affecting the other three basis states. This gate can be converted to a CNOT gate using Hadamard gates in the following way:

$$\begin{aligned} CNOT &= (\mathbb{I}\otimes H)CZ(\mathbb{I}\otimes H) \\ &= \frac{1}{2}\begin{pmatrix} 1 & 1 & 0 & 0 \\ 1 & -1 & 0 & 0 \\ 0 & 0 & 1 & 1 \\ 0 & 0 & 1 & -1 \end{pmatrix} \cdot \begin{pmatrix} 1 & 0 & 0 & 0 \\ 0 & 1 & 0 & 0 \\ 0 & 0 & 1 & 0 \\ 0 & 0 & 0 & -1 \end{pmatrix} \cdot \begin{pmatrix} 1 & 1 & 0 & 0 \\ 1 & -1 & 0 & 0 \\ 0 & 0 & 1 & 1 \\ 0 & 0 & 1 & -1 \end{pmatrix} \\ &= \begin{pmatrix} 1 & 0 & 0 & 0 \\ 0 & 1 & 0 & 0 \\ 0 & 0 & 0 & 1 \\ 0 & 0 & 1 & 0 \end{pmatrix} \end{aligned} \tag{3.60}$$

Another interesting gate is the controlled-Phase gate

$$U_{CPhase}(\phi_2,\phi_1) = \begin{pmatrix} 1 & 0 & 0 & 0 \\ 0 & e^{i\phi_2} & 0 & 0 \\ 0 & 0 & e^{i\phi_1} & 0 \\ 0 & 0 & 0 & 1 \end{pmatrix} \tag{3.61}$$

Using the CPhase gate it is possible to generate the CZ gate and any other transformation CZ_{ij} that adds a phase of π to the basis states $|i,j\rangle \xrightarrow{CZ_{ij}} -|i,j\rangle$, where $i,j \in \{0,1\}$. For $\phi_1 = \phi_2 = \pi/2$ the CPhase gate corresponds to CZ_{ij} up to single-qubit $\hat{z}$ rotations and a global phase.

$$e^{i\phi}CZ_{ij} = R_1^z\left((-1)^j\frac{\pi}{2})\right) \otimes R_2^z\left((-1)^i\frac{\pi}{2}\right) U_{CPhase}\left(\frac{\pi}{2},\frac{\pi}{2}\right) \tag{3.62}$$

where $R^z(\theta) = e^{-i\frac{\theta}{2}\sigma_z}$ are the single qubit rotations. For example the CZ gate can be constructed by:

$$\begin{aligned} e^{i\phi}CZ = e^{i\phi}CZ_{11} &= R_1^z\left(-\frac{\pi}{2}\right) \otimes R_2^z\left(-\frac{\pi}{2}\right) U_{CPhase}\left(\frac{\pi}{2},\frac{\pi}{2}\right) \\ &= \begin{pmatrix} e^{i\frac{\pi}{4}} & 0 \\ 0 & e^{-i\frac{\pi}{4}} \end{pmatrix} \otimes \begin{pmatrix} e^{i\frac{\pi}{4}} & 0 \\ 0 & e^{-i\frac{\pi}{4}} \end{pmatrix} \begin{pmatrix} 1 & 0 & 0 & 0 \\ 0 & i & 0 & 0 \\ 0 & 0 & i & 0 \\ 0 & 0 & 0 & 1 \end{pmatrix} \\ &= \begin{pmatrix} i & 0 & 0 & 0 \\ 0 & 1 & 0 & 0 \\ 0 & 0 & 1 & 0 \\ 0 & 0 & 0 & -1 \end{pmatrix} \begin{pmatrix} 1 & 0 & 0 & 0 \\ 0 & i & 0 & 0 \\ 0 & 0 & i & 0 \\ 0 & 0 & 0 & 1 \end{pmatrix} = i \begin{pmatrix} 1 & 0 & 0 & 0 \\ 0 & 1 & 0 & 0 \\ 0 & 0 & 1 & 0 \\ 0 & 0 & 0 & -1 \end{pmatrix} = e^{i\pi/2}CZ \end{aligned}$$

3.5 Two spin hamiltonian

In the following section we will see how a two spin system, described by the Heisenberg model of spins, can be used to achieve the CPhase. We will then show that the two

spin hamiltonian, described by the extended Hubbard model, in quantum dots reduces to the Heisenberg model, therefore it can be used to create the CPhase gate necessary for universal quantum computation.

3.5.1 Heisenberg model

In a system of two electron spins, the Hamiltonian can be described by the Heisenberg Hamiltonian

$$\hat{H} = J\mathbf{S}_1 \cdot \mathbf{S}_2 + \boldsymbol{\mu}_1 \cdot \mathbf{B}_1 + \boldsymbol{\mu}_2 \cdot \mathbf{B}_2 \tag{3.63}$$

$$= J\mathbf{S}_1 \cdot \mathbf{S}_2 + \mathbf{B}_1 \cdot \mathbf{S}_1 + \mathbf{B}_2 \cdot \mathbf{S}_2 \tag{3.64}$$

where we have obsorbed the physical constants μ_B and the g-factor into the magnetic fields $g\mu_B B \equiv B$. Here $\mathbf{S}_i = \boldsymbol{\sigma}_i/2$ describes the spin of electron i, $\boldsymbol{\sigma}$ is a vector of the Pauli matrices $\boldsymbol{\sigma} = \sigma_x\hat{\mathbf{x}} + \sigma_y\hat{\mathbf{y}} + \sigma_z\hat{\mathbf{z}}$ and $\boldsymbol{\sigma}_i$ labels what qubit is affected, i.e. $\boldsymbol{\sigma}_1 = \boldsymbol{\sigma} \otimes \mathbb{I}$ and $\boldsymbol{\sigma}_2 = \mathbb{I} \otimes \boldsymbol{\sigma}$. J is the exchange interaction between the two spins, i.e. the energy gap between the spin triplet and singlet states. We will use this Hamiltonian to generate the controlled-Phase gate U_{CPhase} up to a basis change. The Heisenberg Hamiltonian in matrix form reads:

$$\frac{1}{2}\begin{pmatrix} B_1^z + B_2^z & B_2^x - iB_2^y & B_1^x - B_1^y & 0 \\ B_2^x + iB_2^y & B_1^z - B_2^z - J & J & B_1^x - iB_1^y \\ B_1^x + iB_1^y & J & B_2^z - B_1^z - J & B_2^x - iB_2^y \\ 0 & B_1^x + iB_1^y & B_2^x + iB_2^y & -B_1^z - B_2^z \end{pmatrix} \tag{3.65}$$

If we consider he magnetic field to only have a z-component, $B_i^x = B_i^y = 0$ the Hamiltonian reads

$$H = \begin{pmatrix} \bar{E}_z & 0 & 0 & 0 \\ 0 & -J/2 + \Delta E_z & J/2 & 0 \\ 0 & J/2 & -J/2 - \Delta E_z & 0 \\ 0 & 0 & 0 & -\bar{E}_z \end{pmatrix} \tag{3.66}$$

where $\bar{E}_z = (B_1^z + B_2^z)/2$ is the average Zeeman energy of the two spins and $\Delta E_z = (B_1^z - B_2^z)/2$ is the diference in Zeeman energy. By diagonalizing the matrix $H = P\lambda P^{-1}$ we find the following eigenvalues:

$$\lambda = \begin{pmatrix} \bar{E}_z & 0 & 0 & 0 \\ 0 & -J/2 + \sqrt{J^2 + \Delta E_z^2} & 0 & 0 \\ 0 & 0 & -J/2 - \sqrt{J^2 + \Delta E_z^2} & 0 \\ 0 & 0 & 0 & -\bar{E}_z \end{pmatrix} \tag{3.67}$$

In the limit $J << \Delta E_z$ we obtain for the eigenvalues of the $|01\rangle$ and $|10\rangle$ states

$$\lambda_\pm = -\frac{J}{2} \pm \Delta E_z \sqrt{1 + \frac{J^2}{\Delta E_z^2}} \approx -\frac{J}{2} \pm \Delta E_z \left(1 + \frac{J^2}{\Delta E_z^2} + O(J^4/\Delta E_z^4)\right)$$

In the lowest order the eigenvalues are

$$\lambda = \begin{pmatrix} \bar{E}_z & 0 & 0 & 0 \\ 0 & -J/2 + \Delta E_z & 0 & 0 \\ 0 & 0 & -J/2 - \Delta E_z & 0 \\ 0 & 0 & 0 & -\bar{E}_z \end{pmatrix} \tag{3.68}$$

The time evolution operator of the hamiltonian in terms of the eigenvalues and the basis transformation P is given by:

$$U = e^{-iHt/\hbar} = Pe^{-i\lambda t/\hbar}P^{-1} = Pe^{-iH_0 t/\hbar} \begin{pmatrix} 1 & 0 & 0 & \\ 0 & e^{-iJt/2\hbar} & 0 & 0 \\ 0 & 0 & e^{-iJt/2\hbar} & 0 \\ 0 & 0 & 0 & 1 \end{pmatrix} P^{-1} \tag{3.69}$$

Where H_0, ($U_0 = e^{-iH_0 t/\hbar}$) is the Hamiltonian due to the Zeeman splitting which causes the single spins to rotate around the $\hat{z}$-axis. In the basis that the Hamiltonian H is diagonal $P^{-1}HP$, the evolution operator reduces to the U_{CPhase} gate up to single qubit $\hat{z}$-rotations.

$$U = U_0 U_{CPhase} = R_1^z \left(\frac{B_1^z}{\hbar} t\right) \otimes R_2^z \left(\frac{B_2^z}{\hbar} t\right) U_{CPhase} \tag{3.70}$$

which is exactly the controlled-Z gate CZ_{ij}. Another interesting gate that can be generated with the Heisenberg Hamiltonian is the SWAP gate, this gate swaps the states $|10\rangle \rightarrow |01\rangle$. The SWAP operation is obtained by switching on the interaction $J(t)$ between the spins $\mathbf{S}_1$ and $\mathbf{S}_2$ for a period of time such that $\int_0^t J(\tau) = \pi$.

$$U_{SWAP} = e^{-i\pi/4} \exp\left(i\pi \mathbf{S}_1 \cdot \mathbf{S_2}\right) = \begin{pmatrix} 1 & 0 & 0 & 0 \\ 0 & 0 & 1 & 0 \\ 0 & 1 & 0 & 0 \\ 0 & 0 & 0 & 1 \end{pmatrix} \tag{3.71}$$

3.5.2 Hubbard model

In section 2.4.2 we have seen that the Hamiltonian for two electrons in a double quantum dot can be written in the basis $\{|\downarrow,\downarrow\rangle, |\downarrow,\uparrow\rangle, |\uparrow,\downarrow\rangle, |\uparrow,\uparrow\rangle, |S,0\rangle, |0,S\rangle\}$ as

$$\hat{H} = \begin{pmatrix} -\bar{E}_z & 0 & 0 & 0 & 0 & 0 \\ 0 & -\Delta E_z & 0 & 0 & t & t \\ 0 & 0 & \Delta E_z & 0 & -t & -t \\ 0 & 0 & 0 & \bar{E}_z & 0 & 0 \\ 0 & t & -t & 0 & U_1 + \epsilon & 0 \\ 0 & t & -t & 0 & 0 & U_2 - \epsilon \end{pmatrix} \tag{3.72}$$

Where $\bar{E}_z = (E_1^z + E_2^z)/2$ is the average zeeman energy of the dots and in terms of the magnetic fields $E_i^z = g\mu_B B_i^z$. Here the constants g and μ_B will be absorbed into the magnetic

fields so $\bar{E}_z = (B_1^z + B_2^z)/2$ and $\Delta E_z = (B_1^z - B_2^z)/2$. To find the Unitary evolution operator of this system we need to diagonalize the Hamiltonian, however this can be incredibly cumbersome in this case since the characterstic equation of the matrix $(H - \lambda I) = 0$ is a 6th-order polynomial. Instead we will follow ref. [21] and use 2nd-order perturbation theory. The hamiltonian can be split in the form $H = H_0 + V$ where H_0 is the diagonal part of the hamiltonian H and V is the off-diagonal part of the hamiltonian H. If V is considered a perturbation of H_0, i.e. the strength of the interaction V must be much smaller than H_0, then it is possible to use the Schrieffer-Wolff (SW) transformation [22]. The SW transformation is a unitary transformation that removes the off-diagonal terms to the first order, hence it is a method of diagonalization in a perturbative manner. It is also useful for projecting out high energy excitations of the Hamiltonian in order to obtain an effective low energy model. Since we want to relate the double dot hamiltonian to the Heisenberg hamiltonian, it is convenient to project the double dot hamiltonian to the subspace $\{|\downarrow,\downarrow\rangle, |\downarrow,\uparrow\rangle, |\uparrow,\downarrow\rangle, |\uparrow,\uparrow\rangle\}$, the Schrieffer-Wolf transformation provides an acccurate effective projected Hamiltonian for this subspace in the case that the eliminated subspace is energetically well seperated from the subspace of interest, meaning the strength of the interaction V must be much smaller than the energy difference between the subspaces, i.e. $U_{1,2} \pm \epsilon - \bar{E}_z >> t$.

The SW transformation is a unitary transformation that diagonalizes the hamiltonian to a desired order

$$H_e = U^\dagger H U = e^S H e^{-S} \tag{3.73}$$

where S is the generator of the transformation and is an anti-hermitian operator, $S^\dagger = -S$. By expanding the unitary transformations e^S in series

$$e^S = 1 + S + \frac{1}{2}S^2 + \dots \tag{3.74}$$

we obtain a series expansion for the transformed hamiltonian H_e in terms of commutators

$$H_e = H + [S, H] + \frac{1}{2}[S, [S, H]] + \dots \tag{3.75}$$

In terms of H_0 and V the transfomation becomes

$$H_e = H_0 + V + [S, H_0] + [S, V] + \frac{1}{2}[S, [S, H_0]] + \frac{1}{2}[S, [S, V]] + \dots \tag{3.76}$$

In order to make the Hamiltonian diagonal, the generator S can be chosen such that $[S, H_0] = -V$, substituting this in the previous equation cancels the off-diagonal term V to the first order, therefore the effective hamiltonian to the second order is given by

$$H_e = H_0 + \frac{1}{2}[S, V] + O(S^3) \tag{3.77}$$

If we could determine S exactly, it is straightforward to compute the SW hamiltonian, however in general finding S is difficult. Ref [22] and [23] discuss methods of finding S.

We will use ref [21] and show the result of the transformation, a full derivation can be found in appendix A. The effective Hamiltonian in the subspace $\{|\downarrow,\downarrow\rangle, |\downarrow,\uparrow\rangle, |\uparrow,\downarrow\rangle, |\uparrow,\uparrow\rangle\}$ reads:

$$H_e = \begin{pmatrix} -\bar{E}_z & 0 & 0 & 0 \\ 0 & -\Delta E_z - 2t^2/U & 2t^2/U & 0 \\ 0 & 2t^2/U & \Delta E_z - 2t^2/U & 0 \\ 0 & 0 & 0 & \bar{E}_z \end{pmatrix} \tag{3.78}$$

which is the same as the Heisenberg hamiltonian 3.66 with the exchange interaction $J = 4t^2/U$. This means that a $CPhase$ gate can be created by a purely electrical gating of the tunneling barrier between the neighboring quantum dots. If the barrier potential is high, i.e. $t \approx 0$, tunneling is forbidden between the dots and the qubit states are stable and do not evolve in time. If the barrier is pulsed to a low voltage, we see that the Hubbard model description of the double dot reduces to a Heisenberg Hamiltonian with a coupling that is time dependent (t' is time)

$$H(t') = J(t')\mathbf{S}_1 \cdot \mathbf{S}_2 \tag{3.79}$$

where $J(t') = 4t^2(t')/U$, here the tunnel matrix element $t(t')$ is made time dependend by lowering and increasing the tunnel barrier, i.e. turning the tunnel matrix on and off, through electrical gating of the potential barrier between the dots. In the previous chapter we saw that the Heisenberg Hamiltonian can be used to obtain the controlled-Z gate CZ_{ij} and the swap gate U_{SWAP}, therefore these gates can be obtained via the two-electron Hamiltonian by pulsing the dots accordingly.

3.6 Grover's Algorithm

In this section we will discuss the famous Grover's algorithm for two qubits and demonstrate its implementation via the two-electron quantum dot. Grover's Algorithm is considered a search algorithm that searches for a specific item in an unstructured set of N items, e.g. a database. The algorithm requires a black-box type predicate that can be evaluated on all the items in the set, usually called the *Oracle*. Consider the function which is always equal to 0 except for a single value v

$$y = f(x) = \begin{cases} 0 & \text{if } x \neq \omega \\ 1 & \text{if } x = \omega \end{cases} \tag{3.80}$$

If x matches a desired entry ω in a database then y will return 1 and 0 for other values of x which represent other items in the database. Conventional algorithms, searching a database for N items require $O(N)$ queries in the worse case to find the desired item ω. However in the quantum domain, this function can be evaluated on a superposition of all database items which results in $O(\sqrt{N})$ queries [24] to find the desired item, this is a quadratic speedup over the classical case. A database of N entries can be represented by

a N-dimensional Hilbert space which can be constructed by only $n = \log_2 N$ qubits. The function $y = f(x)$ maps database entries to 0 or 1, the oracle is constructed in the form of a unitary operator U_ω that acts as follows

$$U_\omega|x\rangle = (-1)^{f(x)}|x\rangle \tag{3.81}$$

This unitary operator marks the desired index ω with a minus sign $-\omega$ by rotating its phase by π radians. Fig. 3.6 show the quantum circuit of Grover's algorithm. The algorithm's first step is to initialize the $n = \log_2 N$ qubits each with value $|0\rangle$. These qubits are then transformed into a equal superposition state by applying one qubit Hadamard gates on each input qubit.

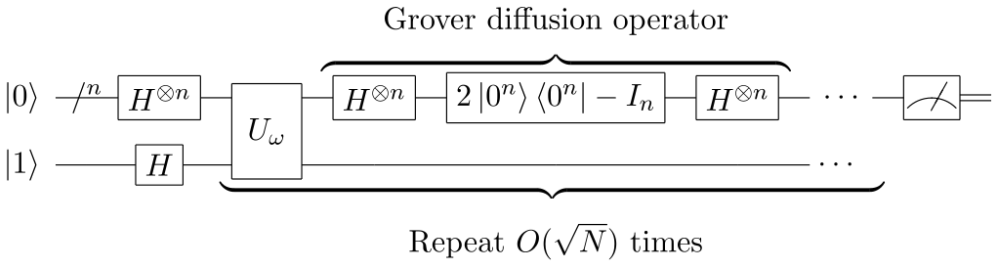

Figure 3.6: *Quantum circuit depiction of Grover's quantum search algorithm.[25]*

The next step is to increase the probability amplitudes of those indices in the superposition that match the search criteria $x = \omega$. This is achieved by additional gates that are applied to increase the probability amplitudes of the marked index ω and decreases the probability amplitudes of the unmarked indices, these are represented by grover's diffusion operator. Each iteration of Grover's algorithm increases the amplitude of the desired state ω by $O(1/\sqrt{N})$. Therefore, at most $\sqrt{N}$ iterations are required to maximize the probability that a measurement will yield the desired state ω. In general, the optimal number of iterations required is $R \approx \frac{\pi}{4}\sqrt{N}$ [26]. For the special case of $N = 4$, corresponding to two qubits, only a single iteration is needed. The oracle for the two qubit case can constructed by the controlled-Z $U_\omega = CZ_{ij}$ gate, since this gate does exactly what we want from the oracle, it marks the desired state $|ij\rangle$ by applying a π radian shift to the state, $|ij\rangle \xrightarrow{CZ_{ij}} -|ij\rangle$. For example consider the two qubit Hilbert space $\mathcal{H}$ with basis states $\{|00\rangle, |01\rangle, |10\rangle, |11\rangle\}$. The equal superposition state is given by

$$|\psi\rangle = \frac{1}{2}\left(|00\rangle + |01\rangle + |10\rangle + |11\rangle\right) \tag{3.82}$$

Let's say the desired state we want to mark is the state $|10\rangle$ then the controlled-Z gate(oracle) applied on the state $|\psi\rangle$ will return

$$U_\omega\,|\psi\rangle = CZ_{10}\,|\psi\rangle = \frac{1}{2}\left(|00\rangle + |01\rangle - |10\rangle + |11\rangle\right) \tag{3.83}$$

In matrix notation

$$CZ_{10}\left|\psi\right\rangle = \begin{pmatrix} 1 & 0 & 0 & 0 \\ 0 & 1 & 0 & 0 \\ 0 & 0 & -1 & 0 \\ 0 & 0 & 0 & 1 \end{pmatrix} \begin{pmatrix} 1/2 \\ 1/2 \\ 1/2 \\ 1/2 \end{pmatrix} = \begin{pmatrix} 1/2 \\ 1/2 \\ -1/2 \\ 1/2 \end{pmatrix} \tag{3.84}$$

In the previous section we've seen that the two electron Hamiltonian (Hubbard model) reduces to CZ_{ij} gate, therefore it can be used as the oracle for a two qubit system. Fig. 3.7 shows the gate sequence of the Grover's algorithm for two qubits.

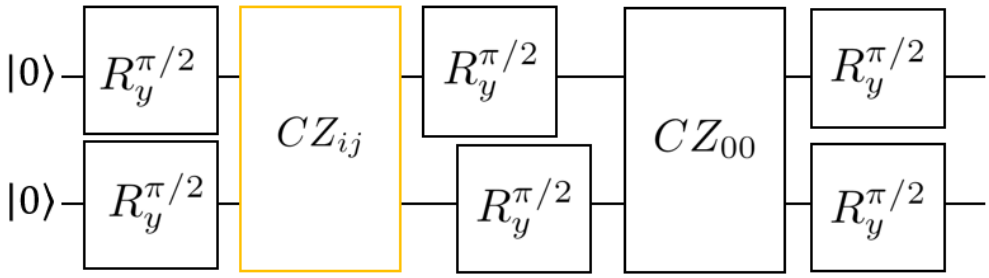

Figure 3.7: ***a****, Gate sequence of single-qubit and controlled-Z gates implementing Grover's algorithm[27],[28].* ***b****, Rotation of the single qubits by π radions around the y-axis obtaining a maximal superposition state.* ***c****, CZ_{ij} is the oracle that marks the desired state $|ij\rangle$ by inerting its phase.* ***d****, the rotation $R_y^{\pi/2}$ of the first qubit turns the state into a Bell state,* ***e****, rotation $R_y^{\pi/2}$ on the second qubit produces a state identical to (d), the application of CZ_{00} undoes the entanglement, producing a maximal superposition state.* ***f****, The last rotations yield the desired output state $|ij\rangle$.*

Both qubits are initialized in the $|0\rangle$ state and rotated around the y-axis by $\pi/2$ degrees to place them in a superposition. Next the oracle CZ_{ij} is applied to mark the desired state and the other single qubit and two qubit gates are applied to increase the amplitude of the desired state while decreasing the amplitude of the other states (Grover diffusion operator).

Chapter 4

Dynamics of Two Spin Qubits

In this chapter we will discuss different methods for solving the Schrödinger numerically for a double dot system. The Schrödinger equation governs the dynamics of the wavefunction Ψ generated by the hamiltonian $\hat{H}$

$$i\hbar\frac{d}{dt}|\psi\rangle = H|\psi\rangle \tag{4.1}$$

In the basis $\{|\downarrow,\downarrow\rangle, |\downarrow,\uparrow\rangle, |\uparrow,\downarrow\rangle, |\uparrow,\uparrow\rangle, |S(0,2)\rangle, |S(2,0)\rangle\}$ the wavefunction takes the form of a vector:

$$\begin{aligned}|\psi\rangle &= c_1|\downarrow,\downarrow\rangle + c_2|\uparrow,\downarrow\rangle + c_3|\downarrow,\uparrow\rangle + c_4|\downarrow,\downarrow\rangle + c_5|S(0,2)\rangle + c_6|S(2,0)\rangle \\ &= \begin{pmatrix} c_1 \\ \vdots \\ c_6 \end{pmatrix}\end{aligned} \tag{4.2}$$

where $c_i = c_i(t)$ are the time dependent coefficients of the wave function. The Hamiltonian $\hat{H}$ takes the form of a matrix H with elements H_{ij}

$$H_{ij} = \langle\psi_i|\hat{H}|\psi_j\rangle \tag{4.3}$$

For clarity we will write the Hamiltonian 2.23 again, in matrix form it reads:

$$H = \begin{pmatrix} -\bar{E}_z & 0 & 0 & 0 & 0 & 0 \\ 0 & -\Delta E_z & 0 & 0 & t_0 & t_0 \\ 0 & 0 & \Delta E_z & 0 & -t_0 & -t_0 \\ 0 & 0 & 0 & \bar{E}_z & 0 & 0 \\ 0 & t_0 & -t_0 & 0 & U_1+\epsilon & 0 \\ 0 & t_0 & -t_0 & 0 & 0 & U_2-\epsilon \end{pmatrix} \tag{4.4}$$

where $\bar{E}_z = \hbar(B_1^z + B_2^z)/2$ is the average zeeman energy of the dots and $\Delta E_z = \hbar(B_1^z - B_2^z)/2$ is the difference in zeeman energy. The constants g, $\hbar$ and μ_B have been absorbed in the

magnetic fields $\frac{g\mu_B}{\hbar}B_k^i \equiv B_k^i$. To control the single-qubit rotations, an oscillating magnetic field in the x-direction which will couple to both electron spins in the dots

$$H_{mw} = \sum_k B_{mw}\cos(\omega_k t + \phi_k)(\sigma_x \otimes \mathbb{I} + \mathbb{I} \otimes \sigma_x) \tag{4.5}$$

Rotation of a particular qubit k is achieved by choosing the frequency of the oscillating magnetic field ω_k such that it corresponds to the larmor frequency $\omega_k = \frac{g\mu_B}{\hbar}B_k^z \equiv B_k^z$ of qubit k. B_{mw} is the driving amplitude of the signal and ϕ_k is the phase. To simplify the calculations, the Hamiltonians are transformed into a rotating frame via the basis transformation

$$\widetilde{H} = UHU^\dagger + i\hbar\frac{dU}{dt}U^\dagger \tag{4.6}$$

where

$$U = e^{-i\frac{\omega_1 t}{2}\sigma_z} \otimes e^{-i\frac{\omega_2 t}{2}\sigma_z} \tag{4.7}$$

The transformed Hamiltonians in the rotating frame are (see Appendix B for derivation)

$$\widetilde{H} = \begin{pmatrix} 0 & 0 & 0 & 0 & 0 & f0 \\ 0 & 0 & 0 & 0 & t_0 e^{i\Delta E_z t/\hbar} & t_0 e^{i\Delta E_z t/\hbar} \\ 0 & 0 & 0 & 0 & -t_0 e^{-i\Delta E_z t/\hbar} & -t_0 e^{-i\Delta E_z t/\hbar} \\ 0 & 0 & 0 & 0 & 0 & 0 \\ 0 & t_0 e^{-i\Delta E_z t/\hbar} & -t_0 e^{i\Delta E_z t/\hbar} & 0 & U_1 + \epsilon & 0 \\ 0 & t_0 e^{-i\Delta E_z t/\hbar} & -t_0 e^{i\Delta E_z t/\hbar} & 0 & 0 & U_2 - \epsilon \end{pmatrix} \tag{4.8}$$

and the microwave Hamiltonian transformed is

$$\widetilde{H}_{mw} = \sum_k \frac{1}{2}\begin{pmatrix} 0 & \Omega_k e^{i(\omega_k-\omega_2)t} & \Omega_k e^{i(\omega_k-\omega_1)t} & 0 & 0 & 0 \\ \Omega_k^* e^{-i(\omega_k-\omega_2)t} & 0 & 0 & \Omega_k e^{i(\omega_k-\omega_1)t} & 0 & 0 \\ \Omega_k^* e^{-i(\omega_k-\omega_1)t} & 0 & 0 & \Omega_k e^{i(\omega_k-\omega_2)t} & 0 & 0 \\ 0 & \Omega_k^* e^{-i(\omega_k-\omega_1)t} & \Omega_k^* e^{-i(\omega_k-\omega_2)t} & 0 & 0 & 0 \\ 0 & 0 & 0 & 0 & 0 & 0 \\ 0 & 0 & 0 & 0 & 0 & 0 \end{pmatrix} \tag{4.9}$$

where $\Omega_k = B_{mw}e^{i\phi_k}$ and the Rabi frequency is $|\Omega_k| = B_{mw}$. The Schrödinger equation $i\hbar\partial_t|\psi\rangle = (\widetilde{H}(t) + \widetilde{H}_{mw}(t))|\psi\rangle$ takes the form of a linear system of ordinary differential equations

$$\dot{c}(t) = A(t)c(t) \tag{4.10}$$

4.1 QuTiP implementation

The Quantum Toolbox in Python (QuTiP) is an open-source framework written in the Python programming lanuage that is designed for simulating the quantum dynamics of

systems. QuTiP is very efficient in describing quantum systems described in second-quantization formalism through vectors (bra/ket vectors) and matrices (operators). It also offers easy implementations of time-dependent Hamiltonians through string based code, this means it is possible to just write the Hamiltonian in string form and QuTiP will handle all the numerics. This allows for an easy-to-use environment which saves substantial code development time. QuTiP's solver's are all based on the ZVODE routine in Scipy, which uses one of the most popular methods (Adams and Backward Differentiation Formula) for solving ODE's like the schrödinger equation 4.16.

4.1.1 Time-dependent solver

To solve the Schrödinger equation $i\hbar\partial_t|\psi\rangle = \left(\widetilde{H}(t) + \widetilde{H}_{mw}(t)\right)|\psi\rangle$ we will be using the *mesolve* function of QuTiP. The time-dependent coefficients $f_i(t)$ of the Hamiltonian are represented by strings in the following way:

$$H_{total} = H_0 - \sum_i f_i(t) H_i \tag{4.11}$$

where H_0 are the time-independent part and H_i denote the positions in the matrix where the coefficients $f_i(t)$ should be placed. To illustrate this, consider the double dot Hamiltonian in the rotating frame

$$\widetilde{H} = \begin{pmatrix} 0 & 0 & 0 & 0 & 0 & 0 \\ 0 & 0 & 0 & 0 & t_0 e^{i\Delta E_z t/\hbar} & t_0 e^{i\Delta E_z t/\hbar} \\ 0 & 0 & 0 & 0 & -t_0 e^{-i\Delta E_z t/\hbar} & -t_0 e^{-i\Delta E_z t/\hbar} \\ 0 & 0 & 0 & 0 & 0 & 0 \\ 0 & t_0 e^{-i\Delta E_z t/\hbar} & -t_0 e^{i\Delta E_z t/\hbar} & 0 & U_1 + \epsilon & 0 \\ 0 & t_0 e^{-i\Delta E_z t/\hbar} & -t_0 e^{i\Delta E_z t/\hbar} & 0 & 0 & U_2 - \epsilon \end{pmatrix} \tag{4.12}$$

The time-independent terms are

$$H_0 = \begin{pmatrix} 0 & 0 & 0 & 0 & 0 & 0 \\ 0 & 0 & 0 & 0 & 0 & 0 \\ 0 & 0 & 0 & 0 & 0 & 0 \\ 0 & 0 & 0 & 0 & 0 & 0 \\ 0 & 0 & 0 & 0 & U_1 + \epsilon & 0 \\ 0 & 0 & 0 & 0 & 0 & U_2 - \epsilon \end{pmatrix} \tag{4.13}$$

while the time-dependent terms are

$$-\sum_i^2 f_i(t) H_i = \begin{pmatrix} 0 & 0 & 0 & 0 & 0 & 0 \\ 0 & 0 & 0 & 0 & f_1(t) & f_1(t) \\ 0 & 0 & 0 & 0 & 0 & 0 \\ 0 & 0 & 0 & 0 & 0 & 0 \\ 0 & 0 & -f_1(t) & 0 & 0 & 0 \\ 0 & 0 & -f_1(t) & 0 & 0 & 0 \end{pmatrix} + \begin{pmatrix} 0 & 0 & 0 & 0 & 0 & 0 \\ 0 & 0 & 0 & 0 & 0 & 0 \\ 0 & 0 & 0 & 0 & -f_2(t) & -f_2(t) \\ 0 & 0 & 0 & 0 & 0 & 0 \\ 0 & f_2(t) & 0 & 0 & 0 & 0 \\ 0 & f_2(t) & 0 & 0 & 0 & 0 \end{pmatrix} \tag{4.14}$$

with $f_1(t) = -t_0 e^{i\Delta E_z t/\hbar}$ and $f_2(t) = -t_0 e^{-i\Delta E_z t/\hbar}$.

The microwave Hamiltonian that controls the single-qubit rotations can be constructed constructed in a similar way, the time independent part of $\widetilde{H}_{mw}$ is zero, while the time-dependent part consist out of the four coefficients

$$f_1(t) = \Omega_k e^{i(\omega_k - \omega_2)t}, \quad f_2(t) = \Omega_k e^{i(\omega_k - \omega_1)t}, \quad f_3(t) = f_1(t)^*, \quad f_4(t) = f_2(t)^* \tag{4.15}$$

where $f_i(t)^*$ is the complex conjugate of $f_i(t)$.

For example consider the double dot system with a negligible tunnel coupling $t_0 \approx 0$ that is subjected to an oscillating magnetic field with a frequency set equal to the Larmor frequency of qubit 1.

```
H0=set_Hamiltonian(B1=0,B2=0,t0=0,U1=1e12,U2=1e12,detuning=0)
```

This creates the time-independent part of the Hamiltonian with on-site energies $U1 = U2 = 10^{12}$ Hz.

```
Hmw1 = np.zeros((6,6),dtype=complex);Hmw1[0,1]=1;Hmw1[2,3]=1;
Hmw2 = np.zeros((6,6),dtype=complex);Hmw2[0,2]=1;Hmw2[1,3]=1;
Hmw3 = np.zeros((6,6),dtype=complex);Hmw3[1,0]=1;Hmw3[3,2]=1;
Hmw4 = np.zeros((6,6),dtype=complex);Hmw4[2,0]=1;Hmw4[3,1]=1;

H0=qt.Qobj(H0);Hmw1=qt.Qobj(Hmw1);Hmw2=qt.Qobj(Hmw2);
Hmw3=qt.Qobj(Hmw3);Hmw4=qt.Qobj(Hmw4)
args = {'B1':2e9, 'B2':1e9, 'Bmw':5e6,'vi':0,'w_k':2e9}
time = '*(0e-9<=t<=1000e-9)'#time interval

Om='-0.5*2*np.pi*Bmw*np.exp(1j*vi)' #complex amplitude
Om_c = '-0.5*2*np.pi*Bmw*np.exp(-1j*vi)'#conjugate

Hmw1_coeff = Om+'*np.exp(1j*2*np.pi*(w_k-B2)*t)'+time
Hmw3_coeff = Om_c+'*np.exp(-1j*2*np.pi*(w_k-B2)*t)'+time
Hmw2_coeff = Om+'*np.exp(1j*2*np.pi*(w_k-B1)*t)'+time
Hmw4_coeff = Om_c+'*np.exp(-1j*2*np.pi*(w_k-B1)*t)'+time
```

The Hmw$i$ terms construct the microwave matrix elements and Hmw$i$_coeff terms are the corresponding time-dependent coefficients, the system starts in the state $|\downarrow\downarrow\rangle$. These are then given to QuTiP's mesolve function in the following way

```
H = [H0,[Hmw1,Hmw1_coeff],[Hmw3,Hmw3_coeff],
     [Hmw2,Hmw2_coeff],[Hmw4,Hmw4_coeff]]
psi0=qt.basis(6,0)

output = qt.mesolve(H,psi0,tlist,[],[],args=args,
                    options=qt.Options(nsteps=200000, method='bdf'))
```

The amplitude of the magnetic field B_{mw} is set to $5 \cdot 10^6$ Hz while the Larmor frequencies of the two electrons are set to $B_1 = 2 \cdot 10^9$ and $B_2 = 10^9$. Since the drive frequency $\omega_k = B_1$ of the ac magnetic field is on resonance with respect to qubit 1 but off-resonance with respect to qubit 2, only qubit 1 will undergo Rabi oscillations with frequency $\sqrt{(\omega_k - B_1)^2 + B_{mw}^2} \approx B_{mw}$.

Plotting the results $|c_i(t)|^2$:

```
tlist = np.linspace(0,1000e-9,1000)
plot_states(tlist,output)
```

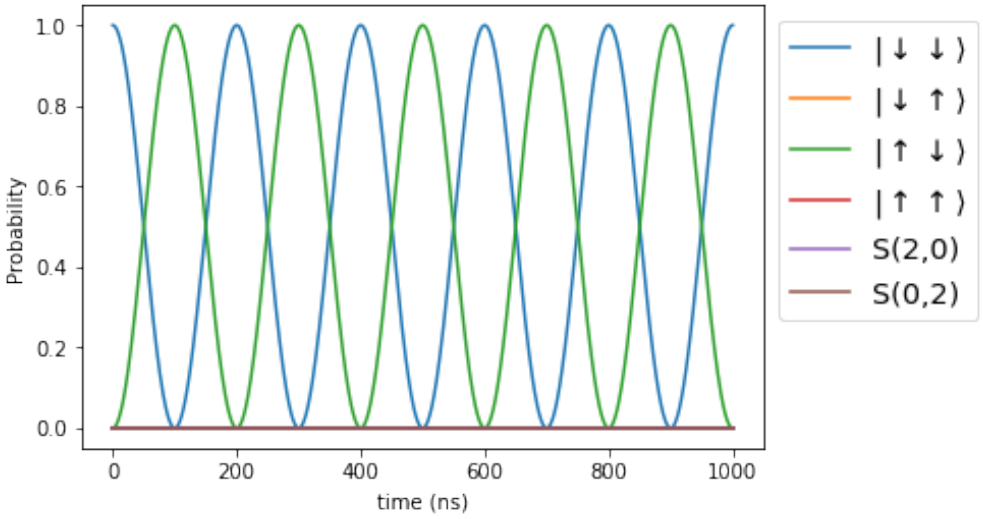

Figure 4.1: *Time evolution of the two electron states using QuTiP mesolve function*

4.1.2 Stiffness slowdown

Most of QuTiP's solver's approach the Schrödinger equation or equivalent equations, e.g. Lindblad Master equation or Bloch-redfield equation, by representing them as a system of ordinary differential equations and subsequently using SciPy's library which provides conventional numerical methods to approximate solutions. Consider the initial value problem (IVP)

$$y'(t) = f(t, y(t)) \tag{4.16}$$

for the complex-valued function y of the real variable t, where $y' \equiv \frac{dy}{dt}$ and f is a given complex-valued function. In terms of the wavefunction and Hamiltonian $y(t) = c(t)$ and

$f(t, y(t)) = A(t)y(t)$. This differential equation will be considered with an initial condition: given two numbers t_0 and y_0, there is a solution to 4.16 for $t > t_0$ such that

$$y(t_0) = y_0 \tag{4.17}$$

SciPy's library uses the the VODE (Variable Coefficient ODE solver)[29] routine to solve 4.16. It uses a general k-step linear multistep formula which has the form

$$\sum_{i=0}^{K_1} = \alpha_i y_{n-i} = h \sum_{i=0}^{K_2} \beta_i f_{n-i} \tag{4.18}$$

Where the coefficients α_i, β_i are computed by interpolating the function f at the previous points f_k , $k = \{0, 1, 2 \ldots n-1\}$ via Lagrange polynomials. For example the Backward Differentiation Formula (BDF) is characterized by setting $K_1 = q$, the order of the method, and $K_2 = 0$

$$\sum_{i=0}^{q} \alpha_i y_{n-i} = h\beta_0 f\left(t_n, y_n\right) \tag{4.19}$$

The stepsize h is the internal stepsize of the solver that determines the amount of times n the solver needs to be called between two timesteps $n = \dfrac{|t_0 - t_1|}{h}$. The stepsize is chosen in such a way that it will satisfy a user defined absolute and relative tolerance. For example, instead of using QuTiP we can directly access SciPy's library to calculate a simple Rabi oscillation.

```
from scipy.integrate import ode
import numpy as np
w1=2e9;w2=1e9;t0=0;B=5e6 #dot parameters
vi=0;wk=2e9;u=1e12
args = [wk,w1,w2,B,t0,u,vi]
y0 = [1,0,0,0,0,0] #initial values
t = np.linspace(0,1000e-9,1001)
dt = t[1]-t[0]
def func(t,y,args): #the function f(t, y(t))
    wk,w1,w2,B,t0,u,vi = args
    x0,x1,x2,x3,x4,x5=y
    dE = np.exp(1j*(w1-w2)/2*t)
    dEc=np.exp(-1j*(w1-w2)/2*t)
    mw1 = B/2*np.exp(1j*vi)*np.exp(1j*(wk-w1)*t/2)
    mw2 = B/2*np.exp(1j*vi)*np.exp(1j*(wk-w2)*t/2)
    mw1c = B/2*np.exp(-1j*vi)*np.exp(-1j*(wk-w1)*t/2)
    mw2c = B/2*np.exp(-1j*vi)*np.exp(-1j*(wk-w2)*t/2)
    f = [mw1*x2+x1*mw2,
```

```
          t0*x4*dE+t0*x5*dE+mw1*x3+mw2c*x0,
          -t0*x4*dEc-t0*x5*dEc+mw1c*x0+mw2*x3,

          mw1c*x1+mw2c*x2,
          t0*x1*dEc-t0*x2*dE+x4*u,
          t0*x1*dEc-t0*x2*dE+x5*u]
    g = [-1j*2*np.pi*i for i in f]

r = ode(func).set_integrator('zvode',atol=1e-8,rtol=1e-6
       ,nsteps=2500,method='bdf')
r.set_initial_value(y0,0).set_f_params(args)
psi = []
while r.successful() and r.t < t[-1]:
    psi.append(r.integrate(r.t+dt))
for i in range(6):
    plt.plot(t/1e-9,abs(np.array(psi)[:,i])**2)
plt.xlabel('t (ns)')
plt.ylabel('probability')
plt.show()
```

This will give us the same result as Fig. 4.1. Now that we know how QuTiP solves the Schrödinger equation, let's look at a more complicated operation. Consider the SWAP gate which can be achieved with the Heisenberg Hamiltonian by turning on the tunnel coupling $J = 4t_0^2/U$, $U_{SWAP} = e^{-i\pi/4}\exp(iJ\mathbf{S_1}\cdot\mathbf{S_2}t/\hbar)$ such that $Jt/\hbar = \pi$[30]

```
Ht1=np.zeros((6,6),dtype=complex);Ht1[4,1]=1;
Ht1[5,1]=1;Ht1[2,4]=-1;Ht1[2,5]=-1;
Ht2=np.zeros((6,6),dtype=complex);Ht2[4,2]=-1;
Ht2[5,2]=-1;Ht2[1,5]=1;Ht2[1,4]=1;
Ht1=qt.Qobj(Ht1);Ht2=qt.Qobj(Ht2)

H0=set_Hamiltonian(0,0,0,U1=1e12,U2=1e12,0)
H0 = qt.Qobj(H0)
args = {'B1':2e9, 'B2':2e9, 'Bmw':5e6,'vi':0,'w_k':2e9,'t0':4.3e9}
tlist = np.linspace(0,20e-9,1000)

Ht1_c = '(5e-9<=t<=11.8e-9)*-2*np.pi*t0*np.exp(-1j*2*np.pi*(B1-B2)/2*t)'
Ht2_c = '(5e-9<=t<=11.8e-9)*-2*np.pi*t0*np.exp(1j*2*np.pi*(B1-B2)/2*t)'
H = [H0,[Ht1,Ht1_c],[Ht2,Ht2_c]]
psi0=qt.basis(6,1)

output = qt.mesolve(H,psi0,tlist,[],[],args=args,
                    options=qt.Options(nsteps=250000, method='bdf')
```

```
                    ,progress_bar=True)
plot_states(tlist,output)
>>> Total run time:  18.19s
```

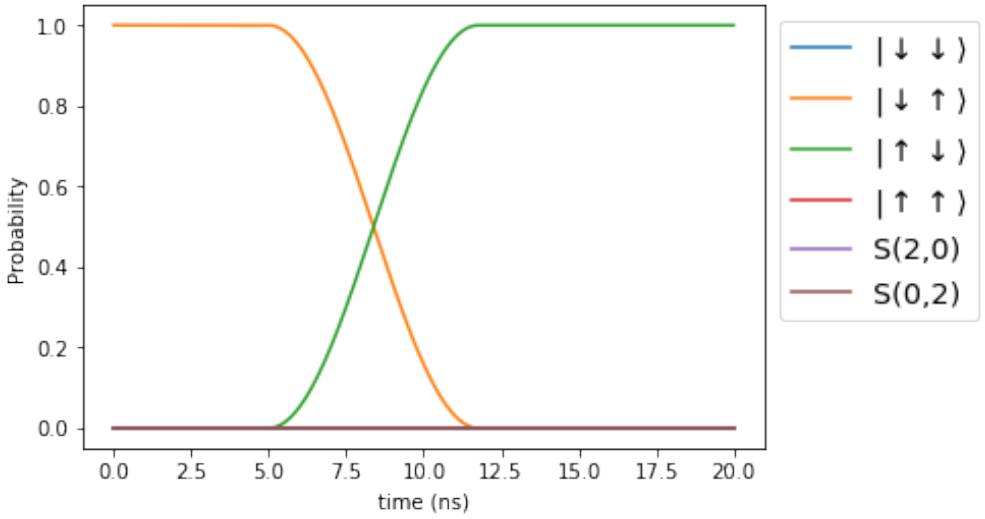

Figure 4.2: *SWAP operation via the Heisenberg exchange interaction* $J = 4t_0^2/U$

Here the exchange interaction has been turned on and off as a step function between 5 ns and 11.8 ns. A problem that arises for this seemingly simple calculation is the amount of time to calculate the solution, it took 18.19 real time seconds to find the solution for only 20 ns simulation time range. The slowdown is apparent when the ODE system contains terms that differ by a large magnitude and that are coupled to eachother via the differential equations. For example in the SWAP operation the differential equation $y' = f(t, y)$ has the following form (for brevity $y(t) \to y$):

$$
\begin{aligned}
\begin{pmatrix} y_0' \\ y_1' \\ y_2' \\ y_3' \\ y_4' \\ y_5' \end{pmatrix} &= \begin{pmatrix} 0 & 0 & 0 & 0 & 0 & 0 \\ 0 & 0 & 0 & 0 & t_0 e^{i\Delta E_z t/\hbar} & t_0 e^{i\Delta E_z t/\hbar} \\ 0 & 0 & 0 & 0 & -t_0 e^{-i\Delta E_z t/\hbar} & -t_0 e^{-i\Delta E_z t/\hbar} \\ 0 & 0 & 0 & 0 & 0 & 0 \\ 0 & t_0 e^{-i\Delta E_z t/\hbar} & -t_0 e^{i\Delta E_z t/\hbar} & 0 & U_1 & 0 \\ 0 & t_0 e^{-i\Delta E_z t/\hbar} & -t_0 e^{i\Delta E_z t/\hbar} & 0 & 0 & U_2 \end{pmatrix} \begin{pmatrix} y_0 \\ y_1 \\ y_2 \\ y_3 \\ y_4 \\ y_5 \end{pmatrix} \\
\begin{pmatrix} y_0' \\ y_1' \\ y_2' \\ y_3' \\ y_4' \\ y_5' \end{pmatrix} &= \begin{pmatrix} 0 \\ t_0 e^{i\Delta E_z t/\hbar}(y_4 + y_5) \\ -t_0 e^{-i\Delta E_z t/\hbar}(y_4 + y_5) \\ 0 \\ t_0 e^{-i\Delta E_z t/\hbar} y_1 - t_0 e^{i\Delta E_z t/\hbar} y_2 + U_1 y_4 \\ t_0 e^{-i\Delta E_z t/\hbar} y_1 - t_0 e^{i\Delta E_z t/\hbar} y_2 + U_2 y_5 \end{pmatrix}
\end{aligned}
\tag{4.20}
$$

The components y_1', y_2' are coupled with the components y_4', y_5' through the term U_1 and U_2 respectively. In the example of Fig. 4.2 the terms $U_1 = U_2$ and $t_0 e^{\pm i\Delta E_z t/\hbar}$ differ by a large magnitude, $\log \frac{U_1}{t_0} \approx 3$ three orders of magnitude. This is a typical problem of *stiffness* of the ODE system. Stiffness is often described in terms of *multiple time scales*. If the ODE system has widely varying time scales and the physical phenomena (i.e. the solution modes) that change on fast scales are stable, then the problem is stiff [31]

In general it is quite difficult to quantitively characterize the stiffness of an ODE system. For constant variable coefficients, it is possible to use the eigenvalues of the matrix A of the ODE system $y' = Ay$ to characterize the stiffness, however for a variable coefficient system $y' = A(t)y$ the eigenvalues are not good indicators for stiffness.[32] To get some general idea of stiffness, consider the following simple initial value problem (following [31]),

$$y' = -100(y - sin(t)), \quad y(0) = 1 \tag{4.21}$$

with a solution that (Fig. 4.3) that rapidly varies for a short time interval $0 \leq t \leq 0.03$ but then varies much more slowly and is approximated by $y(t) \approx \sin t$. The ODE solver will use a small stepsize h for the initial small interval of rapid change, if the timestep is too big, then the initial part of the solution will not be approximated well. When $y(t) \approx \sin t$, it's possible to use a much higher stepsize since the variation is much slower, which will increase computational time. However when the solution contains rapidly varying terms and slowly varying terms throughout the whole solution, then a small stepsize is necessary for the whole range of calculation which will drastically increase computational time.

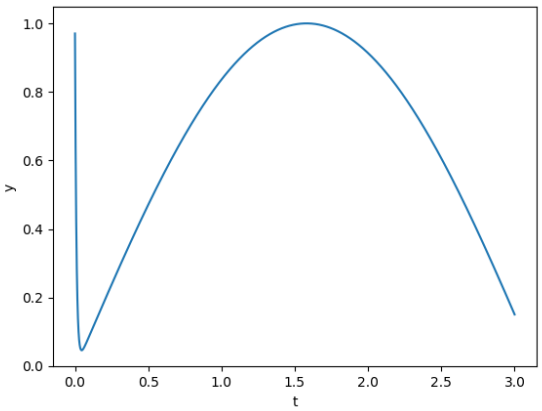

Figure 4.3: *Approximate solution to equation 4.21 using BDF*

Coming back to ODE of the SWAP operation 4.20 the rapidly varying terms are the spin states $|\uparrow\downarrow\rangle, |\downarrow\uparrow\rangle$ while the slowly varying terms are the singlet states $S(2,0)$ and $S(0,2)$. If we set $U_1 = U_2$ such that $\log \frac{U_1}{t_0} \approx= 1$ the rate of the variation of the solutions will be closer to eachother which means that the solver can use a larger stepsize h therefore less computational time is required. Fig. 4.4 is the solution for the same ODE system as the SWAP 4.20 but with values $U_1 = U_2$ and t_0 being of similar size, the variations of the

singlet states become similar to the variation of the other spin states, the computational time for this calculation is reduced from 18.19 sec to 1.93s, which validates the stiffness of the ODE.

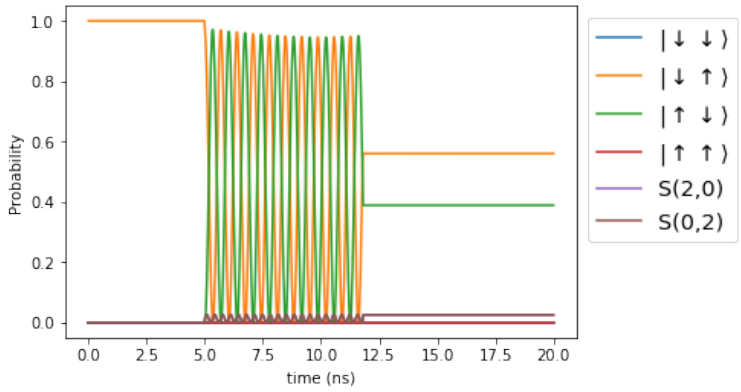

Figure 4.4: *Approximate solution to the SWAP operation 4.20 with U and t_0 being of similar value with Total run time: 1.93s*

For quantum computation we are only interested in the states $\{|\downarrow,\downarrow\rangle, |\downarrow,\uparrow\rangle, |\uparrow,\downarrow\rangle, |\uparrow,\uparrow\rangle\}$ as these correspond to the computational basis states $\{|00\rangle, |01\rangle, |10\rangle |11\rangle\}$. Previously we've seen that the double dot Hamiltonian reduces to the Heisenberg Hamiltonian (via the Schrieffer-Wolff transformation) for values of $U_{1,2} >> t_0$, i.e. the ODE system has a high degree of stiffness, therefore we will only consider Hamiltonians with values that validate this approximation, i.e. high degree of stiffness.

The initial values of the states $y(0)$ will always have zero amplitude for the singlet states $S(2,0)$ and $S(0,2)$, since we are not interested in these states. The Hamiltonians and initial values are such that they induce significant amplitude transitions between the basis states and neglibible amplitude transitions between the basis states and singlet states, e.g. the amplitudes of singlet states remain rather constant on the time scale where the basis states vary rapidly. This is equivalent to approximating the time derivative of the singlet states to zero $y_4' = y_5' \approx 0$.

$$\begin{pmatrix} y_0' \\ y_1' \\ y_2' \\ y_3' \\ 0 \\ 0 \end{pmatrix} = \begin{pmatrix} 0 \\ t_0 e^{i\Delta E_z t/\hbar}(y_4 + y_5) \\ -t_0 e^{-i\Delta E_z t/\hbar}(y_4 + y_5) \\ 0 \\ t_0 e^{-i\Delta E_z t/\hbar} y_1 - t_0 e^{i\Delta E_z t/\hbar} y_2 + U_1 y_4 \\ t_0 e^{-i\Delta E_z t/\hbar} y_1 - t_0 e^{i\Delta E_z t/\hbar} y_2 + U_2 y_5 \end{pmatrix} \tag{4.22}$$

The last two equations can now be used to substitute y_4 and y_5 in terms of y_1 and y_2.

$$y_4 = -(t_0 e^{-i\Delta E_z t/\hbar} y_1 - t_0 e^{i\Delta E_z t/\hbar} y_2)/U_1$$
$$y_5 = -(t_0 e^{-i\Delta E_z t/\hbar} y_1 - t_0 e^{i\Delta E_z t/\hbar} y_2)/U_2$$

Inserting these back into the ODE system 4.22

$$\begin{pmatrix} y_0' \\ y_1' \\ y_2' \\ y_3' \end{pmatrix} = \begin{pmatrix} 0 \\ -\left(\frac{t_0^2}{U_1}+\frac{t_0^2}{U_2}\right) y_1 + e^{2i\Delta E_z t/\hbar}\left(\frac{t_0^2}{U_1}+\frac{t_0^2}{U_2}\right) y_2 \\ e^{-2i\Delta E_z t/\hbar}\left(\frac{t_0^2}{U_1}+\frac{t_0^2}{U_2}\right) y_1 - \left(\frac{t_0^2}{U_1}+\frac{t_0^2}{U_2}\right) y_2 \\ 0 \end{pmatrix} \tag{4.23}$$

Rewriting this in the form $y' = Ay$.

$$\begin{pmatrix} y_0' \\ y_1' \\ y_2' \\ y_3' \end{pmatrix} = \begin{pmatrix} 0 & 0 & 0 & 0 \\ 0 & -\left(\frac{t_0^2}{U_1}+\frac{t_0^2}{U_2}\right) & \left(\frac{t_0^2}{U_1}+\frac{t_0^2}{U_2}\right) e^{2i\Delta E_z t/\hbar} & 0 \\ 0 & \left(\frac{t_0^2}{U_1}+\frac{t_0^2}{U_2}\right) e^{-2i\Delta E_z t/\hbar} & -\left(\frac{t_0^2}{U_1}+\frac{t_0^2}{U_2}\right) & 0 \\ 0 & 0 & 0 & 0 \end{pmatrix} \begin{pmatrix} y_0 \\ y_1 \\ y_2 \\ y_3 \end{pmatrix} \tag{4.24}$$

Since the terms in this ODE system do not differ by a large magnitude, it is not considered stiff and numerical solvers should be able to solve this in a quicker time than the stiff version 4.20. For $U_1 = U_2 = U$ this reduces to the Heisenberg Hamiltonian in the rotating frame with $J/2 = 2t_0^2/U$ in agreement with the Schrieffer-Wolff transformation. Implementing this in QuTiP

```
HJ1 = np.zeros((4,4),dtype=complex);HJ1[1,1]=1;HJ1[2,2]=1
HJ2 = np.zeros((4,4),dtype=complex);HJ2[1,2]=1
HJ3 = np.zeros((4,4),dtype=complex);HJ3[2,1]=1
HJ1=qt.Qobj(HJ1);HJ2=qt.Qobj(HJ2);HJ3=qt.Qobj(HJ3)

H0=qt.Qobj(np.zeros((4,4)))

args = {'B1':2e9, 'B2':2e9, 'Bmw':5e6,'vi':0,'w_k':2e9,'t0':4.3e9,
        'det':0, 'U1':1e12, 'U2':1e12}
tlist = np.linspace(0,20e-9,1000)
det = 'det'
time_int = '*(5e-9<=t<=11.8e-9)'

HJ1c = '-2*np.pi*t0**2*(1/(U1+'+det+')+1/(U2-'+det+'))'+time_int
HJ2c = '2*np.pi*np.exp(2j*2*np.pi*(B1-B2)/2*t)*t0**2*(1/(U1+'+det+\
')+1/(U2-'+det+'))'+time_int
HJ3c = '2*np.pi*np.exp(-2j*2*np.pi*(B1-B2)/2*t)*t0**2*(1/(U1+'+det+\
')+1/(U2-'+det+'))'+time_int

H = [H0,[HJ1,HJ1c],[HJ2,HJ2c],[HJ3,HJ3c]]
```

```
psi0=qt.basis(4,1)

output = qt.mesolve(H,psi0,tlist,[],[],args=args,
                    options=qt.Options(nsteps=250000, method='bdf')
                    ,progress_bar=True)
plot_states(tlist,output)
>>>Total run time: 0.69s
```

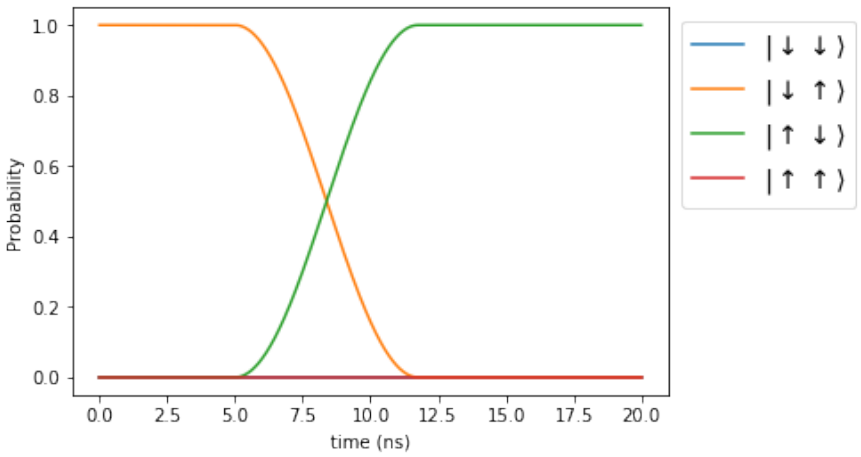

Figure 4.5: *SWAP operation with a reduced double dot ODE system*

Comparing these result with the full ODE system 4.20, the reduced ODE system 4.24 is solved significantly faster, 18.19s versus 0.69s

4.1.3 Grover's algorithm with QuTiP

In this section we will combine a sequence of gates to implement the two qubit Grover's algorithm and test QuTiP's accuracy. The results of the simulations will be compared to the experimental realization of the two qubit algorithm in reference [28]. The parameters in the two-electron Hamiltonian are the following: the Zeeman energies (or qubit frequencies) are B_1 = 18.4 GHz and $B_2 = 19.7$ GHz. The coulomb interactions of the dots are $U_1 = 850$ GHz and $U_2 = 840$ GHz, the tunnel coupling is $t_0 = 210$ MHz. The value for the detuning ϵ for which the CZ gate is implemented is chosen such that $J << \Delta E_z$ so that the eigenstates of the system are still the two-spin product states $\{|\uparrow\downarrow\rangle, |\downarrow\uparrow\rangle\}$ and where the exchange coupling $J = 6$ MHz. As a reminder Fig. 4.6 shows how $J(\epsilon)$ is defined: it is the decrease of the energy of the anti-parallel states compared to their energies at $\epsilon = 0$. $J(\epsilon)$ can be found by diagonlizing the two-electron Hamiltonian as a function of the detuning ϵ. Fig. 4.7 shows the result of calculating J for the given parameters.

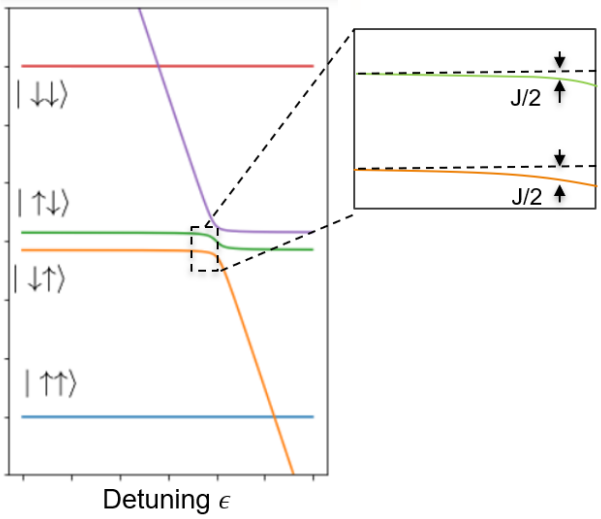

Figure 4.6: *Energy dispersion of the double dot system as a functino of the detuning ϵ. J is defined by the decrease of the energy states compared to their energies at $\epsilon = 0$.*

```
import numpy as np
from scipy import linalg as la

def set_Hamiltonian(B1,B2,t,U1,U2,e):
    '''Initializes the two electron spin hamiltonian

       args:
           B1,B2,t,U1,U2,e (double): the energy terms.

       Returns:
           [6,6] array representing the Hamiltonian
```

```
    '''
    h = np.zeros((6,6))
    h[0,0]=-Ez
    h[1,1]=-dEz/2;h[1,4:6]=t
    h[2,2]=dEz/2;h[3,4:6]=-t
    h[3,3]=Ez
    h[4,1]=t;h[4,2]=-t;h[4,4] = U1+e
    h[5,1]=t;h[5,2]=-t;h[5,5]=U2-e
    return h

def eval_num0(B1,B2,t,U1,U2,erange):
    '''Calculates the eigenvalues of the Hamiltonian as a function
      of detuning
       Parameters:
           B1,B2,t,U: the energy terms.
           erange: the detuning energy range as a 1D numpy array
       Returns:
            eig_vals [6,len(erange)] array where each row is an
     eigenvalue as a function of detuning
    '''
    eig_vals = np.zeros((6,len(erange)))
    for i, e in enumerate(erange):
        h = set_Hamiltonian(B1,B2,t,U1,U2,e)
        w, v = la.eigh(h)
        eig_vals[:,i]=w
    return eig_vals
#function that calculates and plots J
def plot_J(eigen_values,detuning_range,zero_point):
    stat = [r'$|\downarrow\downarrow\rangle$',
            r'$|\uparrow\downarrow\rangle$',
            r'$|\downarrow\uparrow\rangle$',
        r'$|\uparrow\uparrow\rangle$', 'S(2,0)','S(0,2)']
    plt.figure()
    J = abs((eigen_values[1,:]-zero_point[1])/1e6)+\
    abs((eigen_values[2,:]-zero_point[2])/1e6)
    plt.plot(convert_eV(detuning_range)*1000,J,label = 'J')
    plt.legend()
    plt.title('Exchange energy J')
    plt.xlabel('$\epsilon$ (meV)')
    plt.ylabel('Energy (MHz)')
    plt.ylim([-10,10])
    plt.show()
    return J
```

```
#Hamiltonian parameters
B1=18.4e9;B2=19.7e9;t=0.210e9;U1=850e9;U2=840e9;
#the range of the detuning parameter
detuning_range_cphase=invert_eV(np.arange(3.3,3.6,0.0001)*1e-3)
# calculate the eigenvalues are a function of detuning
eigen_values_for_cphase = eval_num0(B1,B2,t,U1,U2,detuning_range_cphase)
#calculate exact zero point where detuning = 0
zero_point,v = la.eigh(set_Hamiltonian(B1,B2,t,U1,U2,e=0))
#calculate and plot J
J = plot_J(eigen_values_for_cphase,detuning_range_cphase,zero_point)
#find the detuning for which J=6 MHz
#value of detuning in Hz
detuning_cphase = detuning_range_cphase[np.argmin(abs(J-6))]
#value of detuning in eV
detuning_cphase_eV = convert_eV(detuning_cphase)
print(detuning_cphase, ' Hz and ',detuning_cphase_eV, ' eV')
>>> 825646613506.6794  Hz and  0.003414600000000242  eV
```

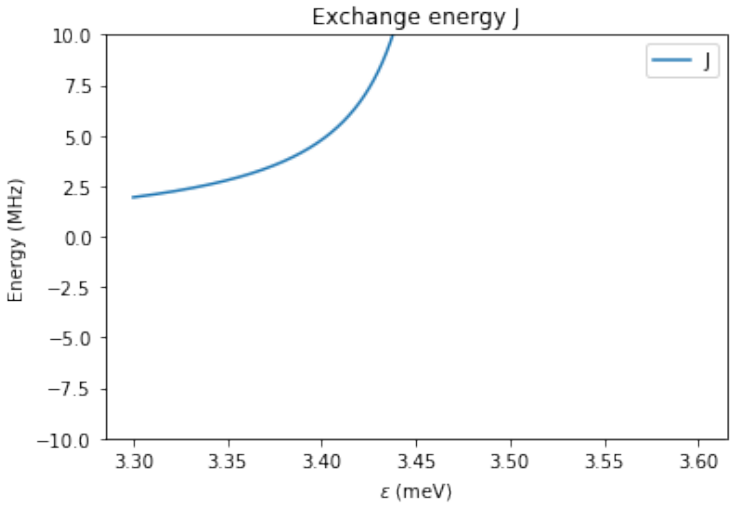

Figure 4.7: *The exchange interaction J as a function of ϵ*

Having the range of detuning ϵ necessary for the CZ gate we can now implement Grover's algorithm in QuTiP through the gate sequence 4.8 We will first use the *stiff* 6×6 Hamiltonian

args = $\{B_1 = 18.4e9, B_2 = 19.7e9, B_{mw} = 2e6, tunnel_coupling = 0.250e9, U_1 = 850e9, U_2 = 840e9, \dots\}$
#Rotate qubit 1 and 2 by $\pi/2$ radians to obtain equal superposition
$Ry_1 =$ add_magnetic_pulse(args, $\omega_k = 18.4e9, 100e-9 <= t <= 225e-9$)

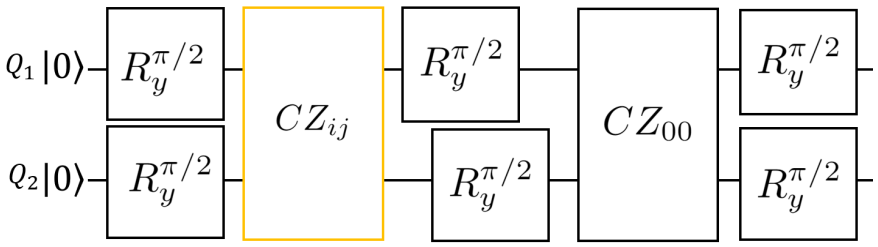

Figure 4.8: *Gate sequence of Grover's algorithm*

$Ry_2 =$ add_magnetic_pulse(args, $\omega_k = 19.7e9, 100e-9 <= t <= 225e-9$)

#Pulse the detuning ϵ to the value as calculated, to obtain the CZ_{ij} gate
$CZ_{ij} =$ add_detuning_pulse(args, $\epsilon, 225e-9 <= t <= 310e-9$)

#Rotate qubit 1 by $\pi/2$ radians to obtain a Bell state, then rotate qubit 2 to obtain an equal superposition
$Ry_1 =$ add_magnetic_pulse(args, $\omega_k = 18.4e9, 325e-9 <= t <= 450e-9$)
$Ry_2 =$ add_magnetic_pulse(args, $\omega_k = 19.7e9, 325e-9 <= t <= 450e-9$)

#Pulse the detuning ϵ to the value as calculated, to apply the CZ_{00} gate
$CZ_{00} =$ add_detuning_pulse(args, $\epsilon, 451e-9 <= t <= 536e-9$)

#Rotate qubit 1 and 2 to undo the superposition
$Ry_1 =$ add_magnetic_pulse(args, $\omega_k = 18.4e9, 560e-9 <= t <= 685e-9$)
$Ry_2 =$ add_magnetic_pulse(args, $\omega_k = 19.7e9, 560e-9 <= t <= 685e-9$)

#adding all of the above to the QuTiP description of the Hamiltonian
H = [...]
psi0=qt.basis(6,0)
output = qt.mesolve(H,psi0,tlist,[],[],args=args,
options=qt.Options(nsteps=60000,method='bdf'),progress_bar=True)

Appedix shows the full code of the QuTiP grover implementation. The CZ_{ij} gates are chosen by choosing the correct $\hat{z}$-rotations $R_z(\theta)$ as we've seen from equation 3.62. Since $\hat{z}$-rotations do not affect the outcome of measuring the computation basis $|0\rangle, |1\rangle$, we simply add these $\hat{z}$-rotations by changing the phase of the reference frame throughout the pulse sequence via microwave pulses instead of actually performing them.[19] Plotting the results of the simulation for the 4×4 and 6×6 Hamiltonian for the $CZ_{ij} = CZ_{00}$ gate in Fig. 4.10

Due to the stiffness of the ODE $6\times$ system, the simulation took 5 hours to finish on a intel core i7. Using the reduced non-stiff 4×4 Hamiltonian with the exact same parameter values the simulation time was 30s. There is a clear difference between the two Hamiltonians, even though the approximation $y_4' = 0$ and $y_5' = 0$ is reasonable, small errors

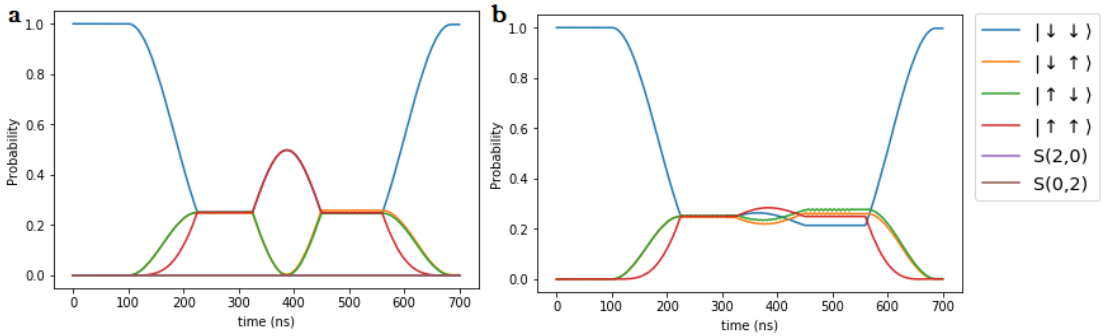

Figure 4.9: *Simulation of Grover's Algorithm using QuTiP for the highly stiff ODE system* **a** *(6×6 Hamiltonian) and non-stiff ODE system* **b***(4×4 Hamiltonian) using the same parameter values.*

can accumulate to large discrepancies for long simulation times, i.e. a large integration domain. By adjusting the tunnel coupling for the reduced Hamiltonian from $0.250 \cdot 10^9$ to $0.190 \cdot 10^9$ we obtain results similar to the full Hamiltonian.

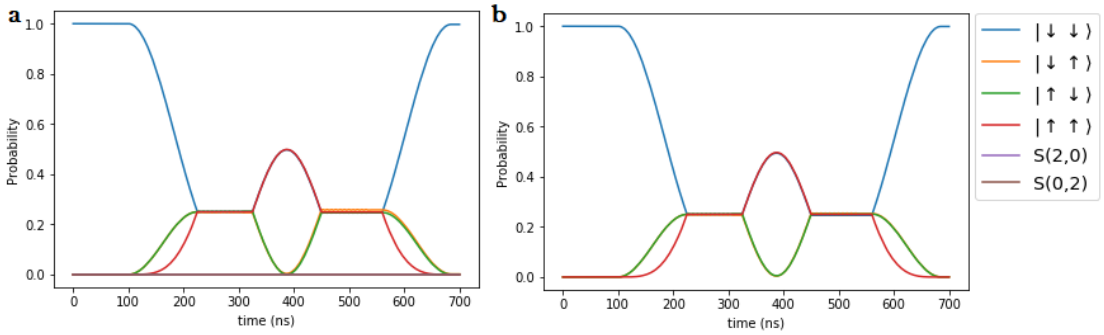

Figure 4.10: *Simulation of Grover's Algorithm using QuTiP for the highly stiff ODE system* **a** *(6×6 Hamiltonian) and non-stiff ODE system* **b***(4×4 Hamiltonian) using a slightly smaller tunnel coupling for the* 4×4 *system.*

The parameter values used in the simulations are based on the experimental values used in the physical realization of Grover's alorithm in [28]. Comparing the QuTiP results with the experimental values in Fig. 4.11

We see that the first half of the simulation quite nicely correspond to the experimental values, however due to experimental errors, environmental magnetic noise, fluctuating nuclear spins in the sample, charge noise of the dots etc. building up over time, the end results of the experiments will be less consistent.

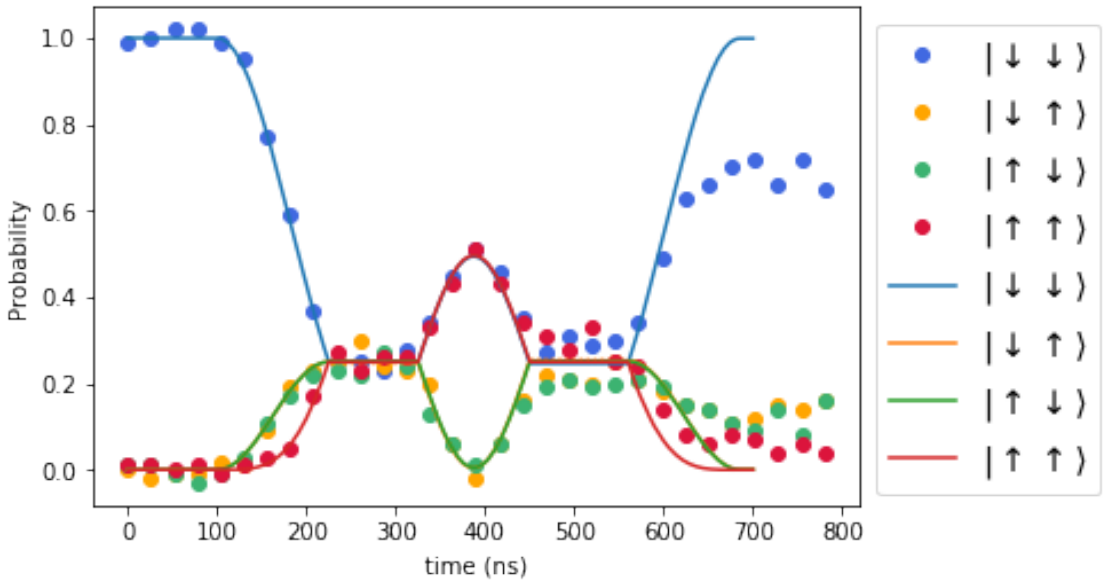

Figure 4.11: *Grover's algorithm QuTiP simulation given by the straight lines and the experimental values given by dots.*

4.2 Numerics with Liouville von Neumann

Instead of solving a system of ODE we can approach the problem more "organically" with Liouville von Neumann equation for the density matrix.

$$i\hbar\frac{\partial\rho}{\partial t} = [H, \rho] \tag{4.25}$$

The time evolution of the density matrix over the time interval between t and $t+\delta t$ is given by

$$\rho(t+\delta t) = G(t+\delta t)\rho(t)G(t+\delta t)^{\dagger} \tag{4.26}$$

where $G(t+\delta t)$ is the wavefunction propagator,

$$G(t+\delta t) = \exp\left(-i\hbar\int_{t}^{t+\delta t} H(t')dt'\right) \tag{4.27}$$

The integral in the exponent can be approximated by a Riemann sum

$$\begin{aligned}\int_a^b H(t)dt &\approx H(a)\delta t + H(a+\delta t)\delta t + H(a+2\delta t)\delta t + \cdots + H(b)\delta t \\ &\approx \sum_{n=0}^{N} H(a+n\delta t)\delta t \quad , a+N\delta t = b\end{aligned} \tag{4.28}$$

From a numerical point of view the most straining issue is the calculation of the matrix exponential $G(t)$. The matrix exponential is defined from the Taylor expansion

$$e^{iH} = \mathcal{I} + iHt + \frac{(iHt)^2}{2!} + \dots \tag{4.29}$$

This method is simple to implement however not recommended as higher terms of the series are lage and of opposite signs, resulting in numerical instability [33]. Another approach would be diagonalize H, since exponents of diagonalizable matrices are simple to evaluate.

$$e^{iHt} = Ue^{iDt}U^{\dagger} \tag{4.30}$$

where D is diagonal and U is unitary. The main problem of this approach is the computational cost of the evaluation of the eigenvalues and eigenvectors which scales as $\sim O(N)^3$. A full diagonalization is computational extremely inefficient. Instead we will use one of the most common methods for matrix exponentiation, the Pade expansion in combination with a scaling and squaring technique[34]. The method is based on the approximation

$$e^A \approx \sum_m P_m(A) \tag{4.31}$$

where P_m are the Padé polynomials. The scaling and squaring technique is based on the following, every matrix exponential can be written as

$$e^A = (e^{2^{-s}A})^{2^s} \tag{4.32}$$

The value of s is such that s is the smallest value for which $||A||/2^s \leq 1$. The Padé expansion is applied to the scaled matrix $e^{2^{-s}A}$, and then e^A is obtained by repeated squaring. This method provides extremely accurate results for any matrix A. The SciPy python library already has a function *expm* that calculates matrix exponentiation via the Padé method so we don't have to write it.

4.2.1 Simulation class

All the necessary elements to calculate the density operator 4.26 have been written in the class *simulation_two_dots()* (see Appendix C). This method is heavily inspired by [28], however it is completely written in python which allows an easy to read and edit code suitable for people who are interested in learning more about manipulating spin qubits. A simulation object is created by calling the simulation class and initializing all the static terms in the Hamiltonian.

```
s = simulation_two_dots(B1=1e9,B2=2e9,tunnel_coupling=0,U1=2e12,U2=2.1e12)
```

As an example we can apply a magnetic field pulse with amplitude $B_{mw} = 5 \cdot 10^6$ for a time $2\pi B_{mw} t = \pi$ that rotates qubit 1 by 180° degrees around the $\hat{x}$-axis.

```
#Rabi_freq, phase, drive_freq, t_start, t_end
s.add_magnetic_pulse(0.5e7,0,1e9,10e-9,110e-9)
```

The system can then be evolved between two user defined times via 4.26, in this case between $0 <= t <= 200$ ns. The initial state is the ground state $|00\rangle$

```
#state to elove, t_start, t_end, nsteps,nsamples
d=s.evolve(0,0,200e-9,1000,nsamples=1)
```

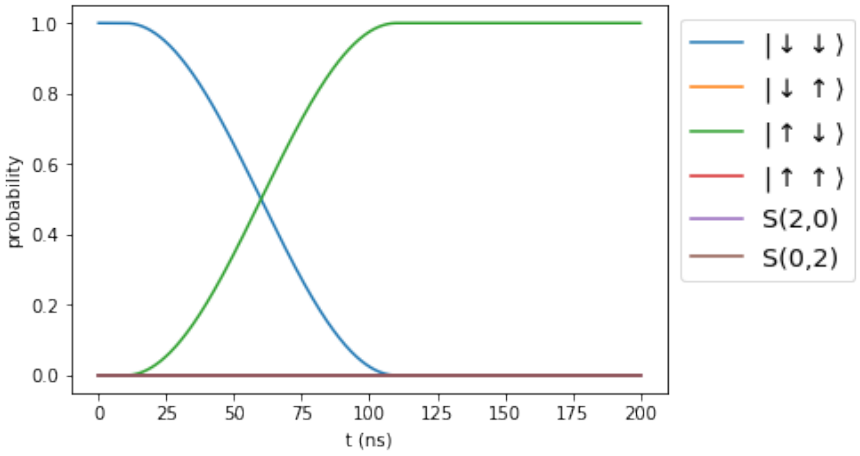

Figure 4.12: *180 degree rotation of a qubit around the $\hat{x}$-axis, initialized in the $|0\rangle$ state*

4.2.2 Grover's algorithm

The Grover's algorithm can be implemented in a succinct and clear manner

```
#phases that determine what CZ gate to apply
phase_q1 = np.pi/2
phase_q2 = np.pi/2

detE = 828.6e9
a = 35e-9
#create a two dot simulation object
grover = simulation_two_dots(19.7e9,18.4e9,0.250e9,850e9,840e9)

#Add magnetic pulses that rotate both qubits pi/2 radians
#to create an equal superposition
grover.add_magnetic_pulse(2e6,np.pi/2,18.4e9,100e-9,225e-9)
```

```
grover.add_magnetic_pulse(2e6,np.pi/2,19.7e9,100e-9,225e-9)

#Add detuning pulse to apply the CZ gate (the oracle of the grover algorithm)
grover.add_detuning_pulse(detE,225e-9,275e-9+a)

#Create Bell state and equal superposition with marked state
grover.add_magnetic_pulse(2e6,np.pi/2+phase_q1,19.7e9,325e-9,450e-9)
grover.add_magnetic_pulse(2e6,np.pi/2+phase_q2,18.4e9,325e-9,450e-9)

grover.add_detuning_pulse(detE,451e-9,501e-9+a)

#Required for readout, "undo" the superposition
grover.add_magnetic_pulse(2e6,np.pi+phase_q1,19.7e9,560e-9,685e-9)
grover.add_magnetic_pulse(2e6,np.pi+phase_q2,18.4e9,560e-9,685e-9)

time0 = time.time()
#Evolve the system
psi0=0
U_t,rhos,psi0_t,sa=grover.evolve(psi0,0,700e-9,nsteps=3000,nsamples=1)
print(np.around(time.time()-time0,2), " s")
>>>Elapsed time for the unitary evolution operator: 1.12 s
```

The Hamiltonians for this simulation used are the full 6×6 Hamiltonian which was calculated in about 1.12s which is much faster than QuTiP's ODE solver which required 5 hours. The results of QuTiP's solver and the numerical solver are in agreement Fig. 4.13 When

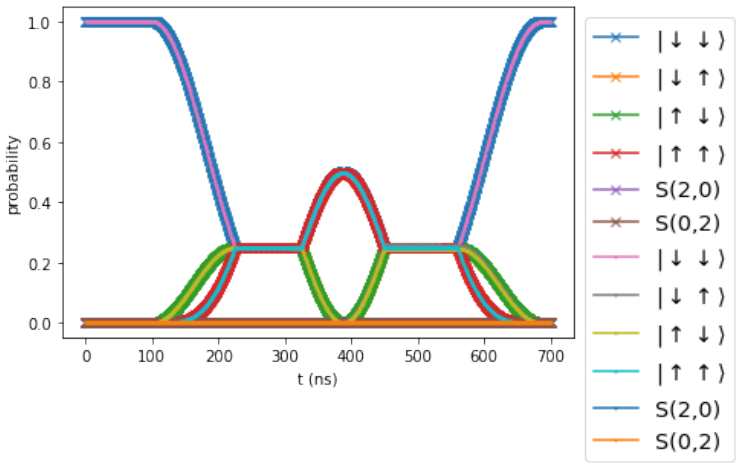

Figure 4.13: *Grover algorithm simulation using QuTiP, marked by the circle and lines, and the numerical solver, marked by the cross and line.*

we considered the reduced 4×4 Hamiltonian with QuTiP, we saw that the approximation

produces an error in contrast to the 6×6 Hamiltonian, this same error is produced by the numerical solver Fig. 4.14 when using the 4×4 Hamiltonian.

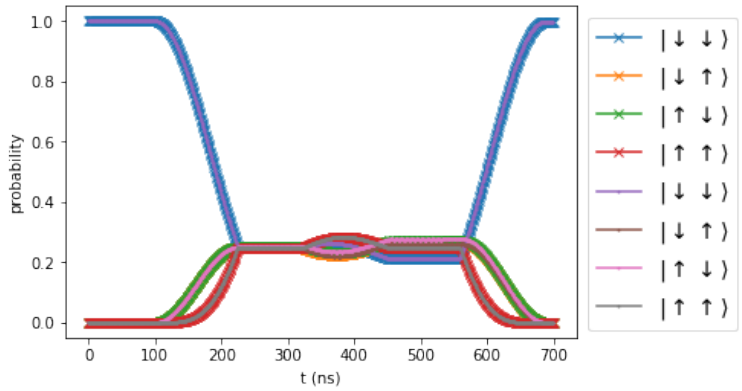

Figure 4.14: *Grover algorithm simulation using QuTiP, marked by the circle and lines, and the numerical solver, marked by the cross and line.*

So we can atleast conclude that the numerical solver properly evolves the schrodinger wavefunction. Since the numerical solver is able to calculate the evolution via the 6×6 Hamiltonians in a timely manner, we don't have to consider using the reduced 4×4 Hamiltonians to improve the computational time, unless QuTiP is used.

4.2.3 Noise considerations

An advantage of the numerical solver, is the ease of manipulating the time-dependent coefficients in the Hamiltonians, we can for example easily add a noise term to the Zeeman energies of the dots and the amplitude of the applied magnetic field. The noise terms added are sampled from a gaussian with probability density

$$p(x) = \frac{1}{\sqrt{2\pi\sigma^2}} e^{-\frac{(x-\mu)^2}{2\sigma^2}} \tag{4.33}$$

where μ is the mean and σ the standard deviation. In the simulation the amplitude B_{mw} of the applied magnetic field and the Zeeman energies B_1, B_2 of the dots are chosen from this distrubition. In the following example Fig. 4.15, the standard deviation is chosen quite large to accentuate the effect of noise on the system.

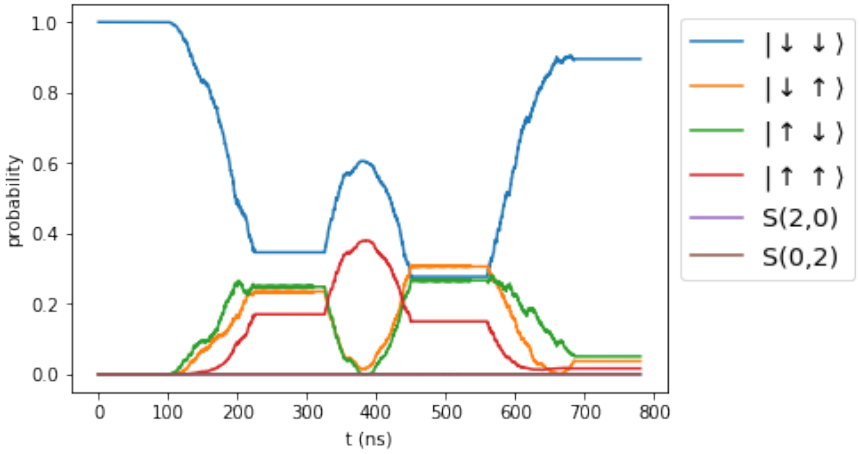

Figure 4.15: *Grover algorithm with the magnetic fields sampled form a gaussian distribution*

To reduce the noise we can run the simulation multiple times by increasing $nsamples$ option and averaging over all simulation runs. For example the following result has been averages over 10 runs, comparing it with the experimental values

The standard deviation and mean of the gaussian distribution was chosen through an educated guess and is most likely not consistent with actual experimental values, here we just show that the addition of noise will result into simulation results similar to experimental values.

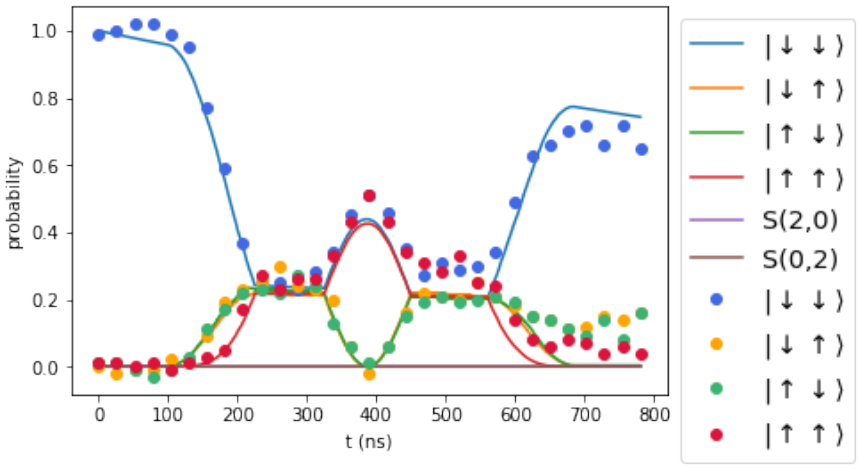

Figure 4.16: *Grover algorithm simulation with gaussan magnetic noise compared to the experimental values (dotted data)*

4.3 Conclusion and Further work

In this thesis we have presented two numerical algorithms for the solution of the Schrödinger Equation (SE) for the system of a two-electron quantm dot. QuTiP offers a user-friendly environment for solving the SE for general Hamiltonians and especially for implementing time-dependent Hamiltonians. The problem we have encountered with QuTiP is that the time-dependent solvers are all based on solving the SE by complicated methods of integration of ODE systems. Computational problems arise when the ODE system has a high degree of stiffness, simulation time of $\sim$ 1000ns require in real time $\sim$ 5 hours to solve on a commercial pc. We've seen that the two-electron Hamiltonian reduces to the proper two-qubit quantum gates CZ and C_{SWAP} if the the subspaces $\{S(2,0), S(0,2)\}$ and $\{|\downarrow,\downarrow\rangle, |\downarrow,\uparrow\rangle, |\uparrow,\downarrow\rangle, |\uparrow,\uparrow\rangle\}$ are energetically well seperated, i.e $U >> t$, which makes the ODE system per definition stiff. This computational slowdown due to the stiffness of the ODE system can be overcome by reducing the Hamiltonian to the subspace of the (1,1) electron configuration, which reduces the real time calculation to the order $\sim$ 30 s, however the approximation does introduce further numerical errors.

The second method relies on the Liouville von Neumann equation, which can be implemented by simple methods as the Riemann sum and scaling and squaring methods. The numerical method shows results in agreement with QuTiP while solving the full Hamiltonian system in mere seconds. Very simple noise models have been implemented in the numerical solver in a monte-carlo esque method to show the effectiveness of noise on the system. Further research based on experimental considerations needs to be done to properly introduce noise into the simulation.

An interesting point of research would be to introduce the noise of the system via coupling to the environment. The Lindblad Master equation is an extension to the Liouville

von Neumann equation for open quantum systems.

$$\frac{\partial \rho(t)}{\partial t} = -\frac{i}{\hbar}[H(t), \rho(t)] + \sum_n \frac{1}{2}\left[2C_n\rho(t)C_n^+ - \rho(t)C_n^+C_n - C_n^+C_n\rho(t)\right] \tag{4.34}$$

where $C_n = \sqrt{\gamma_n}A_n$ are collapse operators and A_n are the operators that couple the environment to the system H, γ_n are the decay rates. The main problem will be to find the correct form of the coupling operators A_n that will properly implement the charge and magnetic noise in the system. Currently the applied pulses are applied as a step function, the simulation will be more realistic if instead of a step function some ramp up function is used to initiate pulses. The numerical solver still has some room for improvement, currently the evolution operator $G(t)$ is calculated in parallel for a range of time t, however there are still some for loops that can be eliminated in the calculations.

Appendix A

Schrieffer-Wolff Transformation

The generator S of the Schrieffer Wolff transfrmation for the double dot Hamiltonian

$$H = H_0 + V = \begin{pmatrix} -\bar{E}_z & 0 & 0 & 0 & 0 & 0 \\ 0 & -\Delta E_z & 0 & 0 & t_0 & t_0 \\ 0 & 0 & \Delta E_z & 0 & -t_0 & -t_0 \\ 0 & 0 & 0 & \bar{E}_z & 0 & 0 \\ 0 & t_0 & -t_0 & 0 & U_1 + \epsilon & 0 \\ 0 & t_0 & -t_0 & 0 & 0 & U_2 - \epsilon \end{pmatrix} \tag{A.1}$$

is given by [21] (see [22] and [23] for methods of finding S for general Hamiltonians)

$$S = \begin{pmatrix} 0 & 0 & 0 & 0 & 0 & 0 \\ 0 & 0 & 0 & 0 & -\gamma\left(-\Delta E_z\right) & -\sigma\left(-\Delta E_z\right) \\ 0 & 0 & 0 & 0 & \gamma\left(\Delta E_z\right) & \sigma\left(\Delta E_z\right) \\ 0 & 0 & 0 & 0 & 0 & 0 \\ 0 & \gamma\left(-\Delta E_z\right) & -\gamma\left(\Delta E_z\right) & 0 & 0 & 0 \\ 0 & \sigma\left(-\Delta E_z\right) & -\sigma\left(\Delta E_z\right) & 0 & 0 & 0 \end{pmatrix} \tag{A.2}$$

where

$$\gamma(\Delta E_z) = \frac{t_0}{U + \epsilon - \Delta E_z}$$
$$\sigma(\Delta E_z) = \frac{t_0}{U - \epsilon - \Delta E_z}$$

To check whether S is indeed a generator, the reader is invited to calculate whether the commutator of S and H_0 indeed results in $-V$, $[S, H_0] = -V$. The Schrieffer-Wolff transformation $e^S H e^{-S}$ up to second order is

$$H_e = H_0 + \frac{1}{2}[S, V] + O(S^3) \tag{A.3}$$

Calculating the commutator $[S,V]$ with V the off-diagonal tunnel elements of the double dot Hamiltonian

$$\frac{1}{2}[S,V] = \frac{1}{2}(SV - VS) = \tag{A.4}$$

$$= \frac{t_0}{2}\begin{pmatrix} 0 & 0 & 0 & 0 & 0 & 0 \\ 0 & -2\alpha(-\Delta E_z) & \beta(\Delta E_z) & 0 & 0 & 0 \\ 0 & \beta(\Delta E_z) & -2\alpha(\Delta E_z) & 0 & 0 & 0 \\ 0 & 0 & 0 & 0 & 0 & 0 \\ 0 & 0 & 0 & 0 & 2\gamma(\Delta E_z) + 2\gamma(-\Delta E_z) & \beta(\Delta E_z) \\ 0 & 0 & 0 & 0 & \beta(\Delta E_z) & 2\sigma(\Delta E_z) + 2\sigma(-\Delta E_z) \end{pmatrix} \tag{A.5}$$

where

$$\begin{aligned} \alpha(\Delta E_z) &= \gamma(\Delta E_z) + \sigma(\Delta E_z) \\ \beta(\Delta E_z) &= \alpha(\Delta E_z) + \alpha(-\Delta E_z) \end{aligned}$$

In the limit $\epsilon << U$ and $\Delta E_z << U$

$$\begin{aligned} t_0\alpha(\Delta E_z) &= \frac{t_0^2}{U + \epsilon - \Delta E_z} + \frac{t_0^2}{U - \epsilon - \Delta E_z} \approx \frac{2t_0^2}{U} \\ t_0\beta(\Delta E_z) &= \frac{t_0^2}{U + \epsilon - \Delta E_z} + \frac{t_0^2}{U - \epsilon - \Delta E_z} + \frac{t_0^2}{U + \epsilon + \Delta E_z} + \frac{t_0^2}{U - \epsilon + \Delta E_z} \\ &\approx \frac{4t_0^2}{U} \end{aligned} \tag{A.6}$$

In the subspace $\{|\downarrow,\downarrow\rangle, |\downarrow,\uparrow\rangle, |\uparrow,\downarrow\rangle, |\uparrow,\uparrow\rangle\}$ the 2nd order correction $\frac{1}{2}[S,V]$ results in

$$\frac{1}{2}[S,V] \approx \begin{pmatrix} 0 & 0 & 0 & 0 \\ 0 & -2t_0^2/U & 2t_0^2/U & 0 \\ 0 & 2t_0^2/U & -2t_0^2/U & 0 \\ 0 & 0 & 0 & 0 \end{pmatrix} \tag{A.7}$$

The effective Hamiltonian now reads

$$H_e = H_0 + \frac{1}{2}[S,V] = \begin{pmatrix} -\bar{E}_z & 0 & 0 & 0 \\ 0 & -\Delta E_z - 2t_0^2/U & 2t_0^2/U & 0 \\ 0 & 2t_0^2/U & \Delta E_z - 2t_0^2/U & 0 \\ 0 & 0 & 0 & \bar{E}_z \end{pmatrix} \tag{A.8}$$

which is the same as the Heisenberg Hamiltonian 3.66 with $J/2 = 2t_0^2/U$.

Appendix B

RWA Two qubit Hamiltonian

In this section we will calculate the double dot Hamiltonian in the rotating frame using the rotating wave approximation (RWA). The double dot Hamiltonian is

$$H = \begin{pmatrix} -\bar{E}_z & 0 & 0 & 0 & 0 & 0 \\ 0 & -\Delta E_z & 0 & 0 & t_0 & t_0 \\ 0 & 0 & \Delta E_z & 0 & -t_0 & -t_0 \\ 0 & 0 & 0 & \bar{E}_2 & 0 & 0 \\ 0 & t_0 & -t_0 & 0 & U_1 + \epsilon & 0 \\ 0 & t_0 & -t_0 & 0 & 0 & U_2 - \epsilon \end{pmatrix} = D + V \tag{B.1}$$

where $\bar{E}_z = \hbar(B_1^z + B_2^z)/2$ is the average zeeman energy of the dots and $\Delta E_z = \hbar(B_1^z - B_2^z)/2$ is the difference in zeeman energy. The constants g, $\hbar$ and μ_B have been absorbed in the magnetic fields $\frac{g\mu_B}{\hbar} B_k^i \equiv B_k^i$. D is the diagonal part and V the off-diagonal part of the Hamiltonian. The control Hamiltonian that controls single qubit rotations

$$H_{mw} = \sum_k B_{mw} \cos\left(\omega_k t + \phi_k\right) \left(\sigma_x \otimes \mathbb{I} + \mathbb{I} \otimes \sigma_x\right) \tag{B.2}$$

These Hamiltonians are transformed to the rotating frame using the basis transformation

$$H' = UHU^\dagger + i\hbar \frac{dU}{dt} U^\dagger \tag{B.3}$$

where

$$U = e^{-i\frac{\omega_1 t}{2}\sigma_z} \otimes e^{-i\frac{\omega_2 t}{2}\sigma_z} \tag{B.4}$$

and $\omega_k = B_k^z$ is the Larmor frequency of qubit k. First let's calculate $i\hbar\frac{dU}{dt}U^\dagger$

$$\begin{aligned}
U &= \begin{pmatrix} e^{-i\frac{\omega_1}{2}t} & 0 \\ 0 & e^{i\frac{\omega_1}{2}t} \end{pmatrix} \otimes \begin{pmatrix} e^{-i\frac{\omega_2}{2}t} & 0 \\ 0 & e^{i\frac{\omega_2}{2}t} \end{pmatrix} \\
&= \begin{pmatrix} e^{-\frac{i}{2}(\omega_1+\omega_2)t} & 0 & 0 & 0 \\ 0 & e^{-\frac{i}{2}(\omega_1-\omega_2)t} & 0 & 0 \\ 0 & 0 & e^{\frac{i}{2}(\omega_1-\omega_2)t} & 0 \\ 0 & 0 & 0 & e^{\frac{i}{2}(\omega_1+\omega_2)t} \end{pmatrix} \\
&= \begin{pmatrix} e^{-i\omega t} & 0 & 0 & 0 \\ 0 & e^{-i\Delta\omega t} & 0 & 0 \\ 0 & 0 & e^{i\Delta\omega t} & 0 \\ 0 & 0 & 0 & e^{i\omega t} \end{pmatrix} \\
&= \begin{pmatrix} e^{-i\bar{E}_z t/\hbar} & 0 & 0 & 0 \\ 0 & e^{-i\Delta E_z t/\hbar} & 0 & 0 \\ 0 & 0 & e^{i\Delta E_z t/\hbar} & 0 \\ 0 & 0 & 0 & e^{i\bar{E}_z t/\hbar} \end{pmatrix}
\end{aligned}$$

where $\omega \equiv= \frac{\omega_1+\omega_2}{2}$ and $\Delta\omega = \frac{\omega_1-\omega_2}{2}$.

Since U_{ij} is a diagonal matrix of exponents $U_{ij} = e^{\lambda_{ij}t}\delta_{ij}$, where δ_{ij} is the kronecker delta that represents the unit matrix, the derivative will be of the form $\frac{dU}{dt} = \lambda_{ij}e^{\lambda_{ij}t}\delta_{ij} = \lambda_{ij}U_{ij}$

$$\begin{aligned}
&i\hbar\frac{dU}{dt} = \\
&i\hbar \begin{pmatrix} -\frac{i}{2}(\omega_1+\omega_2) & 0 & 0 & 0 \\ 0 & -\frac{i}{2}(\omega_1-\omega_2) & 0 & 0 \\ 0 & 0 & \frac{i}{2}(\omega_1-\omega_2) & 0 \\ 0 & 0 & 0 & \frac{i}{2}(\omega_1+\omega_2) \end{pmatrix} U
\end{aligned}$$

Then $\frac{dU_{ij}}{dt}U_{ij}^\dagger = \lambda_{ij}U_{ij}U_{ij}^\dagger = \lambda_{ij}\delta_{ij}$

$$\begin{aligned}
i\hbar\frac{dU}{dt}U^\dagger &= \begin{pmatrix} \frac{\hbar}{2}(\omega_1+\omega_2) & 0 & 0 & 0 \\ 0 & \frac{\hbar}{2}(\omega_1-\omega_2) & 0 & 0 \\ 0 & 0 & -\frac{\hbar}{2}(\omega_1-\omega_2) & 0 \\ 0 & 0 & 0 & -\frac{\hbar}{2}(\omega_1+\omega_2) \end{pmatrix} \\
&= \begin{pmatrix} \Delta\bar{E}_z & 0 & 0 & 0 \\ 0 & \Delta E & 0 & 0 \\ 0 & 0 & -\Delta E & 0 \\ 0 & 0 & 0 & -\bar{E}_z \end{pmatrix}
\end{aligned} \tag{B.5}$$

The double dot Hamiltonian $H = D + V$ in the rotating frame is $UHU^\dagger = UDU^\dagger + UVU^\dagger$. Since D is a diagonal matrix $D_{ij} = d_{ij}\delta_{ij}$ then

$$U_{ij}D_{ij}U_{ij}^\dagger = U_{ij}d_{ij}\delta_{ij}U_{ij}^\dagger = d_{ij}\delta_{ij}U_{ij}U_{ij}^\dagger = d_{ij}\delta_{ij} = D_{ij} \tag{B.6}$$

So the diagonal part of H stays the same in the rotating frame. The off-diagonal part

$$UVU^\dagger = U \begin{pmatrix} 0 & 0 & 0 & 0 & 0 & 0 \\ 0 & 0 & 0 & 0 & t_0 & t_0 \\ 0 & 0 & 0 & 0 & -t_0 & -t_0 \\ 0 & 0 & 0 & 0 & 0 & 0 \\ 0 & t_0 & -t_0 & 0 & 0 & 0 \\ 0 & t_0 & -t_0 & 0 & 0 & 0 \end{pmatrix} U^\dagger \tag{B.7}$$

where U is extended to the 6×6 matrix

$$U = \begin{pmatrix} e^{-i\bar{E}_z t/\hbar} & 0 & 0 & 0 & 0 & 0 \\ 0 & e^{-i\Delta E_z t/\hbar} & 0 & 0 & 0 & 0 \\ 0 & 0 & e^{i\Delta E_z t/\hbar} & 0 & 0 & 0 \\ 0 & 0 & 0 & e^{i\bar{E}_z t/\hbar} & 0 & 0 \\ 0 & 0 & 0 & 0 & 0 & 0 \\ 0 & 0 & 0 & 0 & 0 & 0 \end{pmatrix} \tag{B.8}$$

$$VU^\dagger = \begin{pmatrix} 0 & 0 & 0 & 0 & 0 & 0 \\ 0 & 0 & 0 & 0 & t_0 e^{i\Delta E_z t/\hbar} & t_0 e^{i\Delta E_z t/\hbar} \\ 0 & 0 & 0 & 0 & -t_0 e^{-i\Delta E_z t/\hbar} & -t_0 e^{-i\Delta E_z t/\hbar} \\ 0 & 0 & 0 & 0 & 0 & 0 \\ 0 & t_0 & -t_0 & 0 & 0 & 0 \\ 0 & t_0 & -t_0 & 0 & 0 & 0 \end{pmatrix} \tag{B.9}$$

$$UVU^\dagger = \begin{pmatrix} 0 & 0 & 0 & 0 & 0 & 0 \\ 0 & 0 & 0 & 0 & t_0 e^{i\Delta E_z t/\hbar} & t_0 e^{i\Delta E_z t/\hbar} \\ 0 & 0 & 0 & 0 & -t_0 e^{-i\Delta E_z t/\hbar} & -t_0 e^{-i\Delta E_z t/\hbar} \\ 0 & 0 & 0 & 0 & 0 & 0 \\ 0 & t_0 e^{-i\Delta E_z t/\hbar} & -t_0 e^{i\Delta E_z t/\hbar} & 0 & 0 & 0 \\ 0 & t_0 e^{-i\Delta E_z t/\hbar} & -t_0 e^{i\Delta E_z t/\hbar} & 0 & 0 & 0 \end{pmatrix} \tag{B.10}$$

$UHU^\dagger + i\hbar\frac{dU}{dt}$ is found by adding B.5, B.6 and B.10.

$$UHU^\dagger + i\hbar\frac{dU}{dt} = \begin{pmatrix} 0 & 0 & 0 & 0 & 0 & 0 \\ 0 & 0 & 0 & 0 & t_0 e^{i\Delta E_z t/\hbar} & t_0 e^{i\Delta E_z t/\hbar} \\ 0 & 0 & 0 & 0 & -t_0 e^{-i\Delta E_z t/\hbar} & -t_0 e^{-i\Delta E_z t/\hbar} \\ 0 & 0 & 0 & 0 & 0 & 0 \\ 0 & t_0 e^{-i\Delta E_z t/\hbar} & -t_0 e^{i\Delta E_z t/\hbar} & 0 & U_1 + \epsilon & 0 \\ 0 & t_0 e^{-i\Delta E_z t/\hbar} & -t_0 e^{i\Delta E_z t/\hbar} & 0 & 0 & U_2 - \epsilon \end{pmatrix} \tag{B.11}$$

The microwave Hamiltonian that controls the single-qubit rotations

$$\begin{aligned} H_{mw} &= \sum_k B_k \cos\left(\omega_k t + \phi_k\right) \left(\sigma_x \otimes \mathbb{I} + \mathbb{I} \otimes \sigma_x\right) \\ &\equiv \sum_k B_k(t) \left(\sigma_x \otimes \mathbb{I} + \mathbb{I} \otimes \sigma_x\right) \end{aligned} \tag{B.12}$$

where $B_k(t) = B_k \cos(\omega_k t + \phi_k)$. For brevity the sum term $\sum_k$ will be omitted in the calculations.

$$
\begin{aligned}
UH_{mw} &= \begin{pmatrix} e^{-i\omega t} & 0 & 0 & 0 \\ 0 & e^{-i\Delta\omega t} & 0 & 0 \\ 0 & 0 & e^{i\Delta\omega t} & 0 \\ 0 & 0 & 0 & e^{i\omega t} \end{pmatrix} \begin{pmatrix} 0 & B_k(t) & B_k(t) & 0 \\ B_k(t) & 0 & 0 & B_k(t) \\ B_k(t) & 0 & 0 & B_k(t) \\ 0 & B_k(t) & B_k(t) & 0 \end{pmatrix} \\
&= B_k(t) \begin{pmatrix} 0 & e^{-i\omega t} & e^{-i\omega t} & 0 \\ e^{-i\Delta\omega t} & 0 & 0 & e^{-i\Delta\omega t} \\ e^{i\Delta\omega t} & 0 & 0 & e^{i\Delta\omega t} \\ 0 & e^{i\omega t} & e^{i\omega t} & 0 \end{pmatrix} \\
UH_{mw}U^\dagger &= B_k(t) \begin{pmatrix} 0 & e^{-i\omega t} & e^{-i\omega t} & 0 \\ e^{-i\Delta\omega t} & 0 & 0 & e^{-i\Delta\omega t} \\ e^{i\Delta\omega t} & 0 & 0 & e^{i\Delta\omega t} \\ 0 & e^{i\omega t} & e^{i\omega t} & 0 \end{pmatrix} \begin{pmatrix} e^{i\omega t} & 0 & 0 & 0 \\ 0 & e^{i\Delta\omega t} & 0 & 0 \\ 0 & 0 & e^{-i\Delta\omega t} & 0 \\ 0 & 0 & 0 & e^{-i\omega t} \end{pmatrix} \\
&= B_k(t) \begin{pmatrix} 0 & e^{-i(\omega-\Delta\omega)t} & e^{-i(\omega+\Delta\omega)t} & 0 \\ e^{i(\omega-\Delta\omega)t} & 0 & 0 & e^{-i(\omega+\Delta\omega)t} \\ e^{i(\omega+\Delta\omega)t} & 0 & 0 & e^{-i(\omega-\Delta\omega)t} \\ 0 & e^{i(\omega+\Delta\omega)t} & e^{i(\omega-\Delta\omega)t} & 0 \end{pmatrix} \\
&= B_k(t) \begin{pmatrix} 0 & e^{-i\omega_2 t} & e^{-i\omega_1 t} & 0 \\ e^{i\omega_2 t} & 0 & 0 & e^{-i\omega_1 t} \\ e^{i\omega_1 t} & 0 & 0 & e^{-i\omega_2 t} \\ 0 & e^{i\omega_1 t} & e^{i\omega_2 t} & 0 \end{pmatrix}
\end{aligned} \tag{B.13}
$$

Note that $\omega + \Delta\omega = \frac{1}{2}(\omega_1 + \omega_2 + \omega_1 - \omega_2) = \omega_1$ and $\omega - \Delta\omega = \frac{1}{2}(\omega_1 + \omega_2 - \omega_1 + \omega_2 = \omega_2$. Decomposing $B_k(t)$ into two counter rotating terms $B_k(t) = B_k \cos(\omega_k t + \phi_k) = \frac{B_{mw}}{2}\left(e^{i(\omega_k t+\phi_k)} + e^{-i(\omega_k t+\phi_k)}\right)$.

$$
\begin{aligned}
&UH_{mw}U^\dagger = \\
&\frac{B_k}{2}\begin{pmatrix} 0 & e^{i(\omega_k-\omega_2)t+i\phi_k} + e^{-i(\omega_k+\omega_2)t-i\phi_k} & e^{i(\omega_k-\omega_1)t+i\phi_k} + e^{-i(\omega_k+\omega_1)t-i\phi_k} & 0 \\ e^{i(\omega_k+\omega_2)t+i\phi_k} + e^{-i(\omega_k-\omega_2)t-i\phi_k} & 0 & 0 & e^{i(\omega_k-\omega_1)t+i\phi_k} + e^{-i(\omega_k+\omega_1)t-i\phi_k} \\ e^{i(\omega_k+\omega_1)t+i\phi_k} + e^{-i(\omega_k-\omega_1)t-i\phi_k} & 0 & 0 & e^{i(\omega_k-\omega_2)t+i\phi_k} + e^{-i(\omega_k+\omega_2)t-i\phi_k} \\ 0 & e^{i(\omega_k+\omega_1)t+i\phi_k} + e^{-i(\omega_k-\omega_1)t-i\phi_k} & e^{i(\omega_k+\omega_2)t+i\phi_k} + e^{-i(\omega_k-\omega_2)t-i\phi_k} & 0 \end{pmatrix}
\end{aligned} \tag{B.14}
$$

By applying the RWA, i.e. the dynamics induced by the applied field $B_k(t)$ is much slower than the Larmor frequencies ω_1 and ω_2, the fast rotating terms $\omega_k + \omega_i$ can be neglected.

$$
UH_{mw}U^\dagger = \begin{pmatrix} 0 & \frac{B_k}{2}e^{i\phi_k}e^{i(\omega_k-\omega_2)t} & \frac{B_k}{2}e^{i\phi_k}e^{i(\omega_k-\omega_1)t} & 0 \\ \frac{B_k}{2}e^{-i\phi_k}e^{-i(\omega_k-\omega_2)t} & 0 & 0 & \frac{B_k}{2}e^{i\phi_k}e^{i(\omega_k-\omega_1)t} \\ \frac{B_k}{2}e^{-i\phi_k}e^{-i(\omega_k-\omega_1)t} & 0 & 0 & \frac{B_k}{2}e^{i\phi_k}e^{i(\omega_k-\omega_2)t} \\ 0 & \frac{B_k}{2}e^{-i\phi_k}e^{i(\omega_k-\omega_1)t} & \frac{B_k}{2}e^{-i\phi_k}e^{i(\omega_k-\omega_2)t} & 0 \end{pmatrix} \tag{B.15}
$$

Appendix C

Code

The QuTiP implementation and Numerical Liouville von Neumann solver can be found on github:
https://github.com/AhmadSJ/Two-spin-qubits

Bibliography

[1] D. Deutsch and R. Jozsa. Rapid Solution of Problems by Quantum Computation. *Proceedings of the Royal Society of London Series A*, 439:553–558, December 1992.

[2] P. Harrison and Paul Harrison. *Quantum wells, wires, and dots*. John Wiley & Sons Ltd, 2009.

[3] H. Flentje. *Coherent transport of electron spins in tunnel-coupled quantum dots*. Ph.D. thesis, University Grenoble Alpes, 2016.

[4] R. Hanson, L. P. Kouwenhoven, J. R. Petta, S. Tarucha, and L. M. K. Vandersypen. Spins in few-electron quantum dots. *Rev. Mod. Phys.*, 79:1217–1265, Oct 2007.

[5] M Field, Charles Smith, Michael Pepper, David Ritchie, J.E.F. Frost, G A. C. Jones, and D G. Hasko. Measurements of coulomb blockade with a noninvasive voltage probe. *Physical review letters*, 70:1311–1314, 04 1993.

[6] J. M. Elzerman, R. Hanson, L. H. Willems van Beveren, B. Witkamp, L. M. K. Vandersypen, and L. P. Kouwenhoven. Single-shot read-out of an individual electron spin in a quantum dot. *Nature*, 430(6998):431–435, 2004.

[7] W. G. van der Wiel, S. De Franceschi, J. M. Elzerman, T. Fujisawa, S. Tarucha, and L. P. Kouwenhoven. Electron transport through double quantum dots. *Rev. Mod. Phys.*, 75:1–22, Dec 2002.

[8] J.M. Elzerman. *Electron spin and charge in semiconductor quantum dots*. Ph.D. thesis, Delft University of Technology, 2004.

[9] P. Scarlino. *Spin and Valley physics in a Si/SiGe Quantum Dot*. Ph.D. thesis, Delft University of Technology, 2016.

[10] B. Odom, D. Hanneke, B. D'Urso, and G. Gabrielse. New measurement of the electron magnetic moment using a one-electron quantum cyclotron. *Phys. Rev. Lett.*, 97:030801, Jul 2006.

[11] D. Loss and D. P. DiVincenzo. Quantum computation with quantum dots. *Phys. Rev. A*, 57(1):120–126, 1998.

[12] Jo-Tzu Hung. *Dynamics of Encoded Spin Qubits in Semiconductor Quantum Dots*. Ph.D. thesis, University at Buffalo, 2015.

[13] D. J. Griffiths. *Introduction to Quantum Mechanics*. Pearson Prentice Hall, 2005.

[14] N.W. Ashcroft and N.D. Mermin. *Solid State Physics*. Saunders, Philadelphia, 1976, Chap. 32.

[15] Shuo Yang, Xin Wang, and S. Das Sarma. Generic hubbard model description of semiconductor quantum-dot spin qubits. *Phys. Rev. B*, 83:161301, Apr 2011.

[16] John Clarke and Frank K. Wilhelm. Superconducting quantum bits. *Nature*, 453:1031 EP –, Jun 2008.

[17] D. Leibfried, R. Blatt, C. Monroe, and D. Wineland. Quantum dynamics of single trapped ions. *Rev. Mod. Phys.*, 75:281–324, Mar 2003.

[18] L. M. K. Vandersypen, M. Steffen, G. Breyta, C. S. Yannoni, M. H. Sherwood, and I. L. Chuang. Experimental realization of shor's quantum factoring algorithm using nuclear magnetic resonance. *Nature*, 414:883–887, 2001.

[19] L. M. K. Vandersypen and I. L. Chuang. Nmr techniques for quantum control and computation. *Rev. Mod. Phys.*, 76:1037–1069, Jan 2005.

[20] C.J. Foot. *Atomic Physics*. Oxford University Press, 2004, Chap. 7.

[21] T. Meunier, V. E. Calado, and L. M. K. Vandersypen. Efficient controlled-phase gate for single-spin qubits in quantum dots. *Phys. Rev. B*, 83:121403, Mar 2011.

[22] G.L. Bir and G.E. Pikus. *Symmetry and strain-induced effects in semiconductors*. John Wiley & Sons, Chichester, 1974, Chap.15.

[23] Rukhsan-Ul-Haq Wani. A systematic method for schrieffer-wolff transformation. 04 2016.

[24] Lov K. Grover. A fast quantum mechanical algorithm for database search. In *Proceedings of the Twenty-eighth Annual ACM Symposium on Theory of Computing*, STOC '96, pages 212–219, New York, NY, USA, 1996. ACM.

[25] https://commons.wikimedia.org/wiki/file:grovers_algorithm.svg.

[26] Michael A. Nielsen and Isaac L. Chuang. *Quantum Computation and Quantum Information: 10th Anniversary Edition*. Cambridge University Press, New York, NY, USA, 10th edition, 2011.

[27] L. DiCarlo, J. M. Chow, J. M. Gambetta, Lev S. Bishop, B. R. Johnson, D. I. Schuster, J. Majer, A. Blais, L. Frunzio, S. M. Girvin, and R. J. Schoelkopf. Demonstration of two-qubit algorithms with a superconducting quantum processor. *Nature*, 460:240 EP –, Jun 2009.

[28] T. F. Watson, S. G. J. Philips, E. Kawakami, D. R. Ward, P. Scarlino, M. Veldhorst, D. E. Savage, M. G. Lagally, Mark Friesen, S. N. Coppersmith, M. A. Eriksson, and L. M. K. Vandersypen. A programmable two-qubit quantum processor in silicon. *Nature*, 555:633 EP –, Feb 2018.

[29] P. Brown, G. Byrne, and A. Hindmarsh. Vode: A variable-coefficient ode solver. *SIAM Journal on Scientific and Statistical Computing*, 10(5):1038–1051, 1989.

[30] Guido Burkard, Daniel Loss, David P. DiVincenzo, and John A. Smolin. Physical optimization of quantum error correction circuits. *Phys. Rev. B*, 60:11404–11416, Oct 1999.

[31] Uri M. Ascher and Linda R. Petzold. *Computer Methods for Ordinary Differential Equations and Differential-Algebraic Equations*. Society for Industrial and Applied Mathematics, Philadelphia, PA, USA, 1st edition, 1998, Chap. 3.4.

[32] Wilson J. Rugh. *Linear System Theory (2Nd Ed.)*. Prentice-Hall, Inc., Upper Saddle River, NJ, USA, 1996, Chap. 8.

[33] C. Moler and C. Van Loan. Nineteen dubious ways to compute the exponential of a matrix, twenty-five years later. *SIAM Review*, 45(1):3–49, 2003.

[34] A. Al-Mohy and N. Higham. A new scaling and squaring algorithm for the matrix exponential. *SIAM Journal on Matrix Analysis and Applications*, 31(3):970–989, 2010.